Gait augmentation through co-adaptation

Human-in-the-loop optimization for assistive gait technology

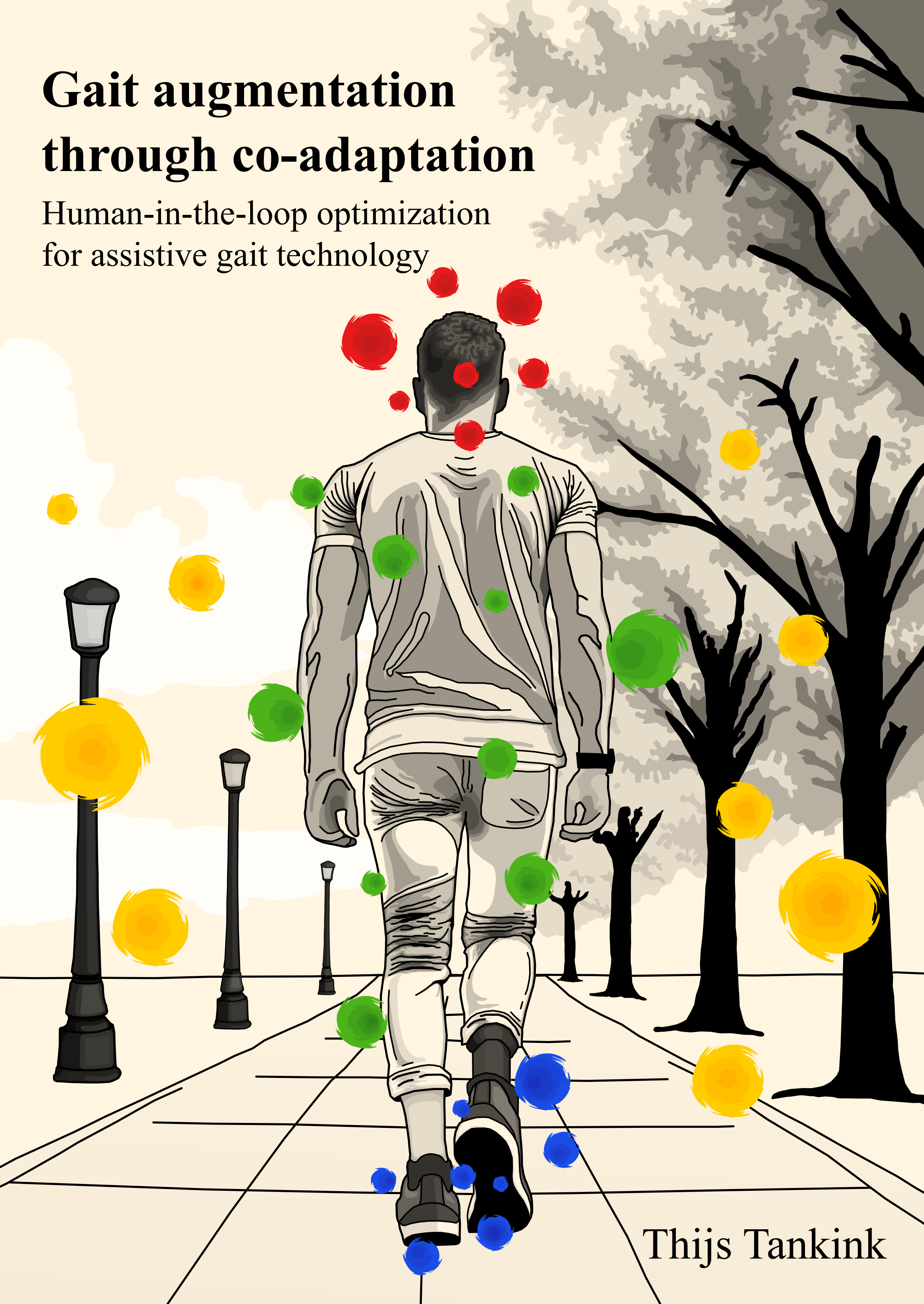

Thijs Tankink

Gait augmentation through co-adaptation

Human-in-the-loop optimization for assistive gait technology

Thijs Tankink

Colophon

The studies in this thesis were conducted within the Health in Context Research Institute of the University Medical Center Groningen (UMCG) and under auspices of the research program SMART movements (SMART).

The printing of this thesis was financially supported by the Graduate School of Medical Sciences of the UMCG, the University of Groningen, OIM Orthopedie, ISPO Nederland, COSMED, OFOM, AIRe, and Stichting Beatrixoord Noord-Nederland.

Paranymphs: Rob Koeken & Alexander Oonk
Cover design and layout: Thijs Tankink
Printed by: Proeschriftspecialist.nl

university of groningen

Gait augmentation through co-adaptation

Human-in-the-loop optimization for assistive gait technology

PhD thesis

to obtain the degree of PhD of the
University of Groningen
on the authority of the
Rector Magnificus Prof. J.M.A. Scherpen
and in accordance with
the decision by the College of Deans.

This thesis will be defended in public on
Wednesday 10 June 2026 at 16.15 hours

by

Thijs Tankink

Born on 20 December 1998

Supervisors

Prof. J.H.P. Houdijk
Prof. R. Carloni
Prof. J.M. Hijmans

Assessment committee

Prof. R. Dekker
Prof. H. van der Kooij
Prof. S.H. Collins

Table of contents

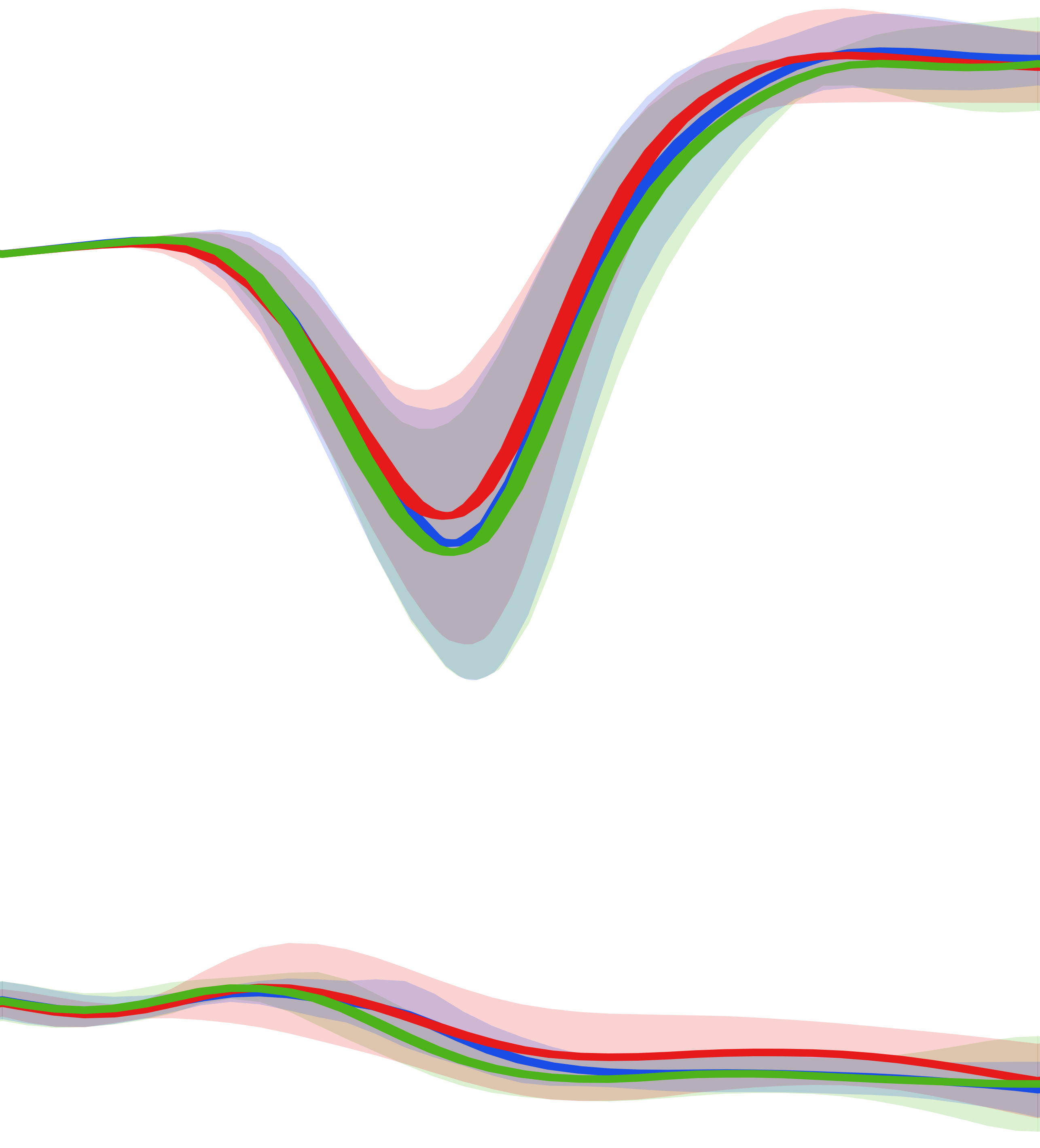

Chapter 1

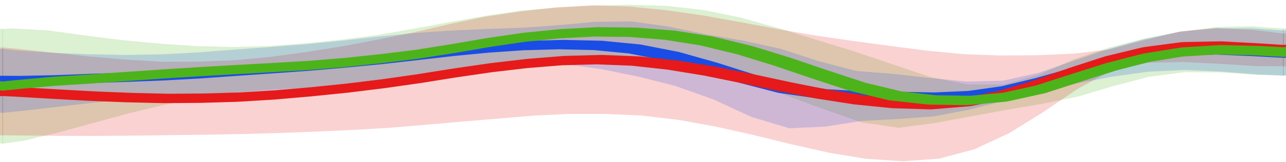

General introduction

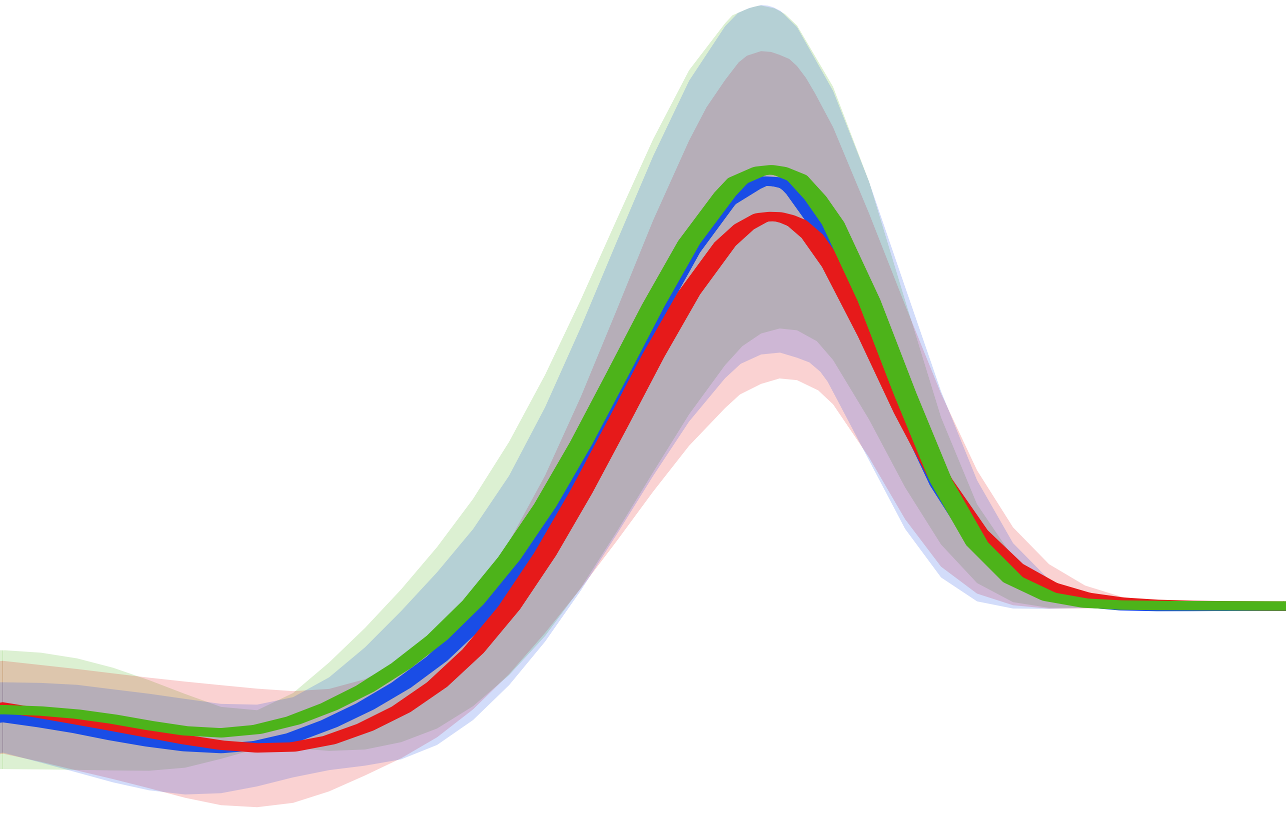

1.1. Human gait

Human bipedal gait, i.e., walking and running, is one of the most important skills of the human species [1]. On average, humans walk almost 120,000 km over their lifetime, the equivalent of travelling around the world three times [2]. Despite the neuromechanical complexity of human gait, which involves the coordinated activity of numerous neurons and muscles, humans have learned to use mechanical laws to find optimal strategies for walking and running. Simple models of human gait have shown that there are general principles that hold [3, 4], and could lead to meaningful insights into the complex dynamics of walking and running [5].

1.1.1. Inverted pendulum model for walking

Human walking is characterized by a center of mass motion similar to that of an inverted pendulum (Figure 1.1) [6]. During the single support phase, the stance leg behaves like a rigid strut that determines the arc movement of the center of mass. This motion allows kinetic energy to be converted to gravitational potential energy during the first half of stance, which can subsequently be recovered during the second half of stance [7]. It hence acts as an energy-saving mechanism. The double support phase of human walking could be seen as a transition from one inverted pendulum to the next. This transition requires negative work produced by the leading leg and positive work produced by the trailing leg in order to redirect the center of mass velocity from one pendular arc to the next [8]. This extension to the original pendulum model explains why walking is not for free.

1.1.2. Spring-mass model for running

Human running can be described by the spring-like behavior of the spring-mass model (Figure 1.1) [3], in which the bounce of the center of mass is caused by the spring-like behavior of the stance leg. During the first half of ground contact in human running, the leg compresses and mechanical energy is partly stored in tendons and other tissues around the joints. This stored energy can then be returned during the second part of ground contact as the leg extends again [9].

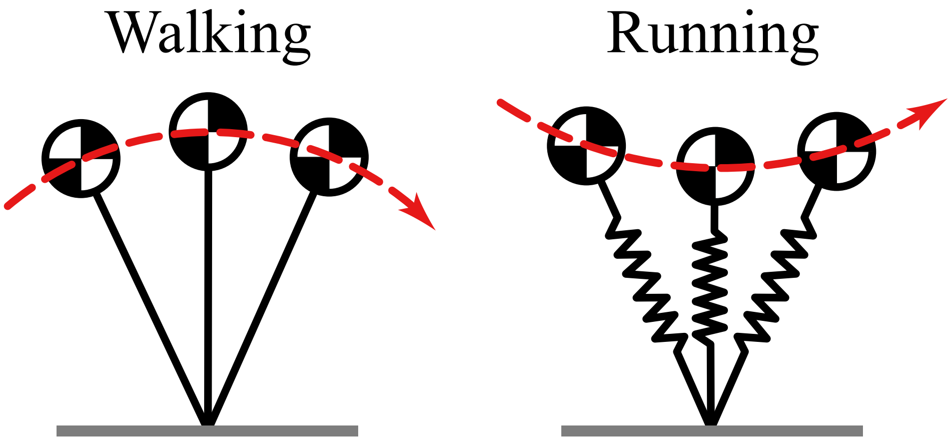

Figure 1.1: Inverted pendulum model for walking (left) and spring-mass model for running (right).

1.2. Foot-ankle system

An important extension of these simple models is the incorporation of the foot-ankle system. The foot and ankle play an important role during human gait, forming a dynamic link between the body and the ground [10]. They continuously adjust their alignment and function to achieve the desired movement [11], e.g., a support surface to enhance stability or a lever system to enhance propulsion and gait economy.

During walking, the foot-ankle system acts as a series of three "rockers", i.e., pivot points, to facilitate a smooth and efficient gait pattern (Figure 1.2) [12]. During running, the foot-ankle system functions as a shock absorption and propulsion system during touch down and push-off, respectively (Figure 1.2) [13]. The following subparagraphs provide a more detailed discussion of the role of the foot-ankle system during the different requirements of gait.

1.2.1. Weight acceptance

A typical characterization of human bipedal walking is heel strike at the initiation of the stance phase, in which the heel makes contact with the ground [14], and the leading leg generates a negative impulse to redirect the center of mass velocity. The dissipated amount of work to redirect the center of mass is proportional to the square of the angle between the legs at heel strike [15]. By landing on the heel, humans

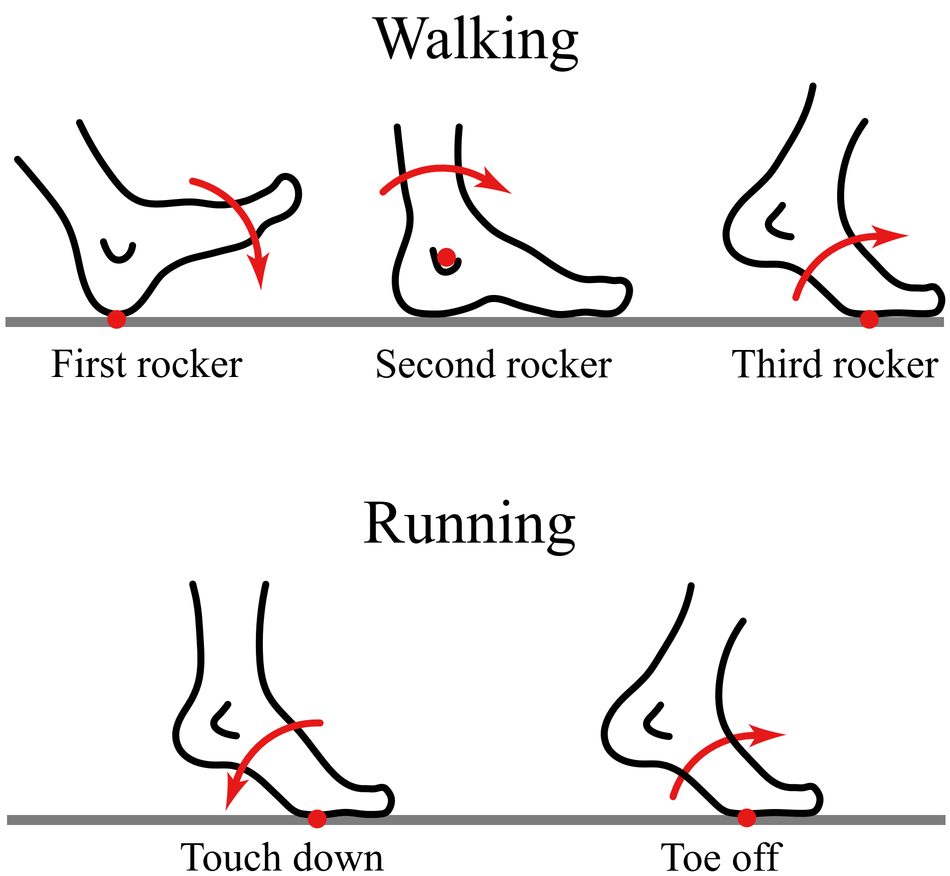

Figure 1.2: Foot-ankle system during different phases of stance during walking (first, second, and third rocker) and running (touch down and toe off).

reduce the angle between their legs at heel strike compared to walking with point feet [16], and therefore reduce the required amount of work. Subsequently, the foot rotates around the point of contact until the foot is flat on the ground, i.e., the first rocker of walking [1]. This extends the heel support period and facilitates shock absorption of the body weight [17].

During running, there is no double support phase, and the energetic advantages of heel strike disappear [18]. Therefore, changing to a forefoot strike pattern, with the ankle in a plantarflexed position at touch down, may be advantageous. Not only can this pattern limit impact forces and prevent injury [19], but it also enables storage and return of mechanical energy in the muscle-tendon complex of the Triceps Surae, which contains morphologies that are suitable for these processes [20].

1.2.2. Progression

During the second rocker of walking, the tibia rotates around the ankle joint, and the center of pressure progresses along the sole of the foot in the anterior direction. Therefore, the pivot point of the inverted pendulum has increased anterior translation during the stance phase, which increases the effective length of the pendulum, resulting in longer stride lengths compared to walking with point feet [21], and mitigating the step-to-step transition cost [16, 22]. Moreover, the ankle dorsi flexion movement allows energy storage in the Achilles tendon due to eccentric contraction of the Triceps Surae, which can be later reused in stance [23, 24]. Altogether, these mechanisms contribute to a reduced metabolic cost of walking [16, 21].

A challenge of human bipedal gait that occurs during the second rocker of walking is the relatively high center of mass above a small base of support [25]. Consequently, even a small perturbation could cause substantial gravitational momentum that accelerates the center of mass away from the base of support [25]. To prevent falls, balance perturbations require rapid adjustment of the base of support and appropriate repositioning of the ground reaction force by the musculoskeletal system to arrest momentum [26]. The foot-ankle system plays an important role in this context by supporting the body [10, 27] and modulating the location of the center of pressure [28, 29]. Additionally, specific features of muscle-tendon units around the ankle joint, e.g., muscle strength and tendon stiffness, contribute to balance control during walking and may help to reduce the risk of falls [26].

1.2.3. Propulsion

During the third rocker of walking, high push-off power at the ankle is produced, with its peak power output exceeding that of any other lower-limb joint by more than threefold [30]. An increased or well-timed push-off from the trailing leg decreases the negative collision work dissipated by the leading leg to redirect the center of mass velocity during the step-to-step transition [8, 31] and the compensatory positive work during mid-stance to maintain center of mass velocity [30, 31]. Therefore, a properly timed and executed push-off could reduce total positive work performed over a stride and reduce the metabolic cost of walking [8, 30].

The structural and functional properties of the foot and ankle enhance an effective push-off. The foot arch and intrinsic foot muscles stiffen the foot during late stance, allowing the foot to act as a rigid lever around the metatarsal-phalangeal (MTP) joints. This reduces energy losses and therefore facilitates a more efficient push-off [32].

During running, mechanical power stored in the tendons and other tissues around the ankle joint could be reused, reducing the need to actively generate push-off power in muscle fibers [33]. Another characteristic of the foot-ankle system that allows efficient propulsion are the long compliant series elastic elements of the Triceps Surae [20]. A considerable part of the reduction/shortening in muscle tendon length during push-off can be taken up by the Achilles tendon, which limits change in muscle fiber length and reduces muscle fiber contraction velocities [34]. More proximal leg muscles have these morphologies to a lesser extent [35], which makes their contractile properties less efficient compared to the distal leg muscles.

1.3. Assistive technology

Assistive technology for gait such as footwear, ankle-foot orthoses, or prosthetic devices, could be used to support, augment or imitate the foot-ankle system to a user's maximum. The applications are diverse, ranging from using orthoses to improve mobility after stroke [36], and using prosthetic devices to improve walking energetics after lower-limb amputation [37], to using newly developed footwear to improve running performance and break world records [38].

One way to enhance the function of the foot-ankle system via footwear is to change the rocker profile of a shoe, i.e., the curvature of the heel and forefoot of the shoe. Changing the starting position of the curvature of the forefoot of the shoe (apex position of a rocker profile) can modify the gear ratio of muscles around the ankle joint by modifying the external moment arm around the ankle joint [39, 40]. Optimizing this gear ratio by adjusting the apex position could allow the calf muscles to maximally utilize their advantageous morphology by operating closer to their optimal length and at lower muscle fiber contraction velocities, thereby improving mechanical efficiency [41] and gait economy [39]. Additionally, the rocker profile could affect the base of support and the roll-off direction of the foot, and therefore, influence gait stability [42].

The role of assistive technology becomes even more important in the field of rehabilitation and specifically rehabilitation of people after transtibial lower-limb amputation, where people are provided with a prosthesis that imitates the function of the biological foot-ankle system. One of the most important prosthetic developments is the introduction of energy storing and return prosthetic feet [43, 44]. These are typically carbon-fiber feet that store energy during the second rocker, which is subsequently re-used during push-off [37]. Increasing the amount of energy stored and proper timing of return could improve the efficiency of push-off power of the prosthetic foot to reduce step-to-step transition costs [45], resulting in more symmetrical joint loading [46, 47] and a decreased metabolic cost of walking [48].

However, despite all innovations, the effectiveness of current state-of-the-art assistive technology lags behind expectations. Physiological and neuromechanical differences between individuals can lead to varying responses to the same device or device settings [49], highlighting the importance of individually prescribing and tuning devices to the individual user [50]. However, technological developments result in more advanced devices with a higher number of parameters to tune. Simultaneously exploring device parameters and their interactions that are optimal for the individual user becomes a complex task. In addition, the voluntary, yet unpredictable, gait adaptations of the user in response to changes in these parameters during the tuning process [51, 52] should also be taken into account. Therefore, smart strategies to help us find individually optimized settings of such sophisticated devices seem to be required.

In current practice, this tuning process is typically performed by trial and error based on the experience and expertise of the clinical specialist involved. This approach lacks a solid evidence base and is getting more complicated with the increasing number of parameters to tune. Other traditional approaches, such as grid search, require tuning time that increases exponentially with the number of tunable parameters, are vulnerable to local optima, or overlook the influence of human adaptations during the tuning process. Computer models of human gait, alternatively, cannot yet replace exploring device settings with humans in this process [53]. Although musculoskeletal simulation models could operate easily and at low cost compared to human experiments, they are not yet able to model human motor adaptations and motor learning, and accurately predict the human response to the dynamic interaction with the device [54]. Therefore, we need to tune assistive devices to a human system that we do not fully understand, and empirical approaches appear to be more effective at present [53].

1.4. Human-in-the-loop optimization

A method that could address present challenges and improve the efficacy of assistive gait technology is human-in-the-loop optimization (Figure 1.3) [53, 55]. During human-in-the-loop optimization, the human is included 'in vivo' in the iterative optimization loop and device parameters are systematically varied during the optimization process using intelligent optimization algorithms in response to measured performance. By means of human-in-the-loop optimization, the device parameters could be tuned to the morphologies (i.e., biological properties) of the user [56], while also taking into account the natural behavior of humans to simultaneously optimize their coordination pattern with respect to gait performance [51].

Human-in-the-loop optimization has led to considerable improvements in performance of individuals using assistive technology [57], e.g., reducing energy cost of walking (-5.8%) [55] or enhancing gait speed (+18.1%) [58] when using optimized exoskeleton assistance compared to generic assistance. Although some aspects within the human-in-the-loop optimization paradigm are well understood, there are many aspects that are hardly explored and open to research (Figure 1.3) [53]. These aspects will be further explained below.

During the optimization process, different performance criteria could be considered as cost functions, such as metabolic cost, mechanical load, gait stability, or user preference. It is however yet unknown whether these different cost functions would result in similar optimal device parameters or not, and which of these cost functions is most responsive to change in the human-in-the-loop approach.

Another important aspect in the human-in-the-loop optimization process is selecting the appropriate optimization algorithm, e.g., evolutionary algorithm [55], Bayesian optimization [59], gradient-based methods [60], along with its configurations. Human-in-the-loop optimization requires a clever algorithm that rapidly and effectively explores the noisy and dynamic search landscape [53]. However, there is no clear consensus on which algorithms are most effective and which configurations of these algorithms should best be employed.

A different aspect open to research is the environment of optimization. Human-in-the-loop optimization is typically performed at a fixed walking speed on level ground, while in daily life, people continuously perform different activities to meet the demands of the changing environment, e.g., the use of different walking speeds. So far, it has not been established whether different activities require different optimal device settings to allow optimal human-device performance.

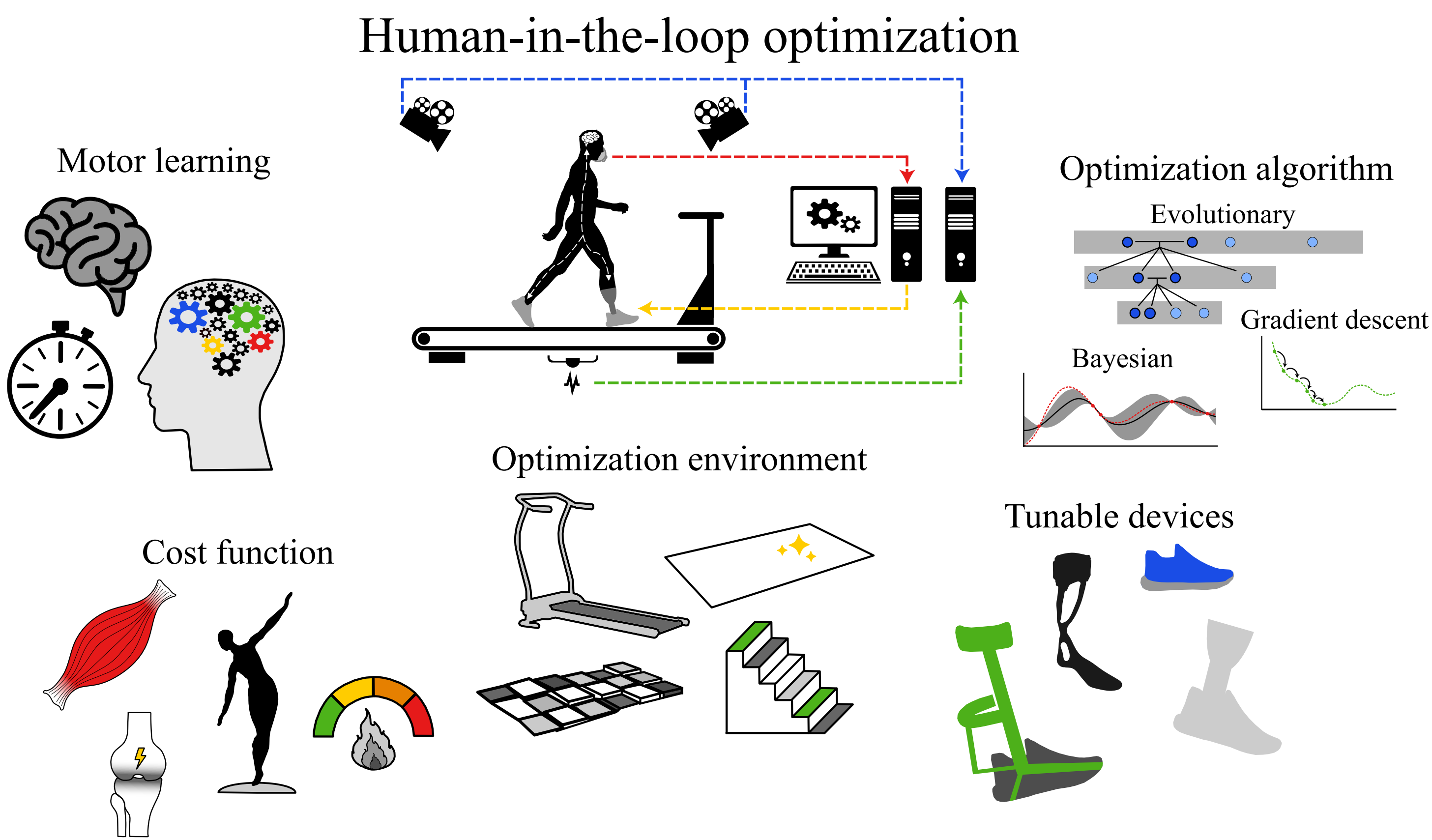

Figure 1.3: Human-in-the-loop optimization (top middle) and aspects within the paradigm that could affect the optimization process and are open to research: appropriateness of different tunable assistive technologies (bottom right), the influence of different cost functions (bottom left), the influence of the optimization environment (bottom middle), the influence of different optimization algorithms (top right), and the influence of motor learning of the user (top left).

The increased gait performance observed after human-in-the-loop optimization of exoskeletons can be attributed both to the optimization of the device settings and the adaptation of the motor control of the user (both +/- 50%) [61]. Apparently, the iterative human-in-the-loop optimization process allows users to explore their motor strategies, co-adapt with the device, and maximally exploit optimal device settings. However, for people using a lower-limb prosthesis the results have been less clear [62], potentially due to poor adaptation skills of the user or limited sensory feedback. Consequently, further developments are needed to enable effective tuning of these devices [62].

Human-in-the-loop optimization is a generic approach that could be performed on many devices with tunable parameters. We will use both shoes and prostheses as showcases in this thesis.

1.5. Aim and outline of thesis

The objective of the current thesis is to explore human-in-the-loop optimization protocols for enhancing gait performance through assistive technologies, spanning from individually optimized footwear to prosthetic ankle-foot devices. This thesis aims to address open questions within the human-in-the-loop paradigm, develop knowledge that could enhance the process of tuning assistive technology to the individual end-user, and explore the potential of human-in-the-loop optimization within clinical practice and beyond.

Firstly, we aim to demonstrate the potential of human-in-the-loop optimization via two proof-of-concept studies. We study how human-in-the-loop optimization influences the optimal rocker profile (apex position and apex angle) of a shoe to enhance running (**Chapter 2**) and walking performance (**Chapter 3**). In **Chapter 2**, we aim to maximize positive ankle work in order to redistribute joint work around the lower-limb joints and improve running economy. In **Chapter 3**, we compare different cost functions (e.g., metabolic cost, mechanical load, and balance) to assess which cost functions are most effective in finding optimal solutions and whether optimal solutions differ between cost functions (**Chapter 3**).

Subsequently, we aim to make the next step towards implementation, by introducing human-in-the-loop optimization as a method that could be used in rehabilitation to optimize assistive technology for gait to the needs of the individual end-user. Therefore, we aim to test human-in-the-loop optimization in a population of people with a transtibial amputation. In this thesis, we used human-in-the-loop optimization to investigate whether this method could be used to individually optimize the stiffness and alignment of an energy storing and return prosthetic foot in order to minimize the metabolic cost of walking of transtibial amputees. We investigate both the effects of changes in prosthetic foot settings (**Chapter 4**) and motor learning of the user (**Chapter 5**) throughout the optimization process, i.e., adaptations of the device and adaptations of the user, on the metabolic cost of walking.

Following up, we will have some critical reflection on human-in-the-loop optimization for prosthetic foot optimization in **Chapters 6** and **7**. More specifically, we study whether optimal stiffness and alignment prosthetic foot settings depend on the walking speed used during optimization, and whether different walking speeds require different device settings (**Chapter 6**). In **Chapter 7**, we aim to explore whether the measured metabolic cost during the human-in-the-loop optimization process correlates with the perceived comfort of the user, and whether user preference might be an interesting optimization objective to use during the tuning of assistive devices as a proxy for metabolic cost.

Finally, a general discussion of the results and future perspectives about the applications of human-in-the-loop optimization and its implementation is provided (**Chapter 8**).

1.6. Reference list

[1] E. B. Simonsen, "Contributions to the understanding of gait control," Danish medical journal, vol. 61, no. 4, Apr, 2014.

[2] A. Hughes. "The average adult "walks around world three times" in their lifetime.," https://www.independent.co.uk/news/health/step-count-adult-lifetime-round-world-three-times-b573751.html.

[3] R. Blickhan, "The spring-mass model for running and hopping," Journal of Biomechanics, vol. 22, no. 11-12, pp. 1217-1227, 1989.

[4] A. D. Kuo, "Energetics of actively powered locomotion using the simplest walking model," Journal of Biomechanical Engineering, vol. 124, no. 1, pp. 113-120, Feb, 2002.

[5] R. M. Alexander, "Simple Models of Human Movement," Applied Mechanics Reviews, vol. 48, no. 8, pp. 461-470, 1995.

[6] J. M. Donelan, R. Kram, and A. D. Kuo, "Simultaneous positive and negative external mechanical work in human walking," Journal of Biomechanics, vol. 35, no. 1, pp. 117-124, Jan, 2002.

[7] G. A. Cavagna, N. C. Heglund, and C. R. Taylor, "Mechanical work in terrestrial locomotion: two basic mechanisms for minimizing energy expenditure," American Journal of Physiology-Regulatory, Integrative and Comparative Physiology, vol. 233, no. 5, pp. R243-R261, 1977.

[8] A. D. Kuo, J. M. Donelan, and A. Ruina, "Energetic consequences of walking like an inverted pendulum: step-to-step transitions," Exercise and sport sciences reviews, vol. 33, no. 2, pp. 88-97, Apr, 2005.

[9] P. U. Saunders, D. B. Pyne, R. D. Telford, and J. A. Hawley, "Factors affecting running economy in trained distance runners," Sports medicine (Auckland, N.Z.), vol. 34, no. 7, pp. 465-485, 2004.

[10] M. Błażkiewicz, I. Wiszomirska, K. Kaczmarczyk, R. Naemi, and A. Wit, "Inter-individual similarities and variations in muscle forces acting on the ankle joint during gait," Gait & posture, vol. 58, pp. 166-170, Oct, 2017.

[11] M. M. Rodgers, "Dynamic biomechanics of the normal foot and ankle during walking and running," Physical Therapy, vol. 68, no. 12, pp. 1822-1830, Dec, 1988.

[12] Z. O. Abu-Faraj, G. F. Harris, P. A. Smith, and S. Hassani, "Human gait and clinical movement analysis," Wiley Encyclopedia of Electrical and Electronics Engineering, vol. 2, pp. 1-34, 2015.

[13] J. M. Czerniecki, "Foot and ankle biomechanics in walking and running: a review," American journal of physical medicine & rehabilitation, vol. 67, no. 6, pp. 246-252, 1988.

[14] N. B. Holowka, and D. E. Lieberman, "Rethinking the evolution of the human foot: insights from experimental research," Journal of experimental biology, vol. 221, no. 17, pp. jeb174425, 2018.

[15] J. M. Donelan, R. Kram, and A. D. Kuo, "Mechanical work for step-to-step transitions is a major determinant of the metabolic cost of human walking," The Journal of experimental biology, vol. 205, no. Pt 23, pp. 3717-3727, Dec, 2002.

[16] P. G. Adamczyk, and A. D. Kuo, "Mechanical and energetic consequences of rolling foot shape in human walking," Journal of Experimental Biology, vol. 216, no. 14, pp. 2722-2731, 2013.

[17] J. A. Blaya, "Force-controllable ankle foot orthosis (AFO) to assist drop foot gait," Massachusetts Institute of Technology, 2002.

[18] C. B. Cunningham, N. Schilling, C. Anders, and D. R. Carrier, "The influence of foot posture on the cost of transport in humans," Journal of Experimental Biology, vol. 213, no. 5, pp. 790-797, 2010.

[19] M. O. Almeida, I. S. Davis, and A. D. Lopes, "Biomechanical Differences of Foot-Strike Patterns During Running: A Systematic Review With Meta-analysis," The Journal of orthopaedic and sports physical therapy, vol. 45, no. 10, pp. 738-755, Oct, 2015.

[20] M. Ishikawa, J. Pakaslahti, and P. V. Komi, "Medial gastrocnemius muscle behavior during human running and walking," Gait & posture, vol. 25, no. 3, pp. 380-384, Mar, 2007.

[21] J. T. Webber, and D. A. Raichlen, "The role of plantigrady and heel-strike in the mechanics and energetics of human walking with implications for the evolution of the human foot," The Journal of experimental biology, vol. 219, no. Pt 23, pp. 3729-3737, Dec 1, 2016.

[22] P. G. Adamczyk, S. H. Collins, and A. D. Kuo, "The advantages of a rolling foot in human walking," Journal of experimental biology, vol. 209, no. 20, pp. 3953-3963, 2006.

[23] R. M. Alexander, "Energy-saving mechanisms in walking and running," Journal of experimental biology, vol. 160, no. 1, pp. 55-69, 1991.

[24] K. E. Zelik, T.-W. P. Huang, P. G. Adamczyk, and A. D. Kuo, "The role of

series ankle elasticity in bipedal walking," Journal of theoretical biology, vol. 346, pp. 75-85, 2014.

[25] S. M. Bruijn, and J. H. van Dieën, "Control of human gait stability through foot placement," Journal of the Royal Society, Interface, vol. 15, no. 143, pp. 20170816, Jun, 2018.

[26] R. E. Smith, A. D. Shelton, G. S. Sawicki, and J. R. Franz, "The effects of plantarflexor weakness and reduced tendon stiffness with aging on gait stability," PloS one, vol. 19, no. 4, pp. e0302021, Apr 16, 2024.

[27] D. N. Karagiannakis, K. I. Iatridou, and D. G. Mandalidis, "Ankle muscles activation and postural stability with Star Excursion Balance Test in healthy individuals," Human movement science, vol. 69, pp. 102563, Feb, 2020.

[28] M. Vlutters, E. H. F. Van Asseldonk, and H. Van der Kooij, "Center of mass velocity-based predictions in balance recovery following pelvis perturbations during human walking," Journal of experimental biology, vol. 219, no. 10, pp. 1514-1523, 2016.

[29] A. L. Hof, "The equations of motion for a standing human reveal three mechanisms for balance," Journal of biomechanics, vol. 40, no. 2, pp. 451-457, 2007.

[30] T. W. Huang, K. A. Shorter, P. G. Adamczyk, and A. D. Kuo, "Mechanical and energetic consequences of reduced ankle plantar-flexion in human walking," The Journal of experimental biology, vol. 218, no. Pt 22, pp. 3541-3550, Nov, 2015.

[31] H. C. Doets, D. Vergouw, H. E. J. D. Veeger, and H. Houdijk, "Metabolic cost and mechanical work for the step-to-step transition in walking after successful total ankle arthroplasty," Human movement science, vol. 28, no. 6, pp. 786-797, 2009.

[32] D. J. Farris, L. A. Kelly, A. G. Cresswell, and G. A. Lichtwark, "The functional importance of human foot muscles for bipedal locomotion," Proceedings of the National Academy of Sciences of the United States of America, vol. 116, no. 5, pp. 1645-1650, Jan 29, 2019.

[33] P. R. Cavanagh, M. L. Pollock, and J. Landa, "A biomechanical comparison of elite and good distance runners," Annals of the New York Academy of Sciences, vol. 301, no. 1, pp. 328-345, 1977.

[34] T. J. Roberts, "The integrated function of muscles and tendons during locomotion," Comparative biochemistry and physiology.Part A, Molecular

& integrative physiology, vol. 133, no. 4, pp. 1087-1099, Dec, 2002.

[35] R. F. Ker, R. M. Alexander, and M. B. Bennett, “Why are mammalian tendons so thick?,” Journal of zoology, vol. 216, no. 2, pp. 309-324, 10, 2021.

[36] G. V. d. Paula, G. J. Luvizutto, L. A. Miranda, T. Regina da Silva, L. T. C. Silva, F. C. Winckler, G. P. Modolo, C. L. M. Chiloff, S. G. Zanati Bazan, and R. D. M. d. Costa, “Articulated ankle-foot orthoses associated with home-based task-specific training improve functional mobility in patients with stroke: a randomized clinical trial,” Topics in Stroke Rehabilitation, vol. 32, no. 3, pp. 280-293, 2025.

[37] G. N. Askew, L. A. McFarlane, A. E. Minetti, and J. G. Buckley, “Energy cost of ambulation in trans-tibial amputees using a dynamic-response foot with hydraulic versus rigid ‘ankle’: insights from body centre of mass dynamics,” Journal of neuroengineering and rehabilitation, vol. 16, no. 1, pp. 019-x, Mar 14, 2019.

[38] W. Hoogkamer, S. Kipp, J. H. Frank, E. M. Farina, G. Luo, and R. Kram, “A Comparison of the Energetic Cost of Running in Marathon Racing Shoes,” Sports medicine (Auckland, N.Z.), vol. 48, no. 4, pp. 1009-1019, Apr, 2018.

[39] S. F. Ray, and K. Z. Takahashi, “Gearing Up the Human Ankle-Foot System to Reduce Energy Cost of Fast Walking,” Scientific reports, vol. 10, no. 1, pp. 8793-5, May 29, 2020.

[40] [40] D. R. Carrier, N. C. Heglund, and K. D. Earls, “Variable gearing during locomotion in the human musculoskeletal system,” Science (New York, N.Y.), vol. 265, no. 5172, pp. 651-653, Jul 29, 1994.

[41] W. O. Fenn, and B. S. Marsh, “Muscular force at different speeds of shortening,” The Journal of physiology, vol. 85, no. 3, pp. 277-297, Nov 22, 1935.

[42] Y. Watanabe, N. Kawabe, and K. Mito, “The apex angle of the rocker sole affects the posture and gait stability of healthy individuals,” Gait & posture, vol. 86, pp. 303-310, May, 2021.

[43] D. H. Nielsen, D. G. Shurr, J. C. Golden, and K. Meier, “Comparison of Energy Cost and Gait Efficiency During Ambulation in Below-Knee Amputees Using Different Prosthetic Feet,” The Iowa orthopaedic journal, vol. 8, pp. 95-100, 1988.

[44] J. M. Casillas, V. Dulieu, M. Cohen, I. Marcer, and J. P. Didier, “Bioenergetic comparison of a new energy-storing foot and SACH foot in traumatic

below-knee vascular amputations," Archives of Physical Medicine and Rehabilitation, vol. 76, no. 1, pp. 39-44, Jan, 1995.

[45] D. Wezenberg, A. G. Cutti, A. Bruno, and H. Houdijk, "Differentiation between solid-ankle cushioned heel and energy storage and return prosthetic foot based on step-to-step transition cost," Journal of Rehabilitation Research & Development, vol. 51, no. 10, 2014.

[46] T. Schmalz, S. Blumentritt, and R. Jarasch, "Energy expenditure and biomechanical characteristics of lower limb amputee gait: The influence of prosthetic alignment and different prosthetic components," Gait & posture, vol. 16, no. 3, pp. 255-263, 2002.

[47] D. H. K. Chow, A. D. Holmes, C. K. L. Lee, and S. W. Sin, "The effect of prosthesis alignment on the symmetry of gait in subjects with unilateral transtibial amputation," Prosthetics and orthotics international, vol. 30, no. 2, pp. 114-128, 2006.

[48] M. J. Major, M. Twiste, L. P. J. Kenney, and D. Howard, "The effects of prosthetic ankle stiffness on ankle and knee kinematics, prosthetic limb loading, and net metabolic cost of trans-tibial amputee gait," Clinical Biomechanics, vol. 29, no. 1, pp. 98-104, January 2014, 2014.

[49] S. Logan, I. Hunter, J. T. J Ty Hopkins, J. B. Feland, and A. C. Parcell, "Ground reaction force differences between running shoes, racing flats, and distance spikes in runners," Journal of sports science & medicine, vol. 9, no. 1, pp. 147-153, Mar 1, 2010.

[50] J. D. Ventura, G. K. Klute, and R. R. Neptune, "The effect of prosthetic ankle energy storage and return properties on muscle activity in below-knee amputee walking," Gait & posture, vol. 33, no. 2, pp. 220-226, Feb, 2011.

[51] R. M. Alexander, "Optimization and gaits in the locomotion of vertebrates," Physiological Reviews, vol. 69, no. 4, pp. 1199-1227, 1989.

[52] J. C. Selinger, S. M. O'Connor, J. D. Wong, and J. M. Donelan, "Humans can continuously optimize energetic cost during walking," Current Biology, vol. 25, no. 18, pp. 2452-2456, 2015.

[53] P. Slade, C. Atkeson, J. M. Donelan, H. Houdijk, K. A. Ingraham, M. Kim, K. Kong, K. L. Poggensee, R. Riener, M. Steinert, J. Zhang, and S. H. Collins, "On human-in-the-loop optimization of human-robot interaction," Nature, vol. 633, no. 8031, pp. 779-788, Sep, 2024.

[54] P. W. Franks, N. A. Bianco, G. M. Bryan, J. L. Hicks, S. L. Delp, and S.

H. Collins, "Testing simulated assistance strategies on a hip-knee-ankle exoskeleton: a case study." pp. 700-707.

[55] J. Zhang, P. Fiers, K. A. Witte, R. W. Jackson, K. L. Poggensee, C. G. Atkeson, and S. H. Collins, "Human-in-the-loop optimization of exoskeleton assistance during walking," Science (New York, N.Y.), vol. 356, no. 6344, pp. 1280-1284, Jun 23, 2017.

[56] F. Scotto di Luzio, D. Simonetti, F. Cordella, S. Miccinilli, S. Sterzi, F. Draicchio, and L. Zollo, "Bio-Cooperative Approach for the Human-in-the-Loop Control of an End-Effector Rehabilitation Robot," Frontiers in neurorobotics, vol. 12, pp. 67, Oct 11, 2018.

[57] M. A. Diaz, M. Vos, A. Dillen, B. Tassignon, L. Flynn, J. Geeroms, R. Meeusen, T. Verstraten, J. Babic, P. Beckerle, and K. De Pauw, "Human-in-the-Loop Optimization of Wearable Robotic Devices to Improve Human-Robot Interaction: A Systematic Review," IEEE transactions on cybernetics, vol. 53, no. 12, pp. 7483-7496, Dec, 2023.

[58] S. Song, and S. H. Collins, "Optimizing exoskeleton assistance for faster self-selected walking," IEEE Transactions on Neural Systems and Rehabilitation Engineering, vol. 29, pp. 786-795, 2021.

[59] Y. Ding, M. Kim, S. Kuindersma, and C. J. Walsh, "Human-in-the-loop optimization of hip assistance with a soft exosuit during walking," Science robotics, vol. 3, no. 15, pp. eaar5438., Feb 28, 2018.

[60] S. C. Senatore, K. Z. Takahashi, and P. Malcolm, "Using human-in-the-loop optimization for guiding manual prosthesis adjustments: a proof-of-concept study," Frontiers in Robotics and AI, vol. 10, pp. 1183170, 2023.

[61] K. L. Poggensee, and S. H. Collins, "How adaptation, training, and customization contribute to benefits from exoskeleton assistance," Science Robotics, vol. 6, no. 58, 2021.

[62] C. G. Welker, A. S. Voloshina, V. L. Chiu, and S. H. Collins, "Shortcomings of human-in-the-loop optimization of an ankle-foot prosthesis emulator: a case series," Royal Society open science, vol. 8, no. 5, pp. 202020, 2021.

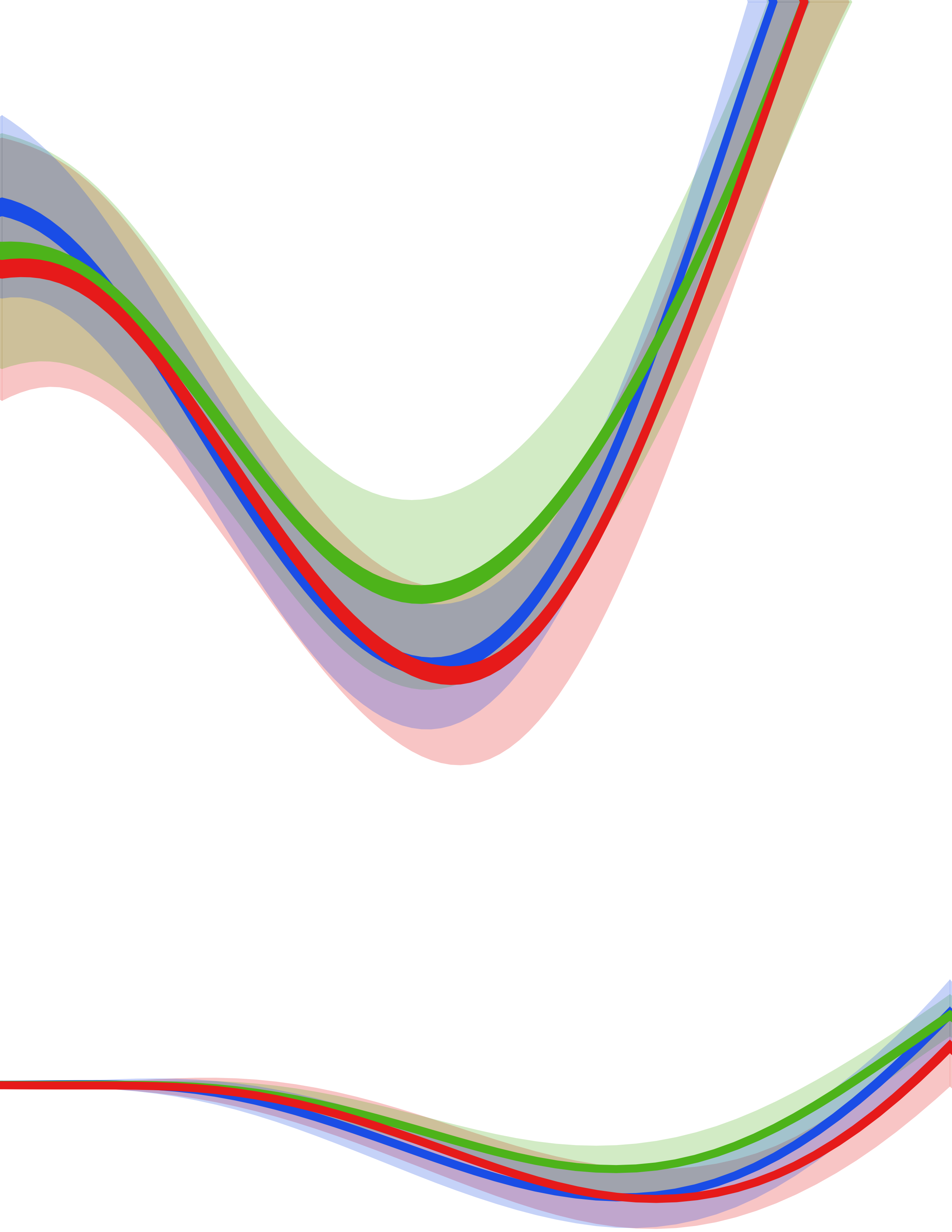

Chapter 2

Human-in-the-loop optimized rocker profile of running shoes to enhance ankle work and running economy

Thijs Tankink
Han Houdijk
Juha M. Hijmans

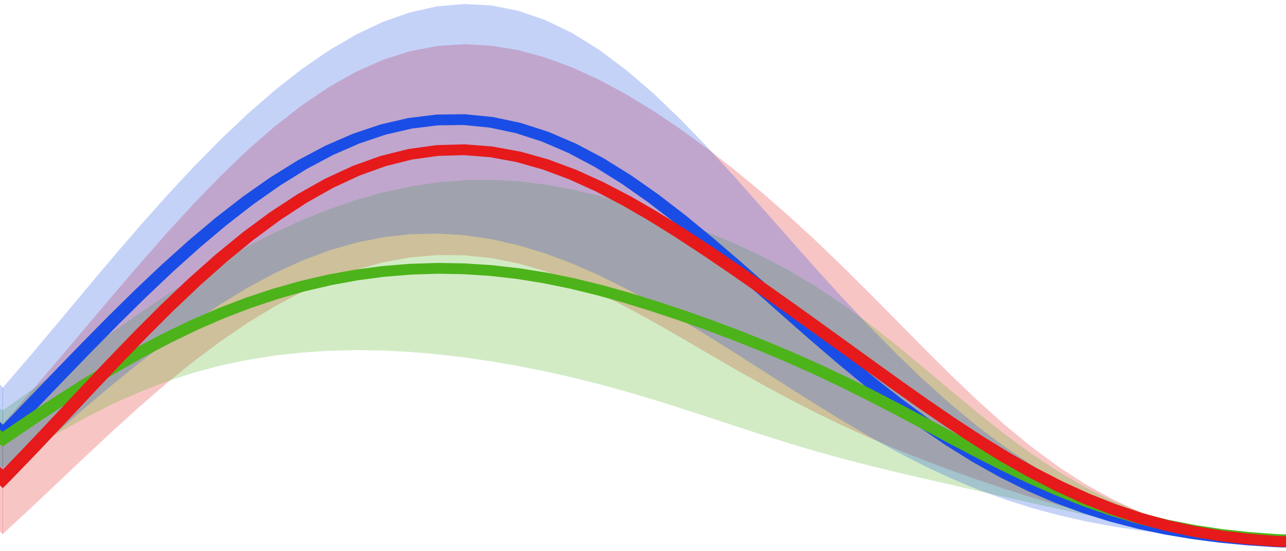

European Journal of Sport Science (2024), 24 (1), 164-173.

Abstract

Increasing the efficiency at which muscles generate mechanical power could improve running economy. A potential way to reduce muscle fiber shortening velocities and enhance energy storing of the Triceps Surae is changing their gear ratio at the ankle via optimization of shoe roll over profile. The aim of the current study was to individually optimize roll over profile of rocker shoes via human-in-the-loop optimization to maximize positive ankle work to redistribute joint work from the hip and knee to the ankle and improve running economy. A total of ten runners ran on a treadmill with experimental rocker shoes in which apex position and angle were optimized using an evolution algorithm to maximize positive ankle work. We compared experimental shoes with optimal settings, with standard settings, and control shoes in terms of biomechanics and running economy. Optimal apex parameters differed considerably between participants. The optimal condition resulted in higher positive ankle work and a higher proportional share of the ankle in the total positive lower limb work compared to the standard condition. A difference in running economy between these conditions was not found. Human-in-the-loop optimization can redistribute joint work from the hip and knee to the ankle by individually optimizing apex parameters. Although this did not improve running economy, the study showed that human-in-the-loop optimization could improve the effectiveness of footwear with respect to the selected optimization parameter on an individual level.

Keywords

Ankle gearing, biomechanics, metabolic rate, rocker shoes, Triceps Surae

2.1. Introduction

Since the marathon distance (42.195 km) was standardized, record times have progressively improved [1]. Despite that these improvements extrapolate to a sub-2-h performance in the near future, some scientists and athletes considered this as physiologically impossible [2, 3]. However, the discussion is more topical than ever, after Eliud Kipchoge recently improved the official world record in 2:01:09 in the 2022 Berlin Marathon and broke the 2-h barrier using pacers and drafting. These achievements were partly assigned to the newly developed running shoes that were worn [4].

Athletes, manufacturers, and scientists have investigated several shoe modifications to improve running performance, especially in terms of running economy [5]. Running economy partially depends on the efficiency in which muscles generate mechanical power [6]. This is dependent on the built-in force-velocity and force-length properties of skeletal muscles [7], where slower shortening velocities of muscle fibers and working close to their optimal length results in more efficient production of force and mechanical work [8]. Another important factor contributing to running economy is the spring-like behavior of the human leg. During the first half of ground contact the leg compresses while negative power is performed on the body's center of mass, and in the second half the leg extends again while positive power is produced. Part of the negative mechanical power can be stored in tendons and other tissues around the lower limb joints, and when returned reducing the need to actively generate power in muscle fibers [9].

Especially the Triceps Surae contain morphologies that are suitable for these processes, because a considerable part of the change of muscle tendon unit can be taken up by stretch and recoil of their long compliant series elastic elements [10], limiting muscle fiber contraction velocities [11]. More proximal leg muscles do have these characteristics to a lesser extent [12], and therefore their change in length is mostly a consequence of change in muscle fiber length. This results in energy loss during eccentric contraction and higher shortening velocities during concentric contraction, which makes the contractile conditions of the proximal leg muscles less efficient compared to the distal leg muscles. A previous study already suggested that a redistribution of joint work from the ankle to the knee and hip could contribute to a reduced running economy [13]. Moreover, runners with higher running economy generally have a higher energy storage capacity in the Triceps Surae compared to runners with lower running economy [14].

One way to enhance energy storing in the tendon of the ankle plantar flexor muscles and reduce muscle fiber shortening velocity is to change the gear ratio at the ankle [15, 16]. This is the ratio of the lever arm of the ground reaction force and the lever arm of the Triceps Surae with respect to the ankle joint. Increasing the gear ratio without changing the magnitude of the ground reaction force would demand a greater force from the calf muscles to generate the required muscle moment. This increased muscle force increases the stretch in the tendon and therewith reduces the required lengthening and shortening of the muscle fiber at a given ankle angular change. Increasing the gear ratio can be caused by a more distally placed apex position of the shoe compared to the metatarsophalangeal (MTP) joint, which causes a distal displacement of the point of application of the ground reaction force [17], with that an increased ankle moment and with the same angular velocity increased positive ankle power.

In addition, the apex angle of a running shoe can affect the gear ratio. Push-off can be performed around different axes: an axis through the MTP joint of the first and second toe (MTP_{1-2}), corresponding with an apex angle of about 90°, and an axis through the MTP joint of the second to the fifth toe (MTP_{2-5}) with an apex angle of 50° – 70° [18]. These two push-off mechanisms result in moment arms with different magnitudes. The ratio between the arms (MTP_{1-2} : MTP_{2-5}) is 1.22 : 1 [18]. Thus, it is expected that an apex angle of about 90° is beneficial for the calf muscle efficiency through increased gearing.

Most previous studies [16, 19] typically investigate only one single shoe parameter out of many that are relevant. This limits the exploration of the interaction between these parameters. To complicate the challenge, physiological and neurological differences between individuals can cause different responses to the same intervention [20], and responses can change substantially during the course of adaptation [21].

A potential method to overcome these challenges is human-in-the-loop optimization [22], in which the human being is included 'in vivo' in the control loop and device parameters are systematically varied during the measurement period using an intelligent optimization algorithm in response to measured performance to optimize human performance. By means of this method, the parameters could be tuned to the needs of the individual [23] while taking into account the natural behavior of humans to simultaneously optimize coordination patterns with respect to locomotor performance [24]. Frequently, metabolic cost is used directly as objective for optimization [22]. However, this requires relatively long measurements, as steady state needs to be reached, which could lead to fatigue when used for running. Mechanical work at the ankle, which requires less measurement time to determine and could enhance running economy via the morphologies of the Triceps Surae as described above, could potentially be used as a proxy for metabolic cost.

Therefore, the aim of the present study is to individually optimize the apex position and apex angle of running shoes through human-in-the-loop optimization to maximize positive ankle work, generated during steady state running. We hypothesize that optimization will result in a more distally placed apex position compared to a normal running shoe and an apex angle close to 90°. We expect that the increase in positive ankle work causes a higher proportional share of positive ankle work to the total positive work generated around the lower limb joints (hip, knee, and ankle), which will result in an improved running economy.

2.2. Method

2.2.1. Participants

A total of 10 (2 female) recreational runners (age: 22.0 ± 1.8 y, height: 183.0 ± 8.5 cm, weight: 77.7 ± 11.1 kg, shoe size range: 38 – 44 EU) participated in this study. Participants had to run at least 15 km per week to be included. Their running distances ranged from 15 to 80 km per week (26.7 ± 20.6 km/week) as part of regular training. All participants were free of injury and pain at time of the experiment and signed an informed consent. The study protocol was approved by the local ethics committee of the department Human Movement Sciences, University Medical Center Groningen (10349).

2.2.2. Shoe Conditions

We used regular athletic shoes (Chris, Dr Comfort, Mequon, WI, USA) as a control condition and experimental shoes (Figure 2.1A) with an adjustable apex position and apex angle [25], made from the same shoe model. The outer sole of the experimental shoes was removed and 3 carbon fiber layers that contained 2 rails with sliders were placed below the shoe, which could be used to manipulate the apex position and angle of the sole (Figure 2.1B). The carbon plates resulted in a higher stiffness (83.6 N/rad) and mass (range: 407 – 560 g/shoe) compared to the control shoe (1.9 N/rad; mass range: 197 – 261 g/shoe). 2 3D-printed cylinders (diameter = 30 mm, height = 13 mm) with tapered rims were screwed onto the sliders with a bolt. The position of the cylinders could be changed across the rails (40 – 90% total shoe length), by manually screwing the bolts. A Polyethylene layer of 3 mm (Streifylast, Streifeneder, Emmering, Germany) was placed between the original outer sole and the cylinders to prevent the outer sole being damaged.

2.2.3. Experimental set-up

Measurements were performed using the GRAIL (Gait Realtime Analysis Interactive Lab; Motekforce Link, Amsterdam, the Netherlands) the department of Human Movement Sciences of the University Medical Center Groningen. The GRAIL consists of a dual-belt treadmill with force sensors beneath each separate belt (Motekforce Link, Amsterdam, the Netherlands; Fs = 900 Hz) and a 10-camera (Vero) motion capture system (Vicon Nexus 2.8.1, Oxford, UK; Fs = 150 Hz) that registered the marker trajectories of 22 reflective markers (diameter = 14 mm) placed according to the lower-limb Human Body Model 2 [26]. We used the D-flow (3.34.3, Motekforce Link, the Netherlands, Amsterdam) online environment for real-time analysis during the optimization period. Respiratory data were collected in the evaluation trials by the portable metabolic analyzer K5 (COSMED, Rome, Italy) in breath-by-breath mode.

2.2.4. Experimental Protocol

The experiment was performed during 1 lab visit and consisted of a warming up, an optimization period, and an evaluation phase. The protocol started with a warming up of 5 min while wearing the experimental shoes with an apex position of 65% total shoe length (middle limits cylinder positions) and an apex angle of 90°. During the warming up, participants chose a self-selected sub-maximal running speed. To minimize the influence of fatigue, participants were instructed to select a speed that they could keep up for 60 min and had a 60-s rest break after every running trial. The self-selected speed (2.67 ± 0.44 m/s) was maintained during the rest of the protocol.

During the optimization period, we aimed to maximize the positive ankle work of the dominant leg (foot used to kick a ball) for every individual participant by optimizing the apex position and apex angle. These parameters were manually adapted by screwing the bolts and changing the cylinder positions of both left and right shoe during the rest periods. We used a covariance matrix adaptation evolution strategy (CMA-ES) [27] to optimize the apex position and angle. The algorithm used a predetermined number (8) of measurements, forming 1 generation, to calculate the parameter values of the next generation. After every generation, the apex parameters of the 4 trials that resulted in the highest positive ankle work were selected as input for the algorithm to generate 8 new candidates for the parameter values of the following generation. These values are around the mean parameters of these 4 best trials. With every new generation, the value of this mean is updated and the area of search around this mean was further reduced to converge to the optimal apex parameter and angle. Based on previous studies [22, 27] we chose to explore a maximum of 4 generations with a generation size of 8. So, during the optimization period, participants ran 32 (4 x 8) times 90 s on the experimental running shoes with intervening rest periods of 60 s. We calculated the mean positive ankle work of the first 6 successive steps of the dominant leg during the last 30 s of a 90-s trial. The result was used as input for the optimization algorithm, with a higher value indicating a better outcome. To ensure that the optimal parameters were an actual measured setting, eventually all 32 trials were compared and the apex position and apex angle that resulted in the highest positive ankle work were chosen as optimal parameters. An example of the results of the optimization period of 1 participant is presented in Figure 2.1C – D. See Appendix for the results of every individual participant.

In the evaluation phase, participants ran 3 times 6 min in different shoe conditions: (1) experimental shoes with optimal parameter settings, (2) experimental shoes with standard parameter settings (apex position: 64% total shoe length, apex angle: 88.0°; copied by visual inspection of the apex of the control shoe), and (3) control shoes. We measured oxygen consumption and carbon dioxide production to compare running economy. Ground reaction forces and marker trajectories were measured for biomechanical analysis. In between trials, participants took a 5-min break while they changed shoes. Shoes were worn in random order.

2.2.5. Data Analysis

Biomechanical data of the dominant leg in the last 2 min of the evaluation period were used in the offline data analysis. Data were filtered with a low-pass second order Butterworth filter with cut-off frequency of 6 Hz. We used a custom-made MATLAB (R2021b, MathWorks, Natick, MA, USA) script with a 10 N vertical ground reaction force threshold to detect the different steps and calculated stance time and step frequency. We calculated the course of vertical ground reaction force and anterior-posterior point of force application over the stance time. For the ankle, knee, and hip joint we calculated joint angles, angular velocities, moments, and powers during the stance phase, using custom MATLAB scripts. Positive and negative joint work was

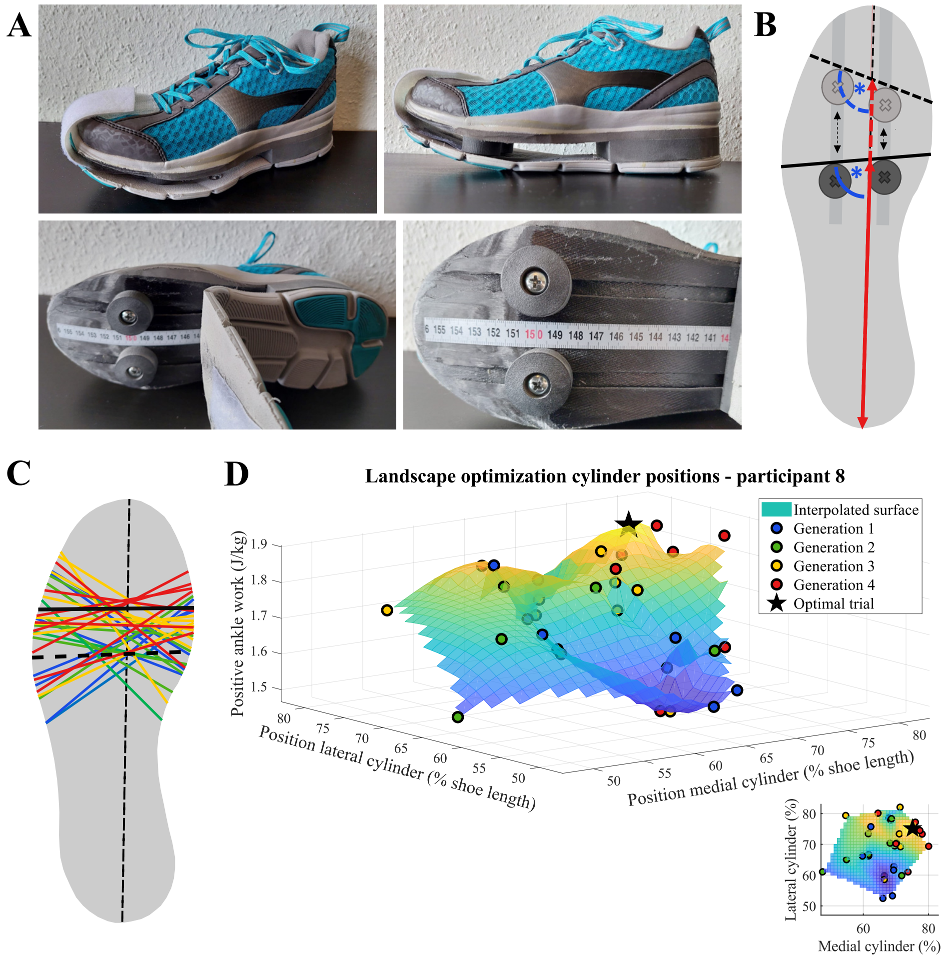

Figure 2.1: (A) Experimental shoes with adjustable apex position and apex angle. The position of the cylinders (bottom) could be changed across the rails, by manually screwing the bolts. (B) Changing the cylinders result in a new (dashed) apex position (red) and apex angle (blue asterisk). (C + D) Example of the optimization results for 1 participant. (C) The apex line of every trial is presented. The colors represent the trials of a given generation as indicated in the legend on the right. The black lines indicate the optimal settings (solid) and standard settings (dashed). (D) Positive ankle work (vertical axis) as a function of the cylinder positions (medial and lateral; as percentage of total shoe length) of every trial. A small 2D top view is inserted in the right bottom corner. The different colored circles indicate the 8 trials of the different generations. The optimal trial is represented by the star.

calculated by integrating the power curves over time, for the intervals of positive and negative power respectively. To gain insight into the contribution of the positive work generated around different joints, we expressed the share as a percentage of the total positive work generated around the lower limb joints. To compare the biomechanical effects of the different shoe conditions, we time normalized all data curves to the duration of the stance phase. The metabolic cost of running was calculated based on the mean $\dot{V}O_2$ and $\dot{V}CO_2$ over the last 2 min of each trial, using the equation of Garby and Astrup [28]:

$$metabolic\ \ power = 16.04 \cdot \dot{V}O_2 + 4.94 \cdot \dot{V}CO_2 \tag{2.1}$$

where $metabolic\ \ power$ is in W and $\dot{V}O_2$ and $\dot{V}CO_2$ are in mL/s. Subsequently, we normalized $metabolic\ \ power$ for body mass (W/kg).

2.2.6. Statistical analysis

We performed repeated measures analyses of variance (ANOVA), in SPSS (version 28.0.1, IBM Corp., Armonk, NY, USA), with shoe condition (optimal, standard, control) as within-subjects factor for 2 dependent variables: positive ankle work and metabolic cost of running. A p-value of 5% was used to indicate statistically significant differences. We used Bonferroni corrected post hoc paired t-tests to compare the different shoe conditions. If the assumption of sphericity was violated, we used a Greenhouse-Geisser correction. Time series of continuous gait variables were compared using 1-dimensional Statistical Parametric Mapping (SPM-1D) [29]. All SPM-1D analyses were performed with a custom MATLAB script and using the open-source software package spm1D 0.4.8 (www.spm1d.org). SPM-1D Repeated measures ANOVA were used to compare the shoe conditions ($p < 0.05$). The p-value of the post hoc paired t-tests were Bonferroni corrected.

2.3. Results

All optimized apex positions were more distally placed compared to the standard apex position (Table 2.1). In 8 of the 10 cases, the final apex angle was smaller than the standard angle (88°).

Table 2.1: Optimized apex position (as percentage of total shoe length) and apex angle for each participant (n=10). Number of trial during the optimization period (maximum=32) that resulted in the optimal parameters is also given.

	Apex position (%)	Apex angle (°)	Optimal trial (n)	Color
Participant 1	77.2	61.1	18	
Participant 2	78.7	115.1	31	
Participant 3	75.9	53.3	11	
Participant 4	78.6	60.8	24	
Participant 5	81.0	54.5	11	
Participant 6	84.2	76.2	13	
Participant 7	81.6	107.5	8	
Participant 8	82.4	87.4	7	
Participant 9	79.5	62.4	20	
Participant 10	84.2	66.9	31	
Standard parameters	64.0	88.0		

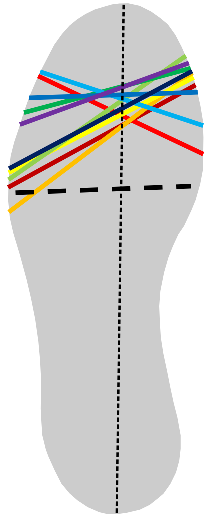

During the evaluation phase, no significant differences were found in step frequency and stance time (Table 2.2). A significant shoe condition effect was found for positive knee and ankle work, and negative ankle work (Table 2.2). Post hoc tests revealed that running on experimental shoes with optimal apex parameters and control shoes resulted in significantly higher positive work compared to experimental shoes with standard apex settings (respectively +22.4%, $p < 0.01$ and +29.6%, $p < 0.01$; Table 2.2). Significant differences between the optimized settings and the control shoe were not found.

SPM-1D with repeated measures ANOVA revealed significant differences between shoe conditions in the vertical ground reaction force during 72 – 97% of stance time ($p < 0.001$; Figure 2.2A). A main effect for the anterior-posterior point of force application was found during 37 – 59% of stance time ($p < 0.001$). Post hoc test showed that the optimal condition resulted in a significantly more distally placed point of force application during this interval, compared to the standard condition (Figure 2.2B).

A main effect for ankle angle was found during 43 – 68% and 76 – 89% of stance time (Figure 2.2C). The optimal apex condition resulted in a larger angle (dorsiflexion) compared to the standard apex condition (47 – 67% stance time, $p < 0.01$). Angular velocity showed most evident contrasts during 59 – 81% of stance time (Figure 2.2D). Post hoc test revealed a significantly higher plantar flexion angular velocity for the optimal (63 – 79% stance time) and control condition (62 – 80% stance time) compared to the standard condition.

Ankle moments differed between conditions 13 – 83% of stance time ($p < 0.001$; Figure 2.2E), with a higher plantar flexion moment for the optimal condition (40 – 82% stance time) and control condition (17 – 67% stance time) compared to the standard condition. The power patterns differed most evident during 18 – 49% ($p < 0.001$; Figure 2.2F) and 58 – 81% ($p < 0.001$) of stance time. Post hoc test revealed that power absorption was reduced for the standard condition compared to the optimal condition (37 – 48% stance time) and control condition (23 – 35% stance time). Significantly more plantar flexion power is generated during the optimal condition (62 – 84% stance time) and control condition (60 – 78% stance time) compared with the standard condition.

The shoe conditions altered the share of positive hip, knee, and ankle work as percentage of the total positive work generated around the lower limb joints (Table 2.2). Post hoc tests revealed that the optimized apex condition resulted in a significantly higher share of positive ankle and lower knee and hip work compared to the standard apex condition. The control shoe also resulted in a higher share of positive ankle work and lower knee work compared to the standard condition.

A significant shoe condition effect was found for metabolic power (Table 2.2). The conditions wearing the experimental shoes with optimal ($p = 0.01$) and standard ($p = 0.02$) apex parameters resulted in a higher metabolic cost of running compared to the control shoe. A significant difference between the optimal condition and standard condition was not found.

Table 2.2: Descriptives (mean (SD)) and results of repeated measure analyses of variance of running parameters, lower limb joint work, and metabolic cost of running for the different shoe conditions (n=10).

	Apex optimal	Apex standard	Control	F(2,18)	p	ES[a]
Step frequency (step/s)	2.67 (0.07)	2.70 (0.08)	2.70 (0.11)	1.20	0.32	0.12
Stance time (s)	0.313 (0.024)	0.316 (0.022)	0.312 (0.023)	1.96	0.17	0.18
Positive hip work (J/kg)	0.22 (0.08)	0.24 (0.08)	0.23 (0.09)	2.25	0.14	0.20
Positive knee work (J/kg)	0.37 (0.08)^{S}	0.42 (0.05)^{O,C}	0.35 (0.09)^{S}	9.15^{b,c}	0.01	0.50
Ankle work (J/kg)						
Positive	1.20 (0.27)^{S}	0.98 (0.20)^{O,C}	1.27 (0.30)^{S}	21.06^{c}	<0.001	0.70
Negative	-0.44 (0.13)^{S}	-0.30 (0.09)^{O,C}	-0.42 (0.11)^{S}	26.37^{c}	<0.001	0.75
Lower limb positive work (% of total)						
Hip	12.09 (3.82)^{S}	14.66 (3.62)^{O,C}	12.38 (5.02)^{S}	8.47c	<0.01	0.49
Knee	21.06 (4.26)^{S,C}	26.07 (3.17)^{O,C}	19.24 (3.97)^{O,S}	56.06^{b,c}	<0.001	0.86
Ankle	66.85 (4.38)^{S}	59.26 (4.46)^{O,C}	68.38 (5.28)^{S}	60.25^{c}	<0.001	0.87
Metabolic cost (W/kg)	14.47 (1.81)^{C}	14.58 (1.59)^{C}	13.88 (1.95)^{O,S}	10.12^{c}	0.001	0.53

Notes: [a]Effect Size = partial η^2

[b]Greenhouse-Geisser correction was used

[c]Bonferroni corrected post hoc tests (^{O}vs. Apex Optimal; ^{S}vs. Apex Standard; ^{C}vs. Control)

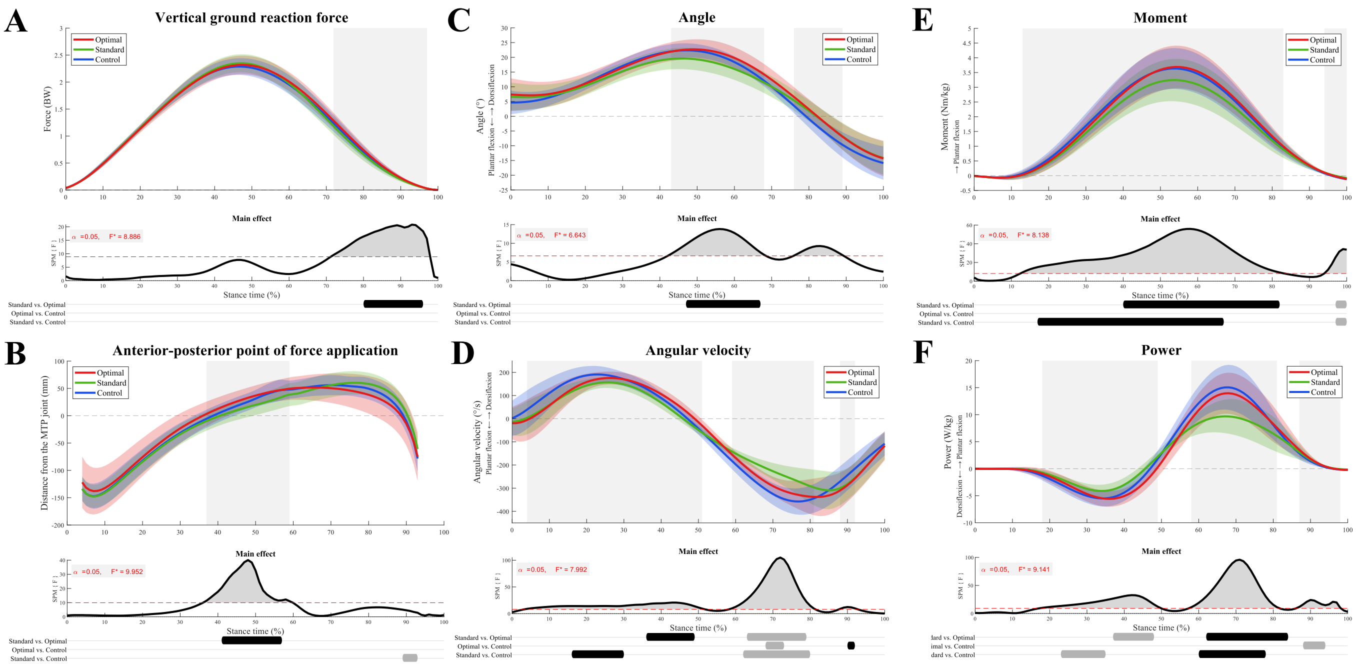

Figure 2.2: (A) Vertical ground reaction force, (B) anterior–posterior distance between point of force application and metatarsophalangeal (MTP) joint, and sagittal ankle (C) angle, (D) angular velocity, (E) moment, and (F) power (Mean ± SD) patterns for all shoe conditions. The gray areas indicate significant differences ($p < 0.05$). The time dependent F-values of the SPM-1D repeated measures ANOVA and results of the post hoc tests between the shoe conditions are given underneath (gray bar = increase; black bar = decrease).

2.4. Discussion

The purpose of the present study was to determine if human-in-the-loop optimization could optimize apex position and angle to maximize positive ankle work and whether this would increase running economy. We hypothesized that this would be achieved by a more distally placed apex position and an apex angle close to 90°. We expected that this would result in a higher percentage of positive ankle work with respect to total lower limb positive work and a lower metabolic cost of running. For all participants, the optimal apex position was placed more distally compared to the standard position. The optimal apex angles showed more variation between participants and were not centered around the expected 90°. Consistent with our hypothesis, the human-in-the-loop optimization resulted in higher positive ankle work and redistribution of joint work compared to the standard settings. However, this did not result in a difference in running economy between the optimal and standard settings.

Our findings show that the optimal condition, with a more distally placed apex position, results in a faster distal travel of the point of force application compared to the standard condition. This increases the moment arm of the ground reaction force with respect to the ankle joint, which requires a higher internal ankle moment. To initiate foot rotation, the internal ankle moment generated by the ankle plantar flexor muscles should exceed the external ankle moment from the ground reaction force [30]. The higher external moment due to the larger moment arm of the ground reaction force in the optimal condition delays the start of foot rotation, which is confirmed by an increase in peak dorsiflexion. The increased ankle moment and increased range of motion of the ankle (and concomitant higher angular velocity), result in an increase of both negative and positive ankle power and work during the optimal condition compared to the standard condition and could explain the corresponding redistribution of joint work from the hip and knee to the ankle.

We expected this would result in an improved running economy compared to the standard condition because due to the increased force on the m. Triceps Surae more negative work could be stored in the tendon of the Triceps Surae [10, 11], and subsequently more stored energy could be reused during the propulsion phase. In addition, muscle fiber shortening could be reduced because the tendon can take up more of the muscle-tendon unit length change. This could limit muscle fiber shortening velocities and enhance muscle mechanical efficiency [7].

However, our results show no difference in metabolic cost between the optimal and standard condition. Unfortunately, the current study design does not allow to assess the muscle-tendon contraction behavior, and test the mechanism described above. A possible explanation for the lack of effect in running economy between optimized and standard shoe condition could be the cost of more force production in the Triceps Surae muscle [31] due to the increased peak dorsiflexion moment [32]. Moreover, the ankle range of motion was increased during the optimal condition, causing an increased change in muscle-tendon unit length [33]. In addition, the higher force might have caused more stretch in the tendon unit at a given range of motion, increasing the shortening of the muscle fibers. Because of this, it could be that muscle fiber shortening velocities were less limited than expected and the hypothesized increase in mechanical efficiency did not occur.

Comparing the optimal condition with the control condition, i.e. a regular athletic shoe, we see that the running biomechanics show many similarities. Although the control shoe had a more proximal apex position, differences in anterior-posterior point of force application were not found. A possible explanation is that due to the lower bending stiffness of the control shoe, intrinsic foot muscles were able to manipulate this position [32] to the individual's optimum. This is in line with previous research [34] that demonstrated that running in minimalist shoes resulted in increased negative and positive ankle work and decreased knee work, showing the same redistribution of joint work.

Despite the biomechanical similarities between the optimal and control condition, there was a difference in running economy. A plausible explanation for this finding could be an increased lower limb moment of inertia [5] due to the extra mass of the experimental shoes. Previous studies [35, 36] found an increase in the oxygen cost of approximately 1% per 100 g of extra shoe mass per foot, where Rodrigo-Carranza et al. (2020) [37] found even a higher increment when running economy was expressed as energy cost instead of oxygen cost only. Given the fact that the mass of the experimental shoes was over 200 g higher per foot than the control shoe, explains the difference in running economy of 4% to a great extent.

2.4.1. Evaluation Human-in-the-loop optimization

The fact that the optimal apex position ranged from 75 to 84% and the optimal apex angles showed even more variance (range: 55 – 115°) emphasizes the importance of this individual approach. Our results demonstrate that human-in-the-loop optimization is able to find optimal parameter values that are beyond the range that is used in regular practice and would not have been found during grid search based on apex parameter values used in existing literature [38].

Another challenge this method is able to deal with, is the fact that humans exhibit individualized adaptation and learning processes [22]. This embedded tuning of motor control could contribute substantial to the final effect [39]. After every generation, the estimate of the optimal parameter values is updated, and the area of search around this estimate is further reduced or increased [27] to explore potentially better parameter settings. Because of this, the effect of motor learning during the optimization process maximally contributes to the measured positive ankle work when the optimal apex parameters are approached, which prevents potentially beneficial apex parameters with early, poorly adapted motor skills to be overlooked [22]. Moreover, the characteristic of human-in-the-loop optimization of variation in practice, followed by more focused training near the optimal solution, have been shown to result in faster adaptations compared to training without variation [39].

Nevertheless, the current results showed that parameter values during the final generations still show relatively high variance and convergence to the optimal setting did not always occur. We used a relatively large generation size of eight, to improve global search capability and robustness of the algorithm [27]. However, a consequence of this decision is reduced convergence speed [27]. It could be that this decision did not match with the chosen initial standard deviation and therefore this value did not decrease sufficiently towards the final generation. This could have caused that the optimized apex parameters may not have been reached after the maximum of four generations and could explain why only two participants had their optimal trial in the final generation.

2.4.2. Limitations and future research

One important note that has to be made is that some participants seemed to run with a high vertical displacement, which resulted in higher amplitudes in the vertical ground reaction force and higher peak moments than previous studies with low running speeds reported [17]. This higher vertical ground reaction force and ankle moments coincided with shorter stance time, longer flight time, and higher vertical pelvis displacement, but we could not find specific explanations for this behavior. The fact that only two participants had their optimal trial in the final generation of the optimization period supports the idea that participants were sufficiently adapted to the shoes and contradicts the idea that this might be an effect of adaptation. Moreover, this atypical running pattern was also seen in the condition with the control shoe and thus not a negative side effect of the experimental shoes. A possible explanation for this result might be the fact that participants wore a portable spirometer on their back during data collection and this load carriage induced the atypical running pattern [40].

Although the generalizability should be considered with caution, the study showed that human-in-the-loop optimization is able to optimize the selected objective, i.e. maximize positive ankle work, and we believe that this method has the potential to individually boost the effectiveness of footwear and assistive devices. However, it did not result in the anticipated increase in running economy. The relation between ankle work and gait economy should be further explored. Moreover, it could be questioned whether ankle work is the most effective cost function for optimizing running shoes [17].

By means of the human-in-the-loop optimization method, the adjustable parameters can be tuned to biomechanical properties of the individual [23] while taking into account the natural behavior of humans to simultaneously optimize coordination patterns with respect to locomotor performance [24]. However, the current design does not reach the methods' full potential. Therefore, future research should investigate whether the current genetic optimization algorithm could be improved or test other potential optimization algorithms to improve the convergence rate of the optimization process, and/or the magnitude of the final effect. Furthermore, it should be investigated how optimization via different cost functions (e.g. physiological, biomechanical, balance) influences human movement in different settings. If we could get a grip on these questions, we will be better able to individually adjust footwear or other assistive devices to the desires of the user.

2.5. Conclusion

The present study shows that human-in-the-loop optimization is able to enhance positive ankle work during running by individually optimizing apex position and apex angle. Although we found an increase in ankle work and redistribution of joint work from the hip and knee to the ankle, the expected improvement in running economy was not found. It needs to be further investigated which factors confound the theoretical benefits of enhanced ankle work on running economy. Furthermore, human-in-the-loop algorithms and cost functions could be further improved to better converge to optimal individual solutions.

2.6. Acknowledgments

We thank Sanne Huisken and Daan Vermeulen for help with data collection.

2.7. Reference list

[1] M. J. Joyner, J. R. Ruiz, and A. Lucia, "The two-hour marathon: who and when?," Journal of applied physiology (Bethesda, Md.: 1985), vol. 110, no. 1, pp. 275-277, Jan, 2011.

[2] A. V. Hill, "The Physiological Basis of Athletic Records," Nature, vol. 116, no. 2919, pp. 544-548, 1925.

[3] M. Weiss, A. Newman, C. Whitmore, and S. Weiss, "One hundred and fifty years of sprint and distance running - Past trends and future prospects," European journal of sport science, vol. 16, no. 4, pp. 393-401, 2016.

[4] W. Hoogkamer, S. Kipp, J. H. Frank, E. M. Farina, G. Luo, and R. Kram, "A Comparison of the Energetic Cost of Running in Marathon Racing Shoes," Sports medicine (Auckland, N.Z.), vol. 48, no. 4, pp. 1009-1019, Apr, 2018.

[5] I. S. Moore, "Is There an Economical Running Technique? A Review of Modifiable Biomechanical Factors Affecting Running Economy," Sports medicine (Auckland, N.Z.), vol. 46, no. 6, pp. 793-807, Jun, 2016.

[6] G. A. Cavagna, and M. Kaneko, "Mechanical work and efficiency in level walking and running," The Journal of physiology, vol. 268, no. 2, pp. 467-81, Jun, 1977.

[7] A. V. Hill, "The heat of shortening and the dynamic constants of muscle," Proceedings of the Royal Society of London.Series B-Biological Sciences, vol. 126, no. 843, pp. 136-195, 1938.

[8] W. O. Fenn, and B. S. Marsh, "Muscular force at different speeds of shortening," The Journal of physiology, vol. 85, no. 3, pp. 277-297, Nov 22, 1935.

[9] P. R. Cavanagh, M. L. Pollock, and J. Landa, "A biomechanical comparison of elite and good distance runners," Annals of the New York Academy of Sciences, vol. 301, no. 1, pp. 328-345, 1977.

[10] M. Ishikawa, J. Pakaslahti, and P. V. Komi, "Medial gastrocnemius muscle behavior during human running and walking," Gait & posture, vol. 25, no. 3, pp. 380-384, Mar, 2007.

[11] T. J. Roberts, "The integrated function of muscles and tendons during

locomotion," Comparative biochemistry and physiology.Part A, Molecular & integrative physiology, vol. 133, no. 4, pp. 1087-1099, Dec, 2002.

[12] R. F. Ker, R. M. Alexander, and M. B. Bennett, "Why are mammalian tendons so thick?," Journal of zoology, vol. 216, no. 2, pp. 309-324, 10, 2021.

[13] M. Sanno, S. Willwacher, G. Epro, and G. P. Brüggemann, "Positive Work Contribution Shifts from Distal to Proximal Joints during a Prolonged Run," Medicine and science in sports and exercise, vol. 50, no. 12, pp. 2507-2517, Dec, 2018.

[14] A. Arampatzis, G. De Monte, K. Karamanidis, G. Morey-Klapsing, S. Stafilidis, and G. P. Brüggemann, "Influence of the muscle-tendon unit's mechanical and morphological properties on running economy," The Journal of experimental biology, vol. 209, pp. 3345-3357, Sep, 2006.

[15] D. R. Carrier, N. C. Heglund, and K. D. Earls, "Variable gearing during locomotion in the human musculoskeletal system," Science (New York, N.Y.), vol. 265, no. 5172, pp. 651-653, Jul 29, 1994.

[16] S. F. Ray, and K. Z. Takahashi, "Gearing Up the Human Ankle-Foot System to Reduce Energy Cost of Fast Walking," Scientific reports, vol. 10, no. 1, pp. 8793-5, May 29, 2020.

[17] S. Sobhani, J. Hijmans, E. van den Heuvel, J. Zwerver, R. Dekker, and K. Postema, "Biomechanics of slow running and walking with a rocker shoe," Gait & posture, vol. 38, no. 4, pp. 998-1004, Sep, 2013.

[18] F. Bojsen-Møller, "The human foot - a two speed construction," American Journal of Anatomy, vol. 147, pp. 71-79, 1978.

[19] J. P. Roy, and D. J. Stefanyshyn, "Shoe midsole longitudinal bending stiffness and running economy, joint energy, and EMG," Medicine and science in sports and exercise, vol. 38, no. 3, pp. 562-569, Mar, 2006.

[20] S. Logan, I. Hunter, J. T. J Ty Hopkins, J. B. Feland, and A. C. Parcell, "Ground reaction force differences between running shoes, racing flats, and distance spikes in runners," Journal of sports science & medicine, vol. 9, no. 1, pp. 147-153, Mar 1, 2010.

[21] K. Hollander, D. Liebl, S. Meining, K. Mattes, S. Willwacher, and A. Zech, "Adaptation of Running Biomechanics to Repeated Barefoot Running: A Randomized Controlled Study," The American Journal of Sports Medicine, vol. 47, no. 8, pp. 1975-1983, Jul, 2019.

[22] J. Zhang, P. Fiers, K. A. Witte, R. W. Jackson, K. L. Poggensee, C. G.

2

Atkeson, and S. H. Collins, “Human-in-the-loop optimization of exoskeleton assistance during walking,” Science (New York, N.Y.), vol. 356, no. 6344, pp. 1280-1284, Jun 23, 2017.

[23] F. Scotto di Luzio, D. Simonetti, F. Cordella, S. Miccinilli, S. Sterzi, F. Draicchio, and L. Zollo, “Bio-Cooperative Approach for the Human-in-the-Loop Control of an End-Effector Rehabilitation Robot,” Frontiers in neurorobotics, vol. 12, pp. 67, Oct 11, 2018.

[24] R. M. Alexander, “Optimization and gaits in the locomotion of vertebrates,” Physiological Reviews, vol. 69, no. 4, pp. 1199-1227, 1989.

[25] R. Reints, “On the design and evaluation of adjustable footwear for the prevention of diabetic foot ulcers,” University of Groningen, 2020.

[26] A. J. van den Bogert, T. Geijtenbeek, O. Even-Zohar, F. Steenbrink, and E. C. Hardin, “A real-time system for biomechanical analysis of human movement and muscle function,” Medical & biological engineering & computing, vol. 51, no. 10, pp. 1069-1077, Oct, 2013.

[27] N. Hansen, “The CMA evolution strategy: a comparing review,” Towards a new evolutionary computation, pp. 75-102, 2006.

[28] L. Garby, and A. Astrup, “The relationship between the respiratory quotient and the energy equivalent of oxygen during simultaneous glucose and lipid oxidation and lipogenesis,” Acta Physiologica Scandinavica, vol. 129, no. 3, pp. 443-444, Mar, 1987.

[29] T. C. Pataky, “Generalized n-dimensional biomechanical field analysis using statistical parametric mapping,” Journal of Biomechanics, vol. 43, no. 10, pp. 1976-1982, 2010.

[30] H. Houdijk, M. F. Bobbert, J. J. De Koning, and G. De Groot, “The effects of klapskate hinge position on push-off performance: a simulation study,” Medicine and science in sports and exercise, vol. 35, no. 12, pp. 2077-2084, Dec, 2003.

[31] T. M. Griffin, T. J. Roberts, and R. Kram, “Metabolic cost of generating muscular force in human walking: insights from load-carrying and speed experiments,” Journal of applied physiology (Bethesda, Md.: 1985), vol. 95, no. 1, pp. 172-183, Jul, 2003.

[32] E. E. Miller, K. K. Whitcome, D. E. Lieberman, H. L. Norton, and R. E. Dyer, “The effect of minimal shoes on arch structure and intrinsic foot muscle strength,” Journal of Sport and Health Science, vol. 3, no. 2, pp. 74-85, 2014.

[33] S. Bohm, F. Mersmann, A. Santuz, and A. Arampatzis, "The force-length-velocity potential of the human soleus muscle is related to the energetic cost of running," Proceedings.Biological sciences, vol. 286, no. 1917, pp. 20192560, Dec 18, 2019.

[34] J. T. Fuller, J. D. Buckley, M. D. Tsiros, N. A. Brown, and D. Thewlis, "Redistribution of Mechanical Work at the Knee and Ankle Joints During Fast Running in Minimalist Shoes," Journal of athletic training, vol. 51, no. 10, pp. 806-812, Oct, 2016.

[35] W. Hoogkamer, S. Kipp, B. A. Spiering, and R. Kram, "Altered Running Economy Directly Translates to Altered Distance-Running Performance," Medicine and science in sports and exercise, vol. 48, no. 11, pp. 2175-2180, Nov, 2016.

[36] J. R. Franz, C. M. Wierzbinski, and R. Kram, "Metabolic cost of running barefoot versus shod: is lighter better?," Medicine and science in sports and exercise, vol. 44, no. 8, pp. 1519-1525, Aug, 2012.

[37] V. Rodrigo-Carranza, F. González-Mohíno, J. Santos-Concejero, and J. M. González-Ravé, "Influence of Shoe Mass on Performance and Running Economy in Trained Runners," Frontiers in physiology, vol. 11, pp. 573660, Sep 23, 2020.

[38] J. D. Chapman, S. Preece, B. Braunstein, A. Höhne, C. J. Nester, P. Brueggemann, and S. Hutchins, "Effect of rocker shoe design features on forefoot plantar pressures in people with and without diabetes," Clinical biomechanics (Bristol, Avon), vol. 28, no. 6, pp. 679-685, Jul, 2013.

[39] K. L. Poggensee, and S. H. Collins, "How adaptation, training, and customization contribute to benefits from exoskeleton assistance," Science Robotics, vol. 6, no. 58, 2021.

[40] H.-H. Wang, W.-C. Tsai, C.-Y. Chang, M.-H. Hung, J.-H. Tu, T. Wu, and C.-H. Chen, "Effect of Load Carriage Lifestyle on Kinematics and Kinetics of Gait," Applied bionics and biomechanics, vol. 2023, pp. 8022635, Feb 8, 2023.

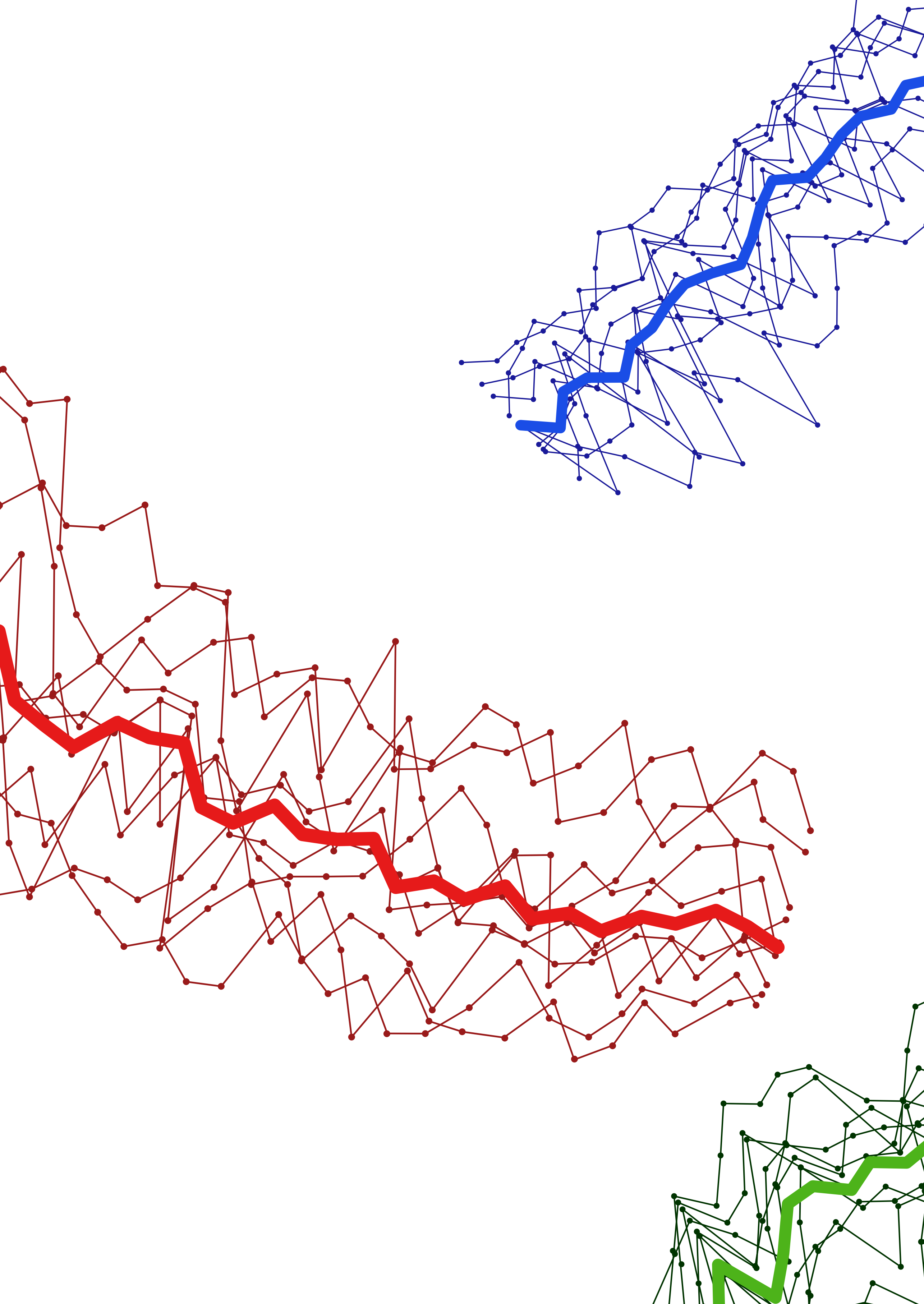

Chapter 3

Human-in-the-loop optimization of rocker shoes via different cost functions during walking

Thijs Tankink
Juha M. Hijmans
Raffaella Carloni
Han Houdijk

Journal of Biomechanics (2024), 166, 112028.

Abstract

Personalized footwear could be used to enhance the function of the foot-ankle complex to a person's maximum. Human-in-the-loop optimization could be used as an effective and efficient way to find a personalized optimal rocker profile (i.e., apex position and angle). The outcome of this process likely depends on the selected optimization objective and its responsiveness to the rocker parameters being tuned. This study aims to explore whether and how human-in-the-loop optimization via different cost functions (i.e., metabolic cost, collision work as measure for external mechanical work, and step distance variability as measure for gait stability) affects the optimal apex position and angle of a rocker profile differently for individuals during walking. Ten healthy individuals walked on a treadmill with experimental rocker shoes in which apex position and angle were optimized using human-in-the-loop optimization using different cost functions. We compared the obtained optimal apex parameters for the different cost functions and how these affected the selected gait related objectives. Optimal apex parameters differed substantially between participants and optimal apex positions differed between cost functions. The responsiveness to changes in apex parameters differed between cost functions. Collision work was the only cost function that resulted in a significant improvement of its performance criteria. Improvements in metabolic cost or step distance variability were not found after optimization. This study showed that cost function selection is important when human-in-the-loop optimization is used to design personalized footwear to allow conversion to an optimum that suits the individual.

Keywords

Cost function, rocker shoes, ankle, gait biomechanics, metabolic rate

3.1. Introduction

Bipedal walking is one of the most important skills of the human species [1]. The foot-ankle system of humans is unique and facilitates our bipedal gait. The foot and the ankle form a dynamic link between the body and the ground [2] , hereby constantly adjusting their alignment and function to achieve the desirable movement [3]. As such, the foot arch and the muscles around the ankle reduce energy losses [4, 5], support the body, enhance stability [6], and generate forward propulsion of the center of mass during the push-off phase of walking [5, 7].

Personalized footwear could be used to enhance the function of the ankle complex to a person's maximum and, therefore, affect different gait related objectives, e.g., metabolic cost, mechanical load, or gait stability. One way to enhance the function of the ankle complex is to personalize the rocker profile of a shoe, i.e., the curvature of the heel and forefoot of the shoe. Changing the rocker profile of a shoe can modify the gear ratio of muscles around the ankle [8]. This could result in more efficient production of mechanical work by the calf muscles as they could operate at lower muscle fiber contraction velocities and closer to their optimal length [9]. Consequently, this could enhance push-off power and reduce metabolic cost. Moreover, the rocker profile could affect the base of support and the roll-off direction of an individual and, therefore, influence gait stability [10].

To develop personalized rocker profiles, the different tuneable parameters (i.e., apex position and apex angle) and their interactions need to be explored simultaneously. To increase the complexity of finding optimal settings, physiological and neuromechanical differences between individuals can cause different responses to the same intervention [11], and responses could change due to voluntary, yet unpredictable, gait adaptations of the user in response to changes in these parameters [12, 13].

A potential method to overcome these challenges is human-in-the-loop optimization [14], in which the human is included 'in vivo' in the control loop and rocker parameters are systematically varied during the optimization process using an intelligent optimization algorithm in response to measured human performance. By means of human-in-the-loop optimization, the rocker parameters can be tuned to the morphologies (i.e., biological properties) of the individual [15] while taking into account the natural behavior of humans, who simultaneously optimize their coordination patterns with respect to locomotor performance [12].

In the optimization of rocker parameters, different performance criteria could be considered as cost functions, as for instance mechanical load, metabolic cost and gait stability that are mentioned above. It is however yet unknown, whether these different cost functions would result in similar optimal rocker parameters or not. There is some evidence that these performance criteria are interrelated [16, 17], but also opposing evidence exists [18, 19]. Moreover, it is unknown which of these cost functions is most responsive to change in the human-in-the-loop approach. Therefore, the aim of this study is to explore whether human-in-the-loop optimization via different cost functions (i.e., metabolic cost, external mechanical work, and gait stability) results in different optimal apex position and apex angle of a rocker profile during walking, and how these potentially different rocker profiles affect the selected performance criteria.

3.2. Method

3.2.1. Participants

10 (4 male, 6 female) healthy individuals (age: 20.3 ± 1.2 y, height: 179.1 ± 5.6 cm, weight: 73.8 ± 10.0 kg, shoe size range: 38 – 44 EU) participated in this study. All participants were free of injury and pain at time of the measurements and signed informed consent. The study protocol was approved by the central ethics committee of the central ethics committee of the University Medical Center Groningen (11440), the Netherlands.

3.2.2. Shoe conditions

In this study, we used regular walking shoes (Chris, Dr Comfort, Mequon, WI, USA) as a control shoe (apex position: 64% total shoe length, apex angle: 88.0°; determined by marking the medial and lateral side of the control shoe where the sole lifts from the ground. We used software Kinovea (version 0.9.5) to draw a line through these points and determine apex parameters) and experimental shoes (Figure 3.1A) with an adjustable apex position and apex angle [20], made from the same shoe model. The outer sole of the experimental shoe was removed and 3 carbon fiber layers, which contained 2 rails with sliders, were placed below the shoe making manipulation of the apex position and apex angle possible (Figure 3.1). The carbon plates resulted in a higher stiffness (83.6 N/rad; determined by a 3-point bending test [21]) and mass (range: 407 – 560 g/shoe) compared to the control shoe (stiffness: 1.9 N/rad; mass range: 197 – 261 g/shoe). 2 3D-printed cylinders (diameter = 30 mm, height

Figure 3.1: A) Experimental shoes with adjustable apex position and apex angle. The position of the cylinders (bottom) could be changed across the rails, by manually screwing the bolts. B) Displayed how changing the cylinders results in a new (dashed) apex position (red) and apex angle (blue asterisk).

= 13 mm) with tapered rims were screwed onto the sliders with a bolt. The position of the cylinders could be changed across the rails (40 – 90% total shoe length), by manually screwing the bolts. A Polyethylene layer of 3 mm (Streifylast, Streifeneder, Emmering, Germany) was placed between the original outer sole and the cylinders to prevent the cylinders from damaging the outer sole.

3.2.3. Experimental set-up

Measurements were performed using the GRAIL (Gait Realtime Analysis Interactive Lab; Motekforce Link, Amsterdam, the Netherlands) at the department of Human Movement Sciences of the University Medical Center Groningen, the Netherlands. The GRAIL consists of a dual-belt treadmill with force sensors beneath each separate belt (Motekforce Link, Amsterdam, the Netherlands; Fs = 1000 Hz) and a 10-camera (Vero) motion capture system (Vicon Nexus 2.8.1, Oxford, UK; Fs = 100 Hz) that registered the marker trajectories of 22 reflective markers (diameter = 14 mm) placed according to the lower-limb Human Body Model 2 [22]. We used the D-flow (3.34.3, Motekforce Link, the Netherlands, Amsterdam) online environment and MATLAB (R2022b, MathWorks, Natick, MA, USA) for real-time analysis during the optimization period. Respiratory data was collected by the portable metabolic analyzer K5 (COSMED, Rome, Italy) in breath-by-breath mode. Measurement systems were calibrated according to the recommended calibration protocols of the manufacturers.

3.2.4. Protocol

Participants visited the gross motor control lab within the department of Human Movement Sciences of the University Medical Center Groningen, the Netherlands, twice (Figure 3.2A). Participants walked on the treadmill during the whole experiment. The protocol consisted of determining the participant's preferred walking speed, 3 optimization periods and 1 evaluation phase.

During the first visit, participants started with a familiarization period of 5 min while wearing the experimental shoes with standard apex settings (apex position: 64% total shoe length, apex angle: 88.0°, similar to the control shoe). During this period, they chose a self-selected walking speed (1.29 ± 0.07 m/s), which was maintained during the rest of the protocol. The rest of the first visit consisted of 2 optimization periods using 2 different cost functions. The second visit consisted of a warm-up, a third optimization period with the remaining cost function, and the evaluation phase. The order of cost functions during the optimization periods was randomized.

Self-selected walking speed was determined by manually increasing the treadmill speed with 0.1 m/s until the participant indicated that comfortable walking speed was reached. Afterwards, the belt speed was further increased to a high walking speed and manually decreased with 0.1 m/s until the participant once again indicated that comfortable walking speed was reached. If there was a difference in the 2 selected speeds, the process was repeated.

During an optimization period (Figure 3.2B), we aimed to optimize the parameters (apex position and apex angle) of the experimental shoes with respect to the optimization parameter of the used cost function (minimizing metabolic cost, minimizing negative collision work, or minimizing step distance variability; Figure 3.3). During one optimization period, participants walked 30 (5 x 6) times 120 s on the experimental shoes with intervening rest periods of 90 s. The apex position and apex angle of every trial were determined by the optimization algorithm as described below. These parameters/settings were manually adjusted by screwing the bolts and changing the cylinder positions of both left and right shoe (symmetrically) during the rest periods between the walking trials.

During the evaluation phase (Figure 3.2C), participants walked 5 times 6 min in different shoe conditions. 4 times wearing the experimental shoes with optimal parameter settings for (1) minimizing metabolic cost, (2) minimizing negative collision work, (3) minimizing step distance variability, (4) standard parameter settings, and 1 time wearing the control shoes. We measured oxygen consumption and carbon dioxide production to compare the metabolic cost of walking. Ground reaction forces and marker trajectories were measured for biomechanical analysis. In between trials, participants took a 5-min break. The order of conditions was randomized.

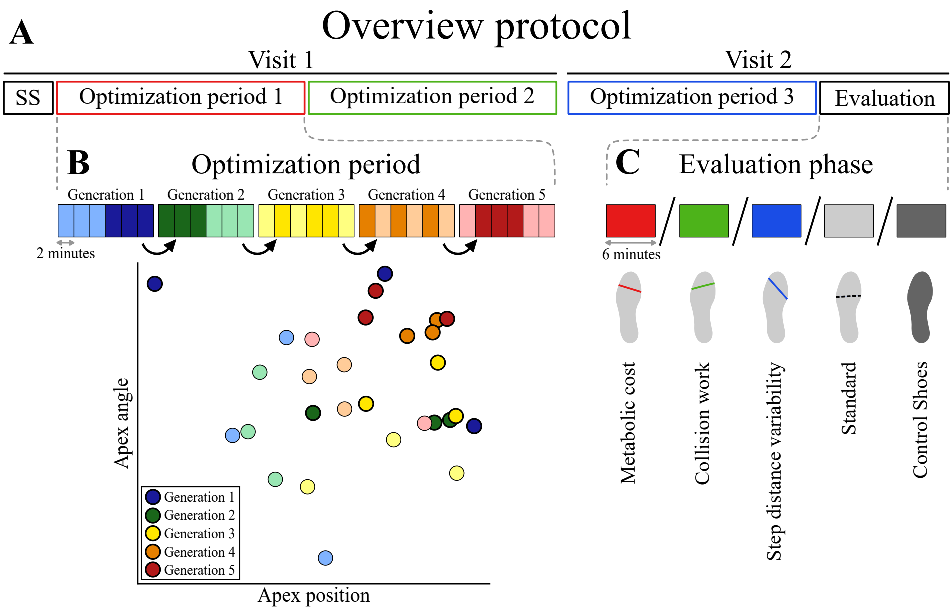

Figure 3.2: A) Structure of the protocol: determination of self-selected speed (SS), 3 optimization periods with different cost functions, and one evaluation phase for all shoe conditions. The protocol is divided over 2 lab visits. B) Optimization period: 30 walking trials of 2 min while walking on the experimental shoes with different apex positions and apex angles. After every generation (6 trials), the 3 trials that resulted in the best outcome of the performance criteria (darker colors) were used to determine the apex settings of the next generation. C) The evaluation phase: 5 walking trials of 6 min. The shoe conditions were experimental shoes (light grey) with apex parameters optimized for the 3 different cost functions, experimental shoes with standard apex parameters, and control shoes (dark grey).

3.2.5. Optimization algorithm

We used a covariance matrix adaptation evolution strategy (CMA-ES) [23] to optimize apex position and apex angle (Figure 3.2B). The calculated values of the optimization parameter during the different walking trials were used as input for the optimization algorithm. The algorithm used a predetermined number of measurements, forming 1 generation, to calculate the parameter values of the next generation. We chose to explore 5 generations with a generation size of 6 [23]. The parameter values of the first generation were pseudo-randomly selected from evenly spaced intervals of the whole parameter search space, to avoid biased sampling that could lead to premature convergence [24]. With every new generation, the mean represents the best estimate of the optimal parameter values, and the area of search around this mean was adapted to end up with the optimal apex position and angle. Eventually, all 30 trials were compared and the apex position and apex angle that resulted in the best (minimum/maximum) value of the optimization parameter were chosen as the optimal parameters for the cost function used.

3.2.6. Data analysis

3.2.6.1. Metabolic cost

The metabolic cost of walking during the trials of the optimization period was estimated by fitting a first-order dynamical model with a time constant of 42 s [13] to 2 min of breath-by-breath metabolic measurements [14] (Figure 3.3A). We fitted an exponential curve to the measured O_2 sconsumption and CO_2 production and used the asymptotes of these fits as estimates for their steady state values. Metabolic cost was calculated using the equation of Garby and Astrup [25]:

$$metabolic \;\; power = 16.04 \cdot \dot{V}O_2 + 4.94 \cdot \dot{V}CO_2 \tag{3.1}$$

where the $metabolic \;\; power$ is in W and $\dot{V}O_2$ and $\dot{V}CO_2$ are in mL/s. Subsequently, we normalized $metabolic \;\; power$ for body mass (W/kg).

The estimated steady state value of the metabolic power was used as input for the optimization algorithm, with a lower value indicating a better outcome.

3.2.6.2. Collision work

The negative collision work performed by the leading leg was determined by using the individual limbs method to calculate the mechanical center of mass (CoM) work described by Donelan et al. (2002) [26] (Figure 3.3B). First, the velocity of the CoM was calculated by integrating its acceleration, which was determined by summing the ground reaction forces under each limb:

$$\overrightarrow{v}_{CoM} = \int \frac{\overrightarrow{F}_{trail} + \overrightarrow{F}_{lead} + m \cdot \overrightarrow{g}}{m} \mathrm{dt} + \begin{bmatrix} c_x \\ c_y \\ c_z \end{bmatrix} \tag{3.2}$$

where $\overrightarrow{v}_{CoM}$ (m/s) is the velocity vector of the CoM, $\overrightarrow{F}_{trail}$ (N) is the ground reaction force exerted by the trailing leg, $\overrightarrow{F}_{trail}$ (N) is the ground reaction force vector of the leading leg, m (kg) is the participants' body mass, and $\overrightarrow{g}$ ([0, -9.81, 0] m/s^2) is the gravitational acceleration. The vertical integration constant (c_y) was found by assuming that the average vertical CoM velocity over a step was 0. The anterior-posterior integration constant (c_z) was obtained by assuming that the average velocity over a step was equal to the belt speed. The medio-lateral integration constant ($\mathrm{c_x}$) was found by assuming that the CoM velocity at the beginning and end of a step was equal in magnitude but opposite in sign [26]. Consequently, the mechanical power on the CoM generated by the trailing and leading leg was calculated by multiplying the force exerted by each individual limb with the CoM velocity:

$$P_{trial} = \overrightarrow{F}_{trail} \cdot \overrightarrow{v}_{CoM} \tag{3.3}$$

$$P_{lead} = \overrightarrow{F}_{lead} \cdot \overrightarrow{v}_{CoM} \tag{3.4}$$

where P is in Watts. Subsequently, we normalized the mechanical power for body mass (W/kg). Finally, collision work was calculated by integrating P_{lead} over time, for the negative interval directly after initial contact.

During the optimization trials, the mean collision work of all successive steps in a 1-min time interval, starting after 45 s of the beginning of the trial, was calculated and used as input for the optimization algorithm, with a less negative value indicating a better outcome.

3.2.6.3. Step distance variability

Step distance was calculated by the following formula:

$$step\ \ distance = \sqrt{(step\ \ length)^2 + (step\ \ width)^2} \tag{3.5}$$

Where $step\ \ distance$, $step\ \ length$, and $step\ \ width$ are in mm. Step distance variability was determined by calculating the standard deviation in step distance (Figure 3.3C).

During the optimization trials, the step distance variability of all successive steps of both legs in a 1-min time interval, starting after 45 s of the beginning of the trial, was calculated and used as input for the optimization algorithm, with a lower value indicating a better outcome [27, 28].

During the trials in the evaluation phase, we determined the steady state $\dot{V}O_2$ and $\dot{V}CO_2$ based on their mean values over the last 2 min of each trial to calculate metabolic cost. For collision work, step distance variability and other spatiotemporal gait parameters, we used the last 2 min of biomechanical data.

3.2.7. Statistical analysis

We performed repeated measures analyses of variance (ANOVA), in SPSS (version 28.0.1.1, IBM Corp. Armonk, NY, USA), with cost function (metabolic cost, collision work, step distance variability) as within-subject factor for 2 dependent variables: apex position and apex angle.

To investigate the effect of the optimized apex settings for the different cost functions during the evaluation phase, we used repeated measures ANOVA with shoe condition (metabolic cost, collision work, step distance variability and standard) as within-subject factor for several dependent spatiotemporal gait variables and the 3 optimization parameters of the different cost functions, i.e., metabolic cost, collision work, and step distance variability. Because of the different stiffness and mass, the condition with the control shoe was excluded from statistical analysis and only added for reverence.

For all tests, a p-value of 5% was used to indicate statistically significant differences. We used Bonferroni correction for post hoc t-tests to compare the different cost functions and shoe conditions. If the assumption of sphericity was violated, we used a Greenhouse-Geisser correction.

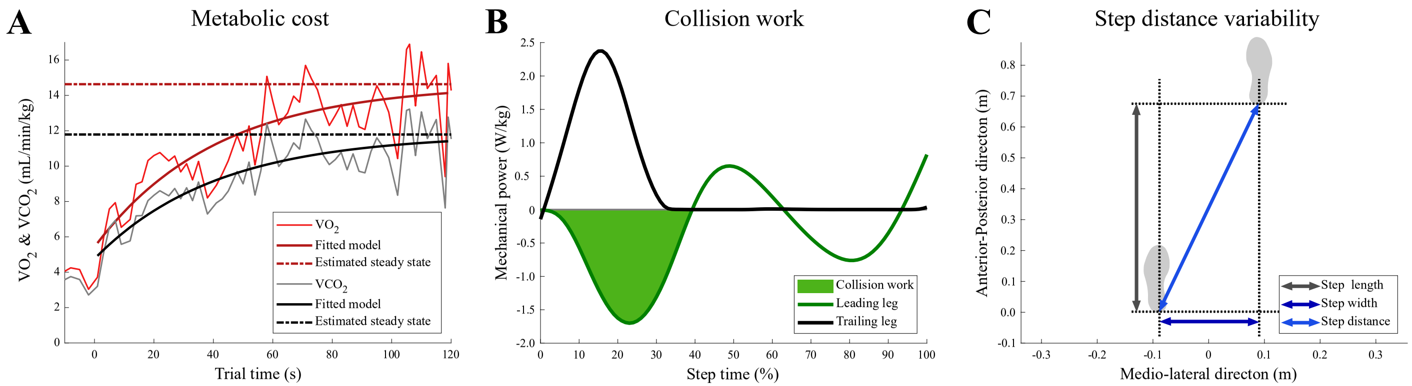

Figure 3.3: Optimization parameters for the different cost functions. A) Metabolic cost was determined by estimating the steady state $\dot{V}O_2$ and $\dot{V}CO_2$ through using the asymptote of a model fitted over 120 s of data. B) Collision work was determined by integrating the negative external mechanical power of the leading leg on the center of mass during heel strike. C) Step distance variability was determined by calculating the standard deviation of step distance, which is the vector that combines step length and step width, in the detected steps.

3

3.3. Results

Optimal apex positions for the different cost functions were located more distal compared to the standard apex position (64% shoe length) and were significantly different between cost functions ($F(2,18) = 3.64$, $p < 0.05$; Figure 3.4). Optimizing for collision work resulted in more distally placed apex positions (78.1 ± 3.4%) compared to step distance variability (74.2 ± 1.4%) and metabolic cost (70.1 ± 1.2%).

Optimized apex angles tended to be larger compared to the standard angle (88.0°) for all cost functions but were quite variable among participants (metabolic cost: 120.0 ± 4.7°, collision work: 94.0 ± 9.1°, and step distance variability: 106.6 ± 7.6°; Figure 3.4). Significant differences in apex angle between cost functions were not found ($F(2,18) = 2.42$, $p = 0.12$). Figure 3.5 shows the progression of designated cost function during the optimization periods.

During the evaluation phase, a significant effect of shoe condition was found for collision work (Table 3.1). Post hoc tests revealed that shoes optimized for collision work resulted in a significant reduction of collision work compared to the standard shoe (-11.3%) and shoes optimized for metabolic cost (-11.5%) and step distance variability (-10.9%). We found no effect of shoe condition for metabolic cost and step distance variability. No significant differences in spatiotemporal gait parameters were found between conditions (Table 3.1).

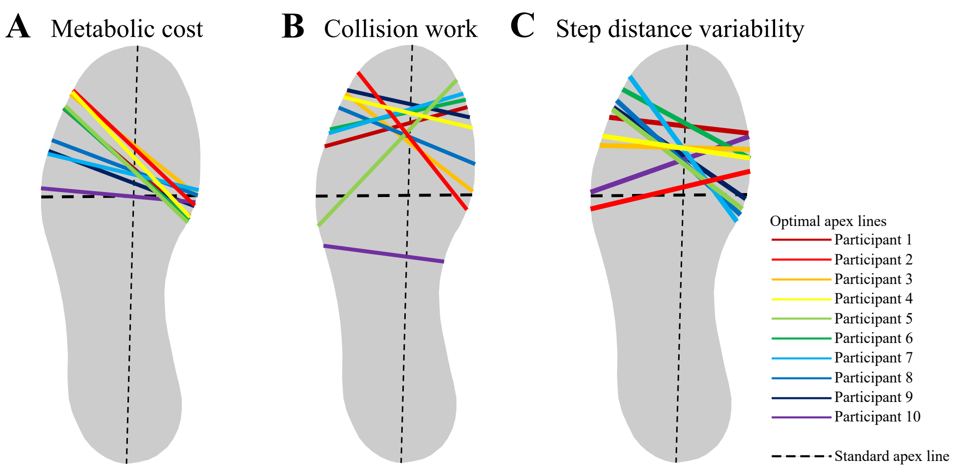

Figure 3.4: Optimized apex lines of each participant (n=10) for the different cost functions: A) metabolic cost, B) collision work, and C) step distance variability. The standard apex line (dashed black) is also given.

Table 3.1: Spatiotemporal gait parameters and cost functions (mean (SD)) for the different shoe condition during the evaluation phase (n=10). Results of the repeated measures analyses of variance of the shoe conditions with the experimental shoe (optimized for metabolic cost, collision work, step distance variability and standard condition) for the different variables are also given.

	Experimental shoes							
	Metabolic cost	Collision work	Step distance variability	Standard	Control shoes[a]	$F(3,27)$	p	ES[b]
Step frequency (Hz)	1.80 (0.06)	1.79 (0.06)	1.78 (0.07)	1.80 (0.06)	1.82 (0.06)	1.55[c]	0.24	0.14
Stride time (s)	1.11 (0.04)	1.12 (0.04)	1.12 (0.04)	1.11 (0.03)	1.10 (0.04)	1.74[c]	0.24	0.15
Stance time (s)	0.74 (0.03)	0.74 (0.03)	0.75 (0.03)	0.75 (0.03)	0.73 (0.03)	1.87	0.16	0.17
Step length (m)	0.72 (0.04)	0.72 (0.04)	0.73 (0.04)	0.72 (0.04)	0.71 (0.04)	1.66	0.22	0.16
Step width (m)	0.13 (0.04)	0.13 (0.03)	0.13 (0.03)	0.13 (0.04)	0.13 (0.04)	0.12	0.95	0.01
Metabolic cost (W/kg)	5.24 (0.58)	5.34 (0.83)	5.21 (0.50)	5.38 (0.64)	5.23 (0.74)	0.77	0.52	0.08
Collision work (J/kg)	-0.19 (0.03)^{CW}	-0.17 (0.03)^{MC,S,SDV}	-0.19 (0.03)^{CW}	-0.19 (0.03)^{CW}	-0.15 (0.03)	11.13[d]	**<0.001**	0.55
Step distance variability (mm)	17.4 (3.12)	18.7 (4.55)	18.1 (3.53)	17.3 (3.02)	17.0 (2.15)	1.61[c]	0.23	0.15

Notes: [a]The condition with the control shoes was excluded from the statistical comparison but only added for reference

[b]Effect Size = partial η^2

[c]Greenhouse-Geisser correction was used

[d]Bonferroni corrected post hoc tests (^{MC}vs. Metabolic Cost; ^{CW}vs. Collision Work; ^{SDV}vs. Step Distance Variability; ^{S}vs. Standard)

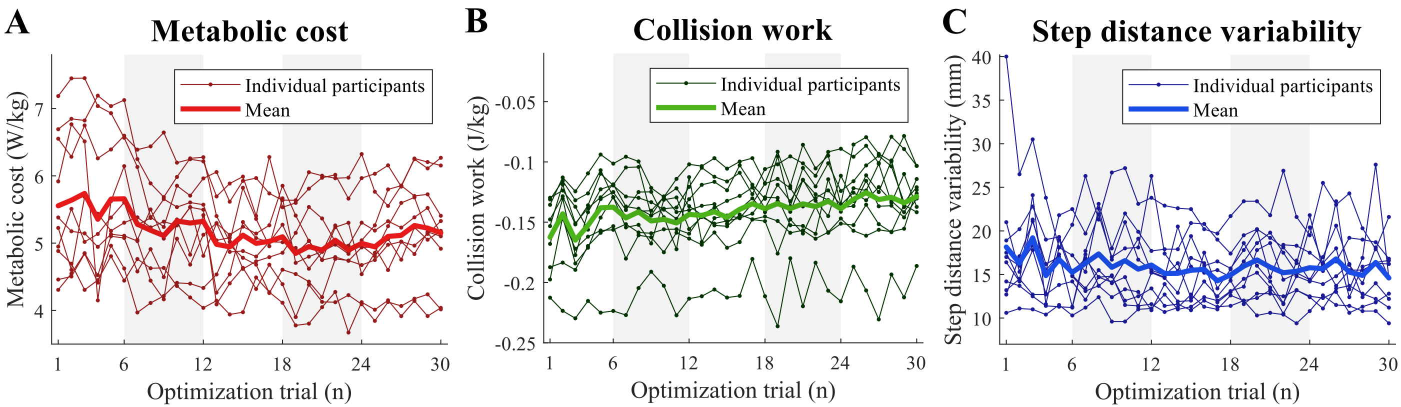

Figure 3.5: Progression of the optimization period for the different cost functions: A) metabolic cost, B) collision work, and C) step distance variability. Both the progression of the individual participants (thin dotted lines) and the mean over all participants (thick line) are given. The shaded areas in the background indicate the different generations during the optimization period.

3.4. Discussion

The aim of the current study was to explore whether human-in-the-loop optimization of rocker profiles (apex position and apex angle) via different cost functions (i.e., metabolic cost, external mechanical work, and gait stability) affected the optimal rocker profile differently during walking. Optimal apex positions (range: 49 – 89%) and angles (range: 42 – 142°) differed substantially between subjects, demonstrating the necessity for individualized tuning. The distal displacement of the apex position compared to the standard condition was the smallest for metabolic cost and largest for collision work during the optimization protocol, but optimal positions did differ between cost functions. The distal displacement of the apex position was the smallest for optimization to metabolic cost and largest for optimization to collision work. Moreover, the responsiveness to changes in apex parameters seemed to differ between cost functions. As indicated by the progression of the cost function during the optimization periods, metabolic cost and collision work were more responsive compared to step distance variability. However, collision work was the only cost function that resulted in a significant improvement of its performance criteria compared to shoes with a standard rocker profile or a rocker profile optimized for the other cost functions. Improvements in metabolic cost or step distance variability were not found after optimization.

The rocker profile optimized for collision work was the only shoe condition during the evaluation phase where the optimized shoe setting showed an improvement of its performance criteria (reduction in collision work in this case) compared to the other experimental shoe conditions. The more distally placed apex position in the shoe optimized for collision work could increase the gear ratio around the ankle [8] and evoke a higher ankle push-off power [29]. As explained by the inverted pendulum model of walking [17, 30], increased push-off work requires less collision work to redirect the center of mass velocity and could therefore explain the decreased collision work for this rocker profile compared to the shoe conditions with a more proximally placed apex position.

We observed a reduction in metabolic cost during the optimization period (Figure 3.5A). This indicates that metabolic cost of walking is affected by the apex parameters and that these features could be used to optimize the rocker profile to increase walking economy. However, the relatively small difference in optimal apex parameters for metabolic cost, which were very similar for all participants, and standard apex parameters seems to indicate that there was only limited room for improvement in healthy individuals. Although the effect of this gain, a 2.6% reduction in metabolic cost during the evaluation phase, might be relevant in practice, metabolic cost as optimization criteria is less appropriate for human-in-the-loop optimization in the current study and this cost function might be better suited for cases with wider search spaces and more room for improvement [14], e.g., clinical populations.

The absence of reduction in step distance variability during the optimization period despite an extensive search space of the apex parameters, combined with the relatively large differences in optimal apex positions and angles between subjects, indicates that there is a broad range of apex parameters which result in similar step distance variability. Although it has been reported that apex angle could affect gait stability [10], our results show that step distance variability is not affected by apex position or angle when the parameter values are within this broad stable area. This indicates that step distance variability is not an adequate optimization objective to optimize apex parameters to improve gait stability in healthy participants.

We expected that the reduction in collision work might simultaneously reduce metabolic cost. Reduced collision work would require less positive work during mid stance to maintain the center of mass velocity, limiting total positive work [17, 30], and potentially reduce metabolic cost. However, the rocker profile optimized for collision work did not reduce metabolic cost during the evaluation phase. This suggests that minimizing collision work for the step-to-step transition, is not the only thriving mechanism for minimizing metabolic cost, which is further supported by the difference in optimal rocker profiles between collision work and metabolic cost. This aligns with previous research [18] and emphasizes the need for more detailed models to explain the relationship between mechanical work and metabolic cost.

3.4.1. Limitations

Human-in-the-loop optimization requires several initial decisions that could affect the outcome of the optimization process, e.g., used optimization algorithm or duration of optimization. In the current study, we selected the best result from all 30 iterations as the optimal apex parameters for that cost function. A potential drawback of this decision is the sensitivity for noise that outcome variables of human measurements entail [31], and optimal shoe settings might have been selected based on measurement error. This is further confirmed by the structural lower values for the cost functions during the optimal trial of the optimization period compared to the values during the evaluation trial with similar apex parameters. However, these values were highly correlated for the cost functions that showed convergence (metabolic cost: Pearson correlation coefficient = 0.84, $p < 0.01$, and collision work: Pearson correlation coefficient = 0.84, $p < 0.01$) and appear not be caused by suboptimal parameter selection due to measurement error. The differences in metabolic cost are more likely to be explained by an underestimation of the steady state values by the estimation model during the short optimization period. The higher values for collision work during the evaluation phase could be attributed to the portable spirometer that was not worn by the participants during the optimization period. Moreover, we verified that the current optimal shoe parameters were mainly in the area of search of the final generation and our outcomes were not negatively affected. Nevertheless, using the estimated optimal parameters of the final generation is recommended for future experiments, because this aligns better with the properties of the optimization algorithm to filter out this measurement noise [14, 23].

3.5. Conclusion

The substantial differences in optimal rocker profiles between participants emphasizes the importance of the individual approach that human-in-the-loop optimization entails. This study also showed that cost function selection is important when human-in-the-loop optimization is used to design personalized footwear or individually tune other assistive devices. Different cost functions generate different optimal solutions. Moreover, using a cost function that is not sensitive for the device parameters that are being tuned (step distance variability in this study), will not enable the optimization algorithm to converge to optimal settings for these parameters. So, to maximize the effectiveness of these personalized devices, it is important to select a cost function that results in an outcome that matches the intended optimization domain of the user and simultaneously is sufficiently sensitive and robust to allow conversion to an optimum that suits the individual.

3.6. Acknowledgments

We gratefully acknowledge Iris van den Anker, Denise Baten Burg, and Twan Ruijgt for their support during data collection.

3.7. Reference list

[1] E. B. Simonsen, "Contributions to the understanding of gait control," Danish medical journal, vol. 61, no. 4, Apr, 2014.

[2] M. Błażkiewicz, I. Wiszomirska, K. Kaczmarczyk, R. Naemi, and A. Wit, "Inter-individual similarities and variations in muscle forces acting on the ankle joint during gait," Gait & posture, vol. 58, pp. 166-170, Oct, 2017.

[3] M. M. Rodgers, "Dynamic biomechanics of the normal foot and ankle during walking and running," Physical Therapy, vol. 68, no. 12, pp. 1822-1830, Dec, 1988.

[4] J. M. Donelan, R. Kram, and A. D. Kuo, "Mechanical work for step-to-step transitions is a major determinant of the metabolic cost of human walking," The Journal of experimental biology, vol. 205, no. Pt 23, pp. 3717-3727, Dec, 2002.

[5] D. J. Farris, L. A. Kelly, A. G. Cresswell, and G. A. Lichtwark, "The functional importance of human foot muscles for bipedal locomotion," Proceedings of the National Academy of Sciences of the United States of America, vol. 116, no. 5, pp. 1645-1650, Jan 29, 2019.

[6] D. N. Karagiannakis, K. I. Iatridou, and D. G. Mandalidis, "Ankle muscles activation and postural stability with Star Excursion Balance Test in healthy individuals," Human movement science, vol. 69, pp. 102563, Feb, 2020.

[7] R. R. Neptune, S. A. Kautz, and F. E. Zajac, "Contributions of the individual ankle plantar flexors to support, forward progression and swing initiation during walking," Journal of Biomechanics, vol. 34, no. 11, pp. 1387-1398, Nov, 2001.

[8] S. F. Ray, and K. Z. Takahashi, "Gearing Up the Human Ankle-Foot System to Reduce Energy Cost of Fast Walking," Scientific reports, vol. 10, no. 1, pp. 8793-5, May 29, 2020.

[9] W. O. Fenn, and B. S. Marsh, "Muscular force at different speeds of shortening," The Journal of physiology, vol. 85, no. 3, pp. 277-297, Nov 22, 1935.

[10] Y. Watanabe, N. Kawabe, and K. Mito, "The apex angle of the rocker sole

affects the posture and gait stability of healthy individuals," Gait & posture, vol. 86, pp. 303-310, May, 2021.

[11] S. Logan, I. Hunter, J. T. J Ty Hopkins, J. B. Feland, and A. C. Parcell, "Ground reaction force differences between running shoes, racing flats, and distance spikes in runners," Journal of sports science & medicine, vol. 9, no. 1, pp. 147-153, Mar 1, 2010.

[12] R. M. Alexander, "Optimization and gaits in the locomotion of vertebrates," Physiological Reviews, vol. 69, no. 4, pp. 1199-1227, 1989.

[13] J. C. Selinger, and J. M. Donelan, "Estimating instantaneous energetic cost during non-steady-state gait," Journal of applied physiology (Bethesda, Md.: 1985), vol. 117, no. 11, pp. 1406-1415, Dec 1, 2014.

[14] J. Zhang, P. Fiers, K. A. Witte, R. W. Jackson, K. L. Poggensee, C. G. Atkeson, and S. H. Collins, "Human-in-the-loop optimization of exoskeleton assistance during walking," Science (New York, N.Y.), vol. 356, no. 6344, pp. 1280-1284, Jun 23, 2017.

[15] F. Scotto di Luzio, D. Simonetti, F. Cordella, S. Miccinilli, S. Sterzi, F. Draicchio, and L. Zollo, "Bio-Cooperative Approach for the Human-in-the-Loop Control of an End-Effector Rehabilitation Robot," Frontiers in neurorobotics, vol. 12, pp. 67, Oct 11, 2018.

[16] J. Jin, J. H. van Dieën, D. Kistemaker, A. Daffertshofer, and S. M. Bruijn, "Does ankle push-off correct for errors in anterior-posterior foot placement relative to center-of-mass states?," PeerJ, vol. 11, pp. e15375, May 29, 2023.

[17] A. D. Kuo, J. M. Donelan, and A. Ruina, "Energetic consequences of walking like an inverted pendulum: step-to-step transitions," Exercise and sport sciences reviews, vol. 33, no. 2, pp. 88-97, Apr, 2005.

[18] J. M. Caputo, and S. H. Collins, "Prosthetic ankle push-off work reduces metabolic rate but not collision work in non-amputee walking," Scientific reports, vol. 4, no. 1, pp. 7213, 2014.

[19] T. Tankink, H. Houdijk, and J. M. Hijmans, "Human-in-the-Loop Optimized Rocker Profile of Running Shoes to Enhance Ankle Work and Running Economy," European Journal of Sport Science, vol. 24, no. 1, pp. 164-173, 2023.

[20] R. Reints, "On the design and evaluation of adjustable footwear for the prevention of diabetic foot ulcers," University of Groningen, 2020.

[21] K. Oh, and S. Park, "The bending stiffness of shoes is beneficial to running

energetics if it does not disturb the natural MTP joint flexion," Journal of Biomechanics, vol. 53, pp. 127-135, Feb 28, 2017.

[22] A. J. van den Bogert, T. Geijtenbeek, O. Even-Zohar, F. Steenbrink, and E. C. Hardin, "A real-time system for biomechanical analysis of human movement and muscle function," Medical & biological engineering & computing, vol. 51, no. 10, pp. 1069-1077, Oct, 2013.

[23] N. Hansen, "The CMA evolution strategy: a comparing review," Towards a new evolutionary computation, pp. 75-102, 2006.

[24] Y. Ding, M. Kim, S. Kuindersma, and C. J. Walsh, "Human-in-the-loop optimization of hip assistance with a soft exosuit during walking," Science robotics, vol. 3, no. 15, pp. eaar5438., Feb 28, 2018.

[25] L. Garby, and A. Astrup, "The relationship between the respiratory quotient and the energy equivalent of oxygen during simultaneous glucose and lipid oxidation and lipogenesis," Acta Physiologica Scandinavica, vol. 129, no. 3, pp. 443-444, Mar, 1987.

[26] J. M. Donelan, R. Kram, and A. D. Kuo, "Simultaneous positive and negative external mechanical work in human walking," Journal of Biomechanics, vol. 35, no. 1, pp. 117-124, Jan, 2002.

[27] S. M. Bruijn, and J. H. van Dieën, "Control of human gait stability through foot placement," Journal of the Royal Society, Interface, vol. 15, no. 143, pp. 20170816, Jun, 2018.

[28] V. L. Chiu, A. S. Voloshina, and S. H. Collins, "The effects of ground-irregularity-cancelling prosthesis control on balance over uneven surfaces," Royal Society open science, vol. 8, no. 1, pp. 201235, Jan 20, 2021.

[29] S. Sobhani, J. Hijmans, E. van den Heuvel, J. Zwerver, R. Dekker, and K. Postema, "Biomechanics of slow running and walking with a rocker shoe," Gait & posture, vol. 38, no. 4, pp. 998-1004, Sep, 2013.

[30] T. W. Huang, K. A. Shorter, P. G. Adamczyk, and A. D. Kuo, "Mechanical and energetic consequences of reduced ankle plantar-flexion in human walking," The Journal of experimental biology, vol. 218, no. Pt 22, pp. 3541-3550, Nov, 2015.

[31] R. J. van Beers, P. Baraduc, and D. M. Wolpert, "Role of uncertainty in sensorimotor control," Philosophical Transactions of the Royal Society of London.Series B: Biological Sciences, vol. 357, no. 1424, pp. 1137-1145, 2002.

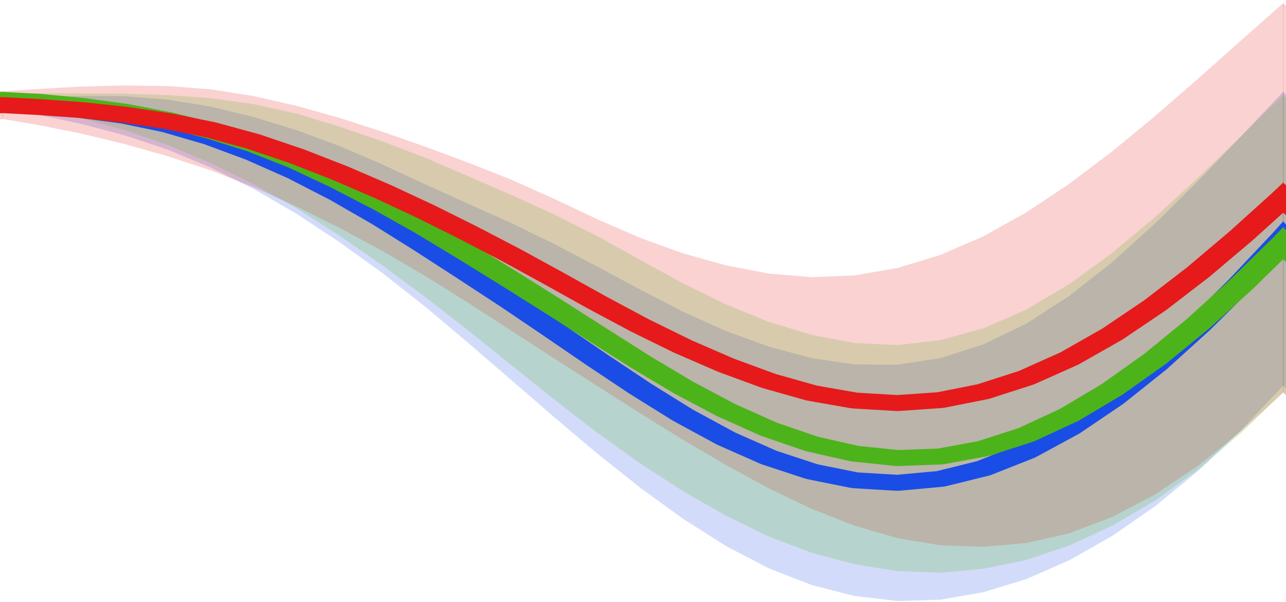

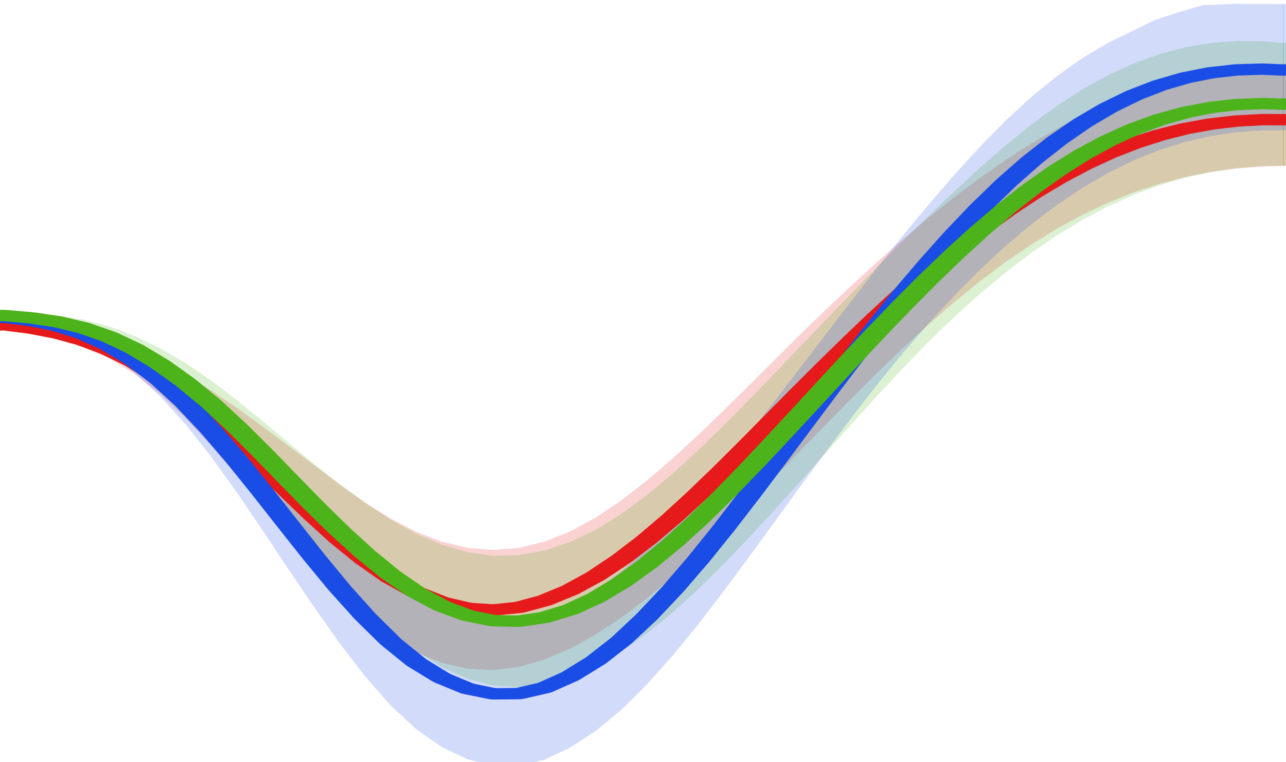

Chapter 4

Human-in-the-loop optimization of the stiffness and alignment of a prosthetic foot to reduce the metabolic cost of walking

Thijs Tankink
Han Houdijk
Johnnidel Tabucol
Marco Leopaldi
Juha M. Hijmans
Raffaella Carloni

IEEE Transactions on Neural Systems and Rehabilitation Engineering (2025), 33, 2823-2833.

Abstract

Improper tuning of prosthetic foot properties to the individual user limits the efficacy of current state-of-the-art prosthetic feet in terms of walking economy. This study aims to explore the potential of human-in-the-loop optimization to individually optimize prosthetic foot stiffness and alignment to decrease the metabolic cost of walking of transtibial amputees. Ten transtibial amputees underwent an optimization protocol while walking on a treadmill with an experimental prosthetic foot with tunable stiffness and alignment. We aimed to minimize the metabolic cost of walking by optimizing the stiffness and alignment of the prosthetic foot, using an evolutionary optimization algorithm. The metabolic cost of walking during the post-test using optimal settings was compared with the pre-test using standard settings, and the post-test using standard settings. Human-in-the-loop optimization of the tunable prosthetic foot resulted in optimal stiffness (4.41 ± 0.17 Nm/°) and alignment (2.40 ± 0.97°) settings that differ between participants. Walking on the prosthetic foot with optimized settings during the post-test resulted in a significant reduction in metabolic cost compared to the pre-test with standard settings (-10.6%). The metabolic cost during the post-test with standard settings was in between the pre-test with standard settings (-6.6%) and the post-test with optimal settings (-4.3%), indicating that part of the decrease in cost could be explained by motor adaptation of the user. Human-in-the-loop optimization can individually tune the stiffness and alignment of a prosthetic foot to lower the metabolic cost of walking for transtibial amputees and provides different optimal settings for each individual participant. Both optimization of prosthetic components and motor adaptation of the user contributed to the reduction in metabolic cost, which corroborates that human-in-the-loop optimization could enhance the efficacy of prosthetic devices.

Key words

Human-in-the-loop optimization (HILO), prosthetics foot, amputee, metabolic cost, human-robot interaction

4.1. Introduction

People with a lower-limb amputation often experience reduced quality of life, which is to a great extent the consequence of diminished level of mobility [1]. To improve mobility, people with lower-limb amputation are provided with a prosthesis that imitates the function of the biological counterpart. However, most of current prostheses do not succeed to fully compensate for the capabilities of the biological system, because their design cannot add energy to the system [2]. To compensate for the missing ankle push-off power, transtibial amputees use the less efficient hip strategy to propel the center of mass forward and upward [3]. Altogether, this results in a 12 – 40% increase in metabolic cost of walking in people with a transtibial prosthesis compared to able bodied controls at similar walking speed [4]. In addition, transtibial amputees load their intact limb more than their prosthetic limb, resulting in more asymmetric load distribution [5, 6], and they prefer a lower self-selected walking speed compared to healthy individuals [4].

To lower the metabolic cost of walking and improve mobility of people with a transtibial amputation, a more natural foot roll-over function and increased push-off power of the prosthetic foot needs to be provided. One of the most important prosthetic developments that has shown to improve walking economy compared to traditional semi-rigid prosthetic ankle-foot systems is the introduction of energy storing and return (ESAR) prosthetic feet [7, 8]. These are typically carbon-fiber feet that store energy during the loading phase, which is subsequently re-used to support forward progression [9]. Two important parameters that could affect the energy storage and return and, therefore, improve the efficacy of this type of prosthesis are stiffness and alignment.

The stiffness of an ESAR prosthetic foot affects walking mechanics. Previous studies showed that a compliant foot can increase the amount of energy stored and returned [10-12], reduce the energetic penalty of redirecting the center of mass velocity during the step-to-step transitions [3], and lower the metabolic cost of walking [13]. However, research in which a higher stiffness, which reduces the prosthetic positive work, was also associated with a lower metabolic cost [14].

Another parameter that could be tuned, but also might interact with prosthetic foot stiffness, is prosthetic alignment. Previous research already showed that prosthetic misalignment can lead to increased or asymmetrical joint forces/moments [15-17] or muscle force [18], and increased metabolic cost of walking [17]. However, it remains unclear what the most optimal alignment for an ESAR would be, and whether optimal alignment depends on the stiffness of the prosthetic foot being tuned.

Improper tuning of stiffness and alignment parameters to the individual user could limit the amount of energy stored and proper timing of energy return. Therefore, the importance of individually prescribing and tuning of prosthetic components to reduce the metabolic cost of amputee walking has already been highlighted [19]. Simultaneously exploring device parameters and their interactions, while also taking into account the voluntary, but unpredictable, gait adaptations of the user in response to changes in these parameters, becomes a complex task [20, 21]. Finding optimal settings is getting even more complicated for innovative prosthetic devices with increasing functionalities.

A method that could address these challenges and improve the efficacy of prosthetic devices is human-in-the-loop optimization [22, 23], in which the human is included 'in vivo' in the iterative optimization loop and the prosthetic foot parameters are systematically varied during the optimization process using an intelligent optimization algorithm in response to measured performance. By means of human-in-the-loop optimization, the prosthetic foot parameters could be tuned to the morphologies (i.e., biological properties) of the user [24], while also taking into account the natural behavior of humans to simultaneously optimize their coordination pattern with respect to gait performance [20].

The aim of the current study is to explore the potential of human-in-the-loop optimization to individually optimize the stiffness and alignment of an ESAR prosthetic foot to decrease the metabolic cost of walking of transtibial amputees. Moreover, we are interested to see whether optimal prosthesis parameters differ between individuals, and what underlying biomechanical parameters and mechanisms could account for the potentially enhanced walking economy.

4.2. Method

4.2.1. Participants

10 individuals with a unilateral transtibial amputation participated in this study. Individuals could be included if they were adult (age $\geq$ 18 years), underwent their amputation more than 1 year ago, and were able to walk independently (without the use of walking aids) on their prosthesis, as defined by Medicare Functional Classification Level (MFC-level) categorization score $\geq$ K3. People were excluded if they had any other condition affecting balance or gait, used drugs or medication that

could negatively affect balance or gait, used orthopedic footwear for their intact leg, used an osseointegrated prosthesis, or had current problems with the alignment or fit of their own prosthesis or socket. The study protocol was approved by the medical ethics committee of the University Medical Center Groningen (under protocol number 17321), the Netherlands. All participants were informed about the purpose of the study and provided written informed consent before the start of the experiments.

4.2.2. The tunable prosthetic foot: MyFlex-η

In this study, we used the MyFlex-η, an ESAR prosthetic foot prototype [25-27] (Figure 4.1) with tunable stiffness and tunable alignment, in combination with an Össur foot shell and regular walking shoes (Chris, Dr Comfort, Mequon, WI, USA), with a combined mass of 1749 g. The MyFlex-η variable stiffness system used the same working principle as MyFlex-ϵ [26]. The MyFlex-η is thoroughly described in Leopaldi et al. (2024) [27].

The stiffness and alignment of the foot could be manually changed as shown in Figure 4.1. Alignment was defined as the pylon-to-vertical angle while the shoe was flat but unloaded on the ground (range 0 – 10° dorsiflexion; intervals of 1°; based on the expertise of certified prosthetic orthotists). Stiffness (range: 3.28 – 5.15 Nm/°; constrained by the mechanical design of the prosthetic foot) was described by the following equation:

$$k = 1.722 + 0.063 \cdot Dx - 0.09386 \cdot \alpha \tag{4.1}$$

where k is the stiffness in Nm/°, Dx is length of the Dx slider in mm (range: 40 – 55 mm; intervals of 1 mm), and α is the alignment expressed in degrees. To determine the stiffness equation above, the foot stiffness of every Dx-length and alignment combination was determined by investigating corresponding roll-over characteristics [28], and applying a linear fit over the moment-angle curves. Afterwards, we applied a linear fit over the data to construct a linear model that described the relation between stiffness, Dx-length, and alignment.

4.2.3. Experimental set-up

Measurements were performed at the GRAIL system (Gait Realtime Analysis Interactive Lab; Motekforce Link, Amsterdam) of the Department of Rehabilitation Medicine, University Medical Center Groningen, the Netherlands. The GRAIL

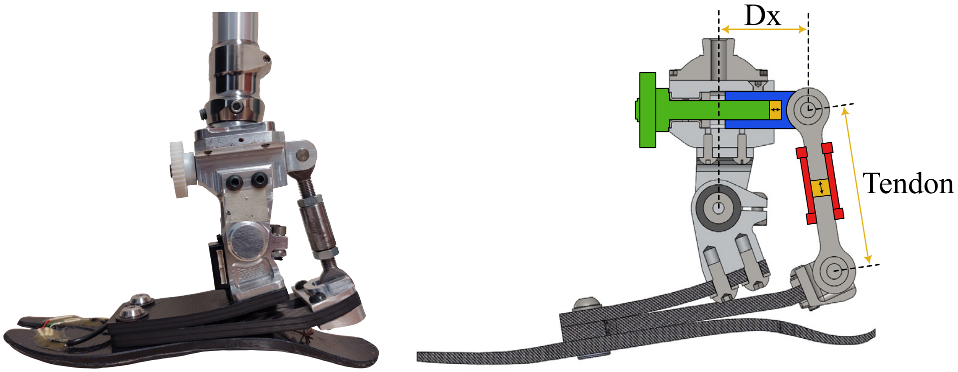

Figure 4.1: Left: The prosthetic foot MyFlex-η with tunable stiffness and tunable alignment. Right: a schematic representation. The stiffness and alignment of the prosthetic foot depended on the Dx-length and the tendon length. The Dx-length could be changed by manually turning the knob (green), horizontally translating the position of the Dx-slider (blue) (note that a change in Dx-length slightly changes the alignment as well). The orientation of the foot plate relative to the pylon could be changed by turning the threaded tube adaptor (red) of the tendon link and changing the tendon length.

consists of 10-camera motion capture system (Vicon Bonita 10, Oxford, United Kingdom; Fs = 100 Hz) that registered the marker trajectories of 22 markers (diameter = 14 mm) placed according to the lower-limb Human Body Model 2 [29] and a dual-belt treadmill with two separate force plates incorporated in the treadmill (Motekforce Link; Amsterdam; Fs = 1000 Hz). Respiratory data were collected by the portable metabolic analyzer K5 (COSMED, Rome, Italy) in breath-by-breath mode, i.e. integrating continuous flow and gas signals over every breathing cycle. Measurement systems were calibrated according to the recommended calibration protocols of the manufacturers.

4.2.4. Protocol

The protocol (Figure 4.2) consisted of a fitting session and 2 visits to the GRAIL lab.

During the fitting session, demographic data and specific body measures were collected. The tunable prosthetic foot was fitted to the participant's own prosthetic socket by a certified prosthetic orthotist and participants walked shortly on the prosthetic foot with standard settings (stiffness: 4.24 Nm/°, alignment: 5°; selected as the middle of the stiffness and alignment range) to get familiar with the device. The alignment between the socket and the pylon of the prosthetic foot was maintained during the remainder of the protocol.

The first visit of the GRAIL lab started with a familiarization period, followed by a pre-test and the first half of the optimization period. The second visit (8.9 ± 8.2 days after the first visit) consisted of a warm-up, the second half of the optimization period and the post-test.

Familiarization period: During the familiarization period, participants chose a self-selected walking speed while using the prosthetic foot with standard settings. Self-selected walking speed was determined by manually increasing the treadmill speed with 0.1 m/s until the participant indicated that comfortable walking speed was reached. Afterwards, the belt speed was further increased to a high walking speed and manually decreased with 0.1 m/s until the participant once again indicated that comfortable walking speed was reached. If there was a difference in the two selected speeds, the process was repeated. The selected speed was maintained during the rest of the protocol.

Pre-test: During the pre-test, participants walked on the treadmill for 6 min using the tunable prosthetic foot with standard settings, followed by a 5-min break.

Optimization period: During the optimization period, which was divided over the 2 lab visits, we aimed to optimize joint stiffness and alignment of the tunable prosthetic foot to minimize the metabolic cost of walking. Participants walked 42 times 120 s on the tunable prosthetic foot with intervening rest periods of 120 s. The optimization period consisted of 6 optimization blocks of 6 trials. The joint stiffness and alignment of every optimization trial were determined by the evolutionary optimization algorithm, as described in section *4.2.5. Optimization algorithm*. At the end of each optimization block, a trial with standard settings was executed to monitor the degree of motor adaptation during the optimization procedure. After every trial, the participant's perceived comfort was determined by using the VAS comfort scale [30] and the prosthetic foot settings were adjusted to the imposed stiffness and alignment for the next trial by manually tuning the Dx-length and tendon length.

Post-test: During the post-test, participants walked 3 times 6 min in different foot conditions. 2 times wearing the tunable prosthetic foot with (1) optimal parameter settings found during the optimization period and (2) standard settings in randomized order, followed by (3) a control condition wearing the participant's own prosthetic foot. After every evaluation trial, participants took a 5-min break in which they

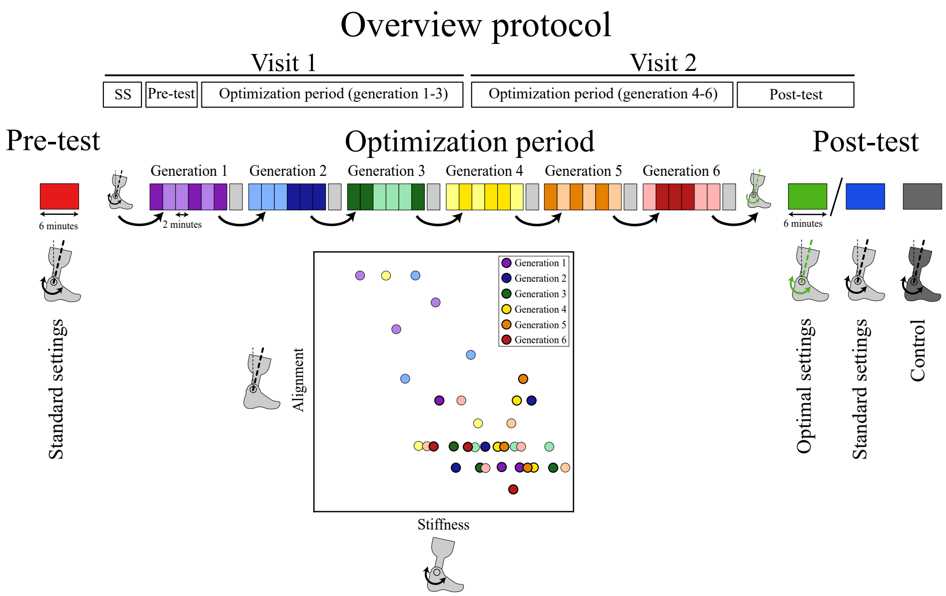

Figure 4.2: Overview of the protocol, consisting of familiarization and determination of self-selected speed (SS), pre-test, optimization period, and post-test. The outcomes of the optimization period for one participant are presented as an example. The optimization period consisted of 42 walking trials while walking on the tunable prosthetic foot with different stiffnesses and alignments. After every generation (6 trials), the 3 trials that resulted in the lowest metabolic cost (dark colors) were used to determine the prosthetic foot settings of the next generation. Every generation was followed by a trial with standard settings (light grey blocks) to monitor motor adaptations. Eventually, the mean calculated after the final generation presented the best estimate of the optimal parameter values and were used as optimal settings (pink star).

reported their perceived comfort.

4.2.5. Optimization algorithm

We used a covariance matrix adaptation evolution strategy (CMA-ES) [31] to optimize the stiffness and alignment of the prosthetic foot. The calculated values of the metabolic cost during the different walking trials were used as input for the optimization algorithm. The algorithm used a predetermined number of measurements, forming 1 generation, to determine the parameter values of the next generation. We chose to explore 6 generations with a generation size of 6 [31, 32]. In the first generation, the parameter settings (stiffness & alignment) of the trials were distributed around the middle of the search space of each optimization parameter, i.e., the standard settings of the prosthetic foot. The area of the search space was determined by σ, i.e., the standard deviation of parameter values within every generation ($\sigma_{initial}$ = 0.50 after standardization of each optimization parameter). After every generation, the settings of the 3 trials that resulted in the lowest metabolic cost were used to update the mean of the search space of the next generation (Figure 4.2), which represented the best estimate of the optimal parameter values, and the area of search around this mean (σ) to end up with the optimal joint stiffness and alignment. Eventually, the mean calculated after the final generation presented the best estimate of the optimal settings and were used as optimal parameter values.

4.2.6. Data analysis

4.2.6.1. Metabolic cost

The metabolic cost of walking during the 2-min trials was estimated by fitting a first-order dynamical model with a time constant of 42 seconds [33] to 120 seconds of breath-by-breath metabolic measurements, because it has shown provide a good balance between limiting estimation errors and trial duration [22]. We fitted an exponential curve to the measured O_2 and CO_2 production and used the asymptotes of these fits as an estimate of their steady state values. During the pre- and post-test, we determined the steady state O_2 and CO_2 based on their mean values over the last 2 min of each trial to calculate metabolic cost of walking. Gross energy consumption was used to account for variations in resting energy consumption between measurement days [34]. Metabolic cost of walking was calculated using the equation of Garby and Astrup [35]:

$$metabolic\ \ power = 16.04 \cdot \dot{V}O_2 + 4.94 \cdot \dot{V}CO_2 \tag{4.2}$$

where $metabolic\ \ power$ is in W and $\dot{V}O_2$ and $\dot{V}CO_2$ are expressed in mL/s. Subsequently, we normalized $metabolic\ \ power$ for body mass (W/kg).

4.2.6.2. Gait biomechanics

We used the last 2 min of the evaluation trials for biomechanical analysis. Data were filtered with a low-pass second order Butterworth filter with a 6 Hz cut-off frequency. We used a custom-made MATLAB (R2023a, MathWorks, Natick, USA) script with a 10 N ground reaction force threshold to detect different steps and calculate spatiotemporal gait parameters: step frequency, stride time, stance time, double support time, step length (variability), and step width (variability). Step length and stance time asymmetry were calculated by the following equation [36]:

$$asymmetry = \frac{prosthetic \;\; leg}{(prosthetic \;\; leg + intact \;\; leg) \;\; / \;\; 2} \cdot 100 \tag{4.3}$$

where $\mathrm{asymmetry}$ is in percentages, and $prosthetic \;\; leg$ and $intact \;\; leg$ represent the values for step length or stance time of each leg.

Mechanical work on the center of mass was determined by using the individual limbs method described by Donelan et al. (2002) [37]. First, the velocity of the center of mass was calculated by integrating its acceleration, which was determined by summing the ground reaction forces under each limb:

$$\overrightarrow{v}_{CoM} = \int \frac{\overrightarrow{F}_{trail} + \overrightarrow{F}_{lead} + m \cdot \overrightarrow{g}}{m} \mathrm{dt} + \begin{bmatrix} c_x \\ c_y \\ c_z \end{bmatrix} \tag{4.4}$$

where $\overrightarrow{v}_{CoM}$ (m/s) is the velocity vector of the center of mass, $\overrightarrow{F}_{trail}$ (N) is the ground reaction force exerted by the trailing leg, $\overrightarrow{F}_{trail}$ (N) is the ground reaction force vector of the leading leg, m (kg) is the participants' body mass, and $\overrightarrow{g}$ ([0, -9.81, 0] m/s^2) is the gravitational acceleration. The vertical integration constant (c_y) was found by assuming that the average vertical center of mass velocity over a step was 0. The anterior-posterior integration constant (c_z) was obtained by assuming that the average velocity over a step was equal to the belt speed. The medio-lateral integration constant ($\mathrm{c_x}$) was found by assuming that the center of mass velocity at the beginning and end of a step was equal in magnitude but opposite in sign [37]. Consequently, the mechanical power on the center of mass generated by the trailing and leading leg was calculated by multiplying the force exerted by each individual limb with the center of mass velocity:

$$P_{trial} = \overrightarrow{F}_{trail} \cdot \overrightarrow{v}_{CoM} \tag{4.5}$$

$$P_{lead} = \overrightarrow{F}_{lead} \cdot \overrightarrow{v}_{CoM} \tag{4.6}$$

where P is in W. Subsequently, we normalized the mechanical power for body mass (W/kg). Finally, collision work was calculated by integrating P_{lead} over time, for the negative interval directly after initial contact. Push-off work was determined by integrating the positive interval of P_{trail} over time.

Ankle push-off work was calculated by integrating the ankle power curve over time, for the positive interval directly before toe off. The maximum value of the ankle power curve was taken as peak push-off power.

All work variables were determined for both the prosthetic and intact leg. To compare the timing of energy storage and return of the different conditions, we time normalized the center of mass power curves to the stance duration and ankle power curves to the stride duration.

4.2.7. Statistical analysis

We performed repeated measures analyses of variance (ANOVA), in SPSS (Version 28.0.1.1, IBM Corp. Armonk, NY, USA) with prosthetic foot condition (pre-test standard settings, post-test optimal settings, post-test standard settings) as within-subject factor and metabolic cost of walking as dependent variable. A Pearson correlation coefficient was calculated to determine the association between optimal stiffness and alignment settings. To investigate whether the different conditions affected walking biomechanics, we used repeated measures ANOVA with prosthetic foot condition (pre-test standard, post-test optimal, post-test standard) as within-subject factor for several dependent spatiotemporal, asymmetry, and mechanical work parameters. Because of the different characteristics of the participants' own prosthetic feet, the control condition with their own prosthesis was excluded from statistical analyses and only added for reverence. To measure perceived comfort during the post-test, we used repeated measures ANOVA with prosthetic foot condition (post-test optimal, post-test standard, post-test control) as within-subject factor and VAS-comfort score as dependent variable. For all tests, we used a p-value of 5% to indicate statistically significant differences. We used Bonferroni correction for post hoc t-tests to compare the different prosthetic foot conditions. If the assumption of sphericity was violated, we used a Greenhouse-Geisser correction.

Time series of continuous gait variables were compared using 1-dimensional Statistical Parametric Mapping (SPM-1D) [38]. All SPM-1D analyses were performed with a custom MATLAB script using the open-source software package spm1D 0.4.10 (www.spm1d.org). SPM-1D repeated measures ANOVA were used to compare the different prosthetic foot conditions ($p < 0.05$). The p-values of the post hoc t-tests were Bonferroni corrected.

4.3. Results

4.3.1. Study population characteristics

10 male transtibial amputees (age: 57.2 ± 16.6 y, height: 180.0 ± 4.0 cm, mass: 85.3 ± 14.6 kg, shoe size range: 42 – 45 EU) participated in this study. Participants had undergone amputation because of trauma (5), vascular disease (3), cancer (1), autoimmune disease (1), and congenital growth disorder (1). The combined mass of their own prosthesis and shoe was 1338.9 ± 228.8 g. The self-selected walking speed was 1.02 ± 0.12 m/s.

4.3.2. Optimal settings prosthetic foot

Human-in-the-loop optimization of the tunable prosthetic foot resulted in optimal stiffness (4.41 ± 0.17 Nm/°) and alignment (2.40 ± 0.97°) settings that differed between participants (Figure 4.3). Optimal alignment settings (i.e., pylon-to-vertical angles) were always smaller than the standard alignment (5°). Optimal stiffness was

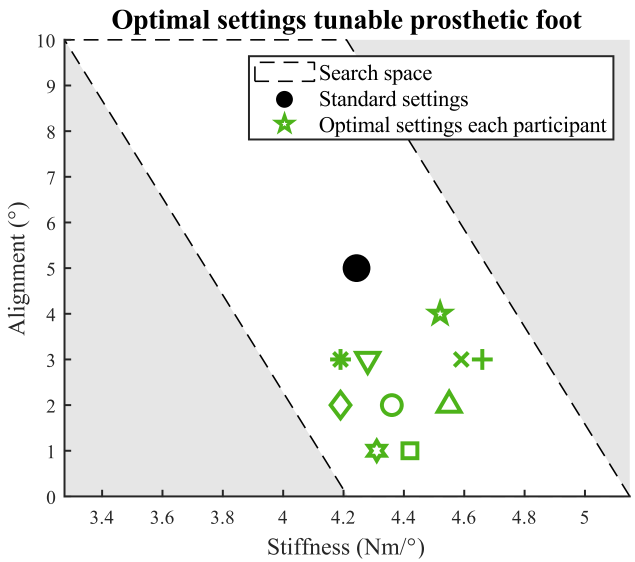

Figure 4.3: Optimal stiffness and alignment settings for every participant (n=10) within the search space of the tunable prosthetic foot (white area). The standard setting (black dot) is also given.

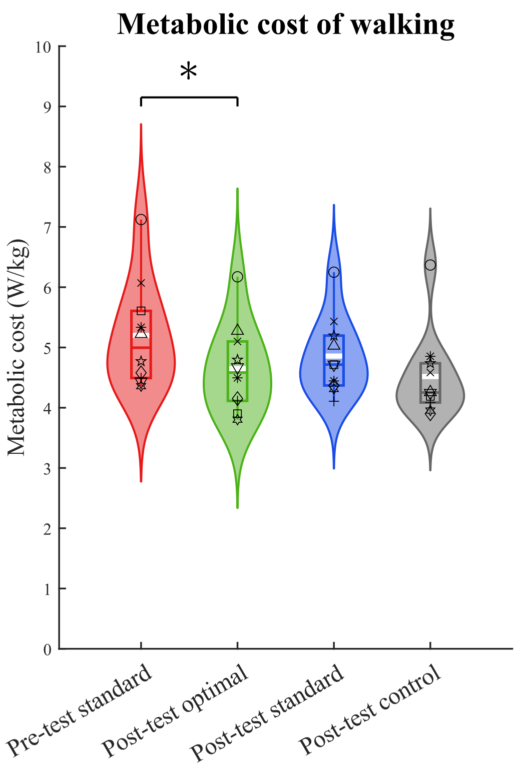

Figure 4.4: Metabolic cost of walking for each prosthetic foot condition (n=10). The colored bars and error bars show mean ± standard deviation. Individual observations are also given. Post-test control condition is displayed for reference and not statistically tested. *p<0.05.The colored bars and error bars show mean ± standard deviation. Individual observations are also given. Post-test control condition is displayed for reference and not statistically tested. *p<0.05.

higher than the standard stiffness (4.24 Nm/°) in 8 of the 10 cases. For 6 out of 10 participants, their optimal stiffness was in the lower half of the stiffness range corresponding with their optimal alignment. No significant relation between optimal stiffness and alignment settings was found (Pearson correlation coefficient = 0.28, p = 0.44). The progression of the prosthetic foot stiffness and alignment settings throughout the optimization period are presented in Figure 4.6. The area of search of stiffness and alignment landscape (σ) during the optimization period decreased towards the final generation (σ_{final} = 0.25 ± 0.03, range: 0.19 – 0.30; Figure 4.6), indicative of convergence.

During the post-test, perceived comfort of walking with the prosthetic foot with optimal settings was higher compared to walking with the prosthetic foot with standard settings (Table 4.1).

4.3.3. Metabolic cost

In the evaluation trials, we found a significant main effect of prosthetic foot condition on metabolic cost of walking (Table 4.1, Figure 4.4). Post hoc test revealed that walking on the tunable prosthetic foot with optimal settings during the post-test resulted in a significant reduction of metabolic cost compared to walking on the prosthetic foot with standard settings during the pre-test (-10.6%, $p < 0.05$). The differences between the pre-test and post-test with standard settings (-6.6%) and between the optimal settings and standard settings during post-test (-4.3%) were not

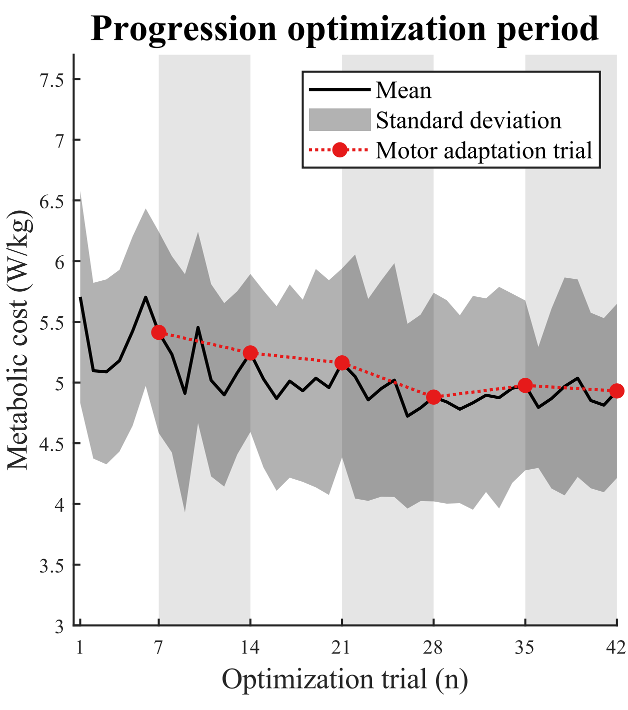

Figure 4.5: Progression of metabolic cost during the optimization period. Mean ± standard deviation over all participants (black line ± shared area) are given. The shaded areas in the background indicate the different generations during the optimization period. Note that every generation was followed by a trial with standard settings to monitor motor adaptation (red dotted line).

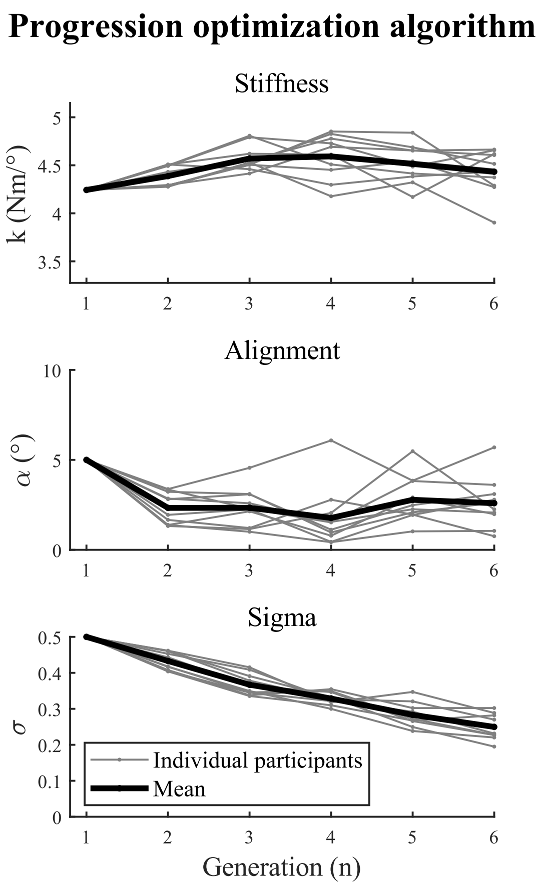

Figure 4.6: Progression of the optimization algorithm parameters during the optimization period. Mean optimization parameter values (stiffness and alignment) and search space (sigma) are presented for every generation. Both the progression for the individual participants (thin lines) and the mean over all participants (bold line) are given.

significant. The progression of metabolic cost throughout the optimization period is presented in Figure 4.5.

4.3.4. Gait biomechanics

Prosthetic foot condition also affected gait parameters. A significant main effect of prosthetic foot condition for total double support time and initial double support time (during loading response) of the intact leg was found (Table 4.1). Post hoc tests

Table 4.1: Spatiotemporal, energetic, biomechanical gait parameters, and perceived comfort for the different prosthetic foot conditions during the pre-test and post-test (n=10). Results of the repeated measures analysis of variance of the tunable prosthetic foot conditions (pre-test standard, post-test optimal, post-test standard) for the different variables are also given.

	Tuneable prosthetic foot			Own prosthetic foot			
	Pre-test standard	Post-test optimal	Post-test standard	Post-test control^{A}	F(2,18)	p	ES^{B}
Spatiotemporal							
Step frequency (Hz)	1.68 (0.08)	1.65 (0.08)	1.65 (0.09)	1.69 (0.08)	2.19^{C}	0.17	0.20
Stride Time (s)	1.19 (0.05)	1.22 (0.07)	1.22 (0.07)	1.18 (0.06)	2.19^{C}	0.17	0.20
Double support time (% stride)	38.9 (2.58)$^{\phi}$	37.8 (2.84)*	38.0 (2.98)	36.9 (2.72)	6.89	**<0.01^{D}**	0.43
Initial double support time prosthetic leg (% stride)	19.7 (1.62)	19.5 (1.88)	19.8 (2.18)	19.1 (1.59)	0.62	0.55	0.06
Initial double support time intact leg (% stride)	19.2 (1.37)$^{\phi\,\times}$	18.3 (1.25)*	18.2 (1.11)*	17.8 (1.51)	21.9^{C}	**<0.001^{D}**	0.71
Stance time (s)							
Prosthetic leg	0.81 (0.03)	0.82 (0.05)	0.81 (0.05)	0.80 (0.05)	0.76^{C}	0.42	0.08
Intact leg	0.85 (0.05)	0.86 (0.05)	0.87 (0.06)	0.83 (0.05)	1.21C	0.31	0.12
Step length (m)							
Prosthetic leg	0.61 (0.10)	0.63 (0.08)	0.62 (0.08)	0.61 (0.07)	0.93^{C}	0.37	0.09
Intact leg	0.61 (0.08)	0.62 (0.09)	0.63 (0.10)	0.60 (0.08)	1.68^{C}	0.23	0.16
Step width (m)	0.16 (0.02)$^{\times}$	0.14 (0.03)	0.14 (0.02)*	0.15 (0.03)	12.0^{C}	**<0.01^{D}**	0.58
Step length variability (mm)	40.4 (14.0)	41.9 (19.7)	46.6 (24.8)	51.8 (33.3)	0.25	0.75	0.03
Step width variability (mm)	35.9 (7.93)	32.0 (6.35)	33.5 (5.55)	33.7 5.89)	4.04	**<0.05^{D}**	0.31
Asymmetry (%)							
Step length	100.2 (4.74)	100.8 (5.02)	99.3 (5.43)	100.9 (5.16)	0.57^{C}	0.56	0.06
Stance time	97.2 (1.90)	97.2 (2.58)	96.8 (2.61)	98.07 (1.60)	0.41^{C}	0.57	0.04

Table 4.1: continued.

	Tuneable prosthetic foot			Own prosthetic foot			
	Pre-test standard	Post-test optimal	Post-test standard	Post-test control[A]	F(2,18)	p	ES[B]
Metabolic cost (W/kg)	5.20 (0.88)$^{\phi}$	4.65 (0.73)*	4.86 (0.64)	4.52 (0.72)	6.89	**<0.01[D]**	0.43
Mechanical work on the center of mass (J/kg)							
Intact leg leading							
Collision	-0.22 (0.06)	-0.21 (0.06)	-0.24 (0.07)	-0.14 (0.06)	1.54[C]	0.25	0.15
Push-off	0.09 (0.05)	0.08 (0.03)	0.07 (0.02)	0.11 (0.04)	1.50[C]	0.25	0.14
Prosthetic leg leading							
Collision	-0.08 (0.04)	-0.07 (0.04)	-0.07 (0.05)	-0.06 (0.05)	0.60	0.56	0.06
Push-off	0.13 (0.06)	0.14 (0.04)	0.14 (0.04)	0.15 (0.04)	1.47[C]	0.26	0.14
Ankle joint mechanics							
Push-off work (J/kg)							
Prosthetic leg	0.26 (0.10)	0.32 (0.13)	0.30 (0.11)	0.29 (0.11)	2.20	0.14	0.20
Intact leg	0.41 (0.16)	0.43 (0.15)	0.44 (0.15)	0.40 (0.13)	0.45	0.64	0.05
Peak push-off power (W/kg)							
Prosthetic leg	2.75 (1.10)	3.15 (1.01)	3.09 (1.04)	2.85 (0.92)	1.93[C]	0.20	0.18
Intact leg	3.58 (1.39)	3.53 (1.60)	3.79 (1.25)	3.60 (1.01)	0.45	0.65	0.05
VAS comfort score (0-10)[E]		7.40 (1.27)$^{\times}$	6.20 (1.48)$^{\phi\,\dagger}$	8.30 (1.06)$^{\times}$	22.20[C]	**<0.001[F]**	0.69

[A]Condition with the participants' own prosthetic foot was excluded from the statistical comparison but only added for reference.
[B]ES = partial η^2.
[C]Greenhouse-Geisser correction was used.
[D]Bonferroni corrected post hoc tests: *vs. pre-test standard, $^{\phi}$vs. post-test optimal, $^{\times}$vs. post-test standard.
[E]VAS comfort score of pre-test standard condition was not collected. Result of the repeated measures analysis of variance of the tuneable prosthetic foot conditions (post-test optimal, post-test standard, post-test control) is given.
[F]Bonferroni corrected post hoc tests: $^{\phi}$vs. post-test optimal, $^{\times}$vs. post-test standard, †vs. post-test control.

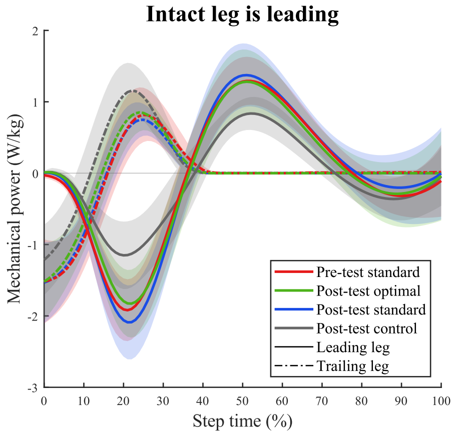

Figure 4.7: The external mechanical power generated on the center of mass by the leading intact (solid) and trailing prosthetic (dashed) leg during a step. Group average ± standard deviation when the intact leg is leading are presented. Significant differences between conditions were not found (p>0.05).

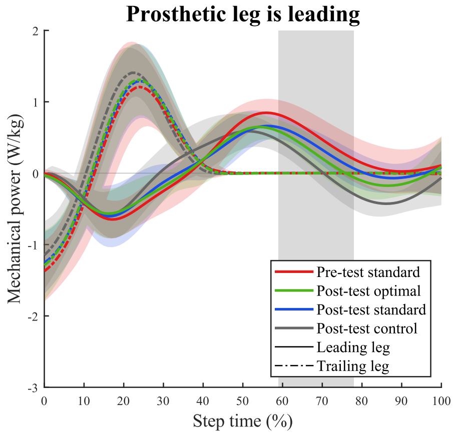

Figure 4.8: The external mechanical power on the center of mass generated by the leading prosthetic (solid) and trailing intact (dashed) leg during a step. Group average ± standard deviation when the prosthetic leg is leading are presented. The grey area indicates a significant difference between conditions (p<0.05; post hoc tests were not significant, p>0.05).

revealed that participants decreased their double support time during the post-test with optimal settings compared to the pre-test with standard settings (-2.7%, $p < 0.05$), and that participants decreased the initial double support time of their intact leg during the post-test with both optimal and standard settings compared to the pre-test with standard settings (-4.7%, $p < 0.01$ and -5.2%, $p < 0.01$, respectively). We also found a main effect of prosthetic foot condition for step width and step width variability (Table 4.1). Post hoc test revealed that participants walked with a decreased step width during the post-test conditions with optimal and standard settings compared to the pre-test condition with standard settings (-14.5%, $p < 0.01$, respectively). We did not find significant differences in asymmetry parameters and variables related to mechanical work performed on the body's center of mass, ankle push-off work or peak power among foot conditions (Table 4.1).

SPM-1D with repeated measures ANOVA revealed a significant main effect between prosthetic foot conditions for the mechanical power on the center of mass of the prosthetic leg during 59 – 78% of step time (i.e., midstance) while being the leading leg ($p < 0.01$; Figure 4.8). The post-test condition with optimal settings had a lower power compared to the pre-test and post-test conditions with standard settings, but post hoc test did not show significant differences. SPM-1D did not reveal any other significant differences between conditions for ankle power (Figure 4.9) or mechanical power on the center of mass for the prosthetic or intact leg while being either the leading or trailing leg (Figure 4.7, Figure 4.8).

4.4. Discussion

The aim of the present study was to determine whether human-in-the-loop optimization could optimize the stiffness and alignment of an ESAR prosthetic foot to decrease the metabolic cost of walking of transtibial amputees. Walking on the prosthetic foot with optimized settings during the post-test resulted in a significant 10% reduction in metabolic cost compared to the pre-test with standard settings. This seemed partly due to changes in stiffness and alignment settings of the prosthetic foot, but also partly due to motor adaptations of the user.

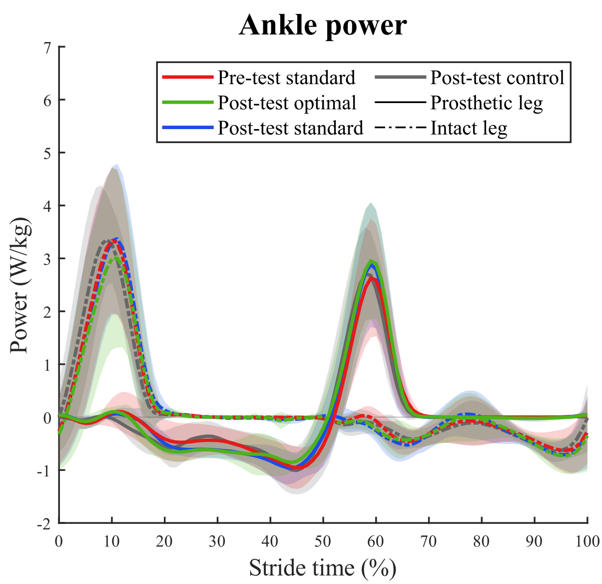

Figure 4.9: Ankle power of the prosthetic (solid line) and intact (dashed line) leg during a stride. Group average ± standard deviation when the prosthetic leg is leading are presented. Significant differences between conditions were not found ($p>0.05$).

Optimal alignment (range: 1 – 4°) and stiffness (range: 4.19 – 4.65 Nm/°) settings differed between participants and appeared quite independent of each other. While previous research [17] showed that a 10° change in alignment could affect metabolic cost, our results show that even smaller differences in prosthetic foot alignment can already influence energy expenditure. Optimal stiffness settings found in the current study were relatively high compared to commercially available prosthetic feet (2.51 – 4.67 Nm/°) [28], but were scattered over the search space of the tunable prosthetic foot. Apparently, optimal stiffness and alignment vary independently individually, and no general guideline can be provided. This underlines the complexity and unpredictability of the user-prosthesis system and highlights the need for individually optimizing prosthetic devices.

The 10.6% decrease in energy cost is larger than seen in previous studies comparing metabolic cost for different prosthetic foot types or settings. Most studies found differences that were not significant [2, 39], or only small significant differences (2.7 – 8%) that appeared to be not clinically relevant [2, 13, 14, 17]. Although the reduction in metabolic cost is smaller than found by previous human-in-the-loop studies in people without amputation (15 – 24%) [22, 40, 41], the reduction is higher than found in a case study using human-in-the-loop optimization of an ankle-foot prosthesis in a person with an amputation (3.5%) [32], and our results show that optimizing prosthetic devices via human-in-the-loop optimization has the potential to obtain more substantial and meaningful effects than observed before.

The 10.6% reduction in metabolic cost during the post-test with optimal settings compared to the pre-test with standard settings was accompanied by a 6.6% decrease in metabolic cost during the post-test using standard settings compared to the pre-test with standard settings. The variable practice that human-in-the-loop optimization entails, which has been suggested to enhance motor learning [42, 43], could have contributed to the reduction in metabolic cost with the post-test optimal setting. This is in line with previous research about human-in-the-loop optimization of exoskeletons [44], in which training also accounted for half of the final reduction in energy cost. However, in the current study the 6.6% in post-test standard condition was not statistically different from pre-test, nor was the difference between post-test with standard and optimal settings significant. Hence it remains unclear to what extent motor learning contributed to the total reduction with optimal settings. Nevertheless, it appears that the effect of human-in-the-loop optimization should not only be ascribed to adaptations of the settings, but also to motor adaptations of the user.

We expected that the reduction in metabolic cost for the optimized prosthetic foot could be explained by increased energy storing in the foot and improved timing of return. This could reduce collision work on the center of mass and therefore the energetic penalty for the step-to-step transition [3, 45]. However, we did not find convincing evidence that this mechanism could account for the reduced metabolic energy cost. Push-off and collision work did not differ significantly between foot conditions, nor did ankle joint work. It could be argued that the amount of push-off power that can be derived from the elastic energy storage of an ESAR foot is still too limited to affect energy consumption [2]. SPM analysis showed a main effect for single support work, which was highest during the pre-test standard condition, although this difference was not statistically different in post hoc test. The higher single support work in the pre-test standard condition could indicate that more compensatory work during single support was required in that condition. However, given that follow-up post hoc results were not significant this interpretation should be taken with caution. Although SPM analysis did not show clear trends in timing of energy return on a group level either, it could be possible that the optimal settings improved push-off timing on an individual level, but this was too subtle to be detected in our current analyses. To test this hypothesis, a follow-up study testing different levels of stiffness and alignment normalized to the individually optimized settings would be needed. Additionally, it is worth exploring whether these different settings affect self-selected walking speed.

Another explanation for the decrease in metabolic cost could be a reduction in balance-related effort. Previous research [46] demonstrated that controlling prosthetic push-off work could decrease metabolic cost, even if average push-off work did not change. They attributed the reduction to a decreased muscular effort related to medio-lateral foot placement. This is in line with our current results, in which participants walked with decreased step width and step width variability during the post-test with optimal settings compared to the pre-test with standard settings, indicating that less active balance control was required [46-48]. Moreover, double support time was decreased during the post-test with optimal settings, spending less time with two feet on the ground. This could indicate that participants needed less alterations in their gait to correct for deviations [49]. Since participants also decreased their double support time and step width during the post-test with standard settings compared to pre-test with standard settings, this effect might be partially attributed to motor learning.

4.4.1. Limitations and future research

Some limitations of our study should be acknowledged. The outcomes of the optimization process are dependent on the settings of the optimization algorithm. One setting of the optimization algorithm that might have affected the outcomes of the current study is the way it dealt with generated optimization parameters outside the search space. If there was a stiffness-alignment combination generated that was outside the search space of the prosthetic foot, the algorithm regenerated these parameter values until there was a stiffness-alignment combination generated within the search space. A potential drawback of this decision is that the areas around the border are insufficiently explored, and the area of search is pushed away from the borders. An alternative would be that parameter values outside the search space are adjusted with the value on the boundary.

Furthermore, it remains uncertain whether full convergence of the two optimization parameters (stiffness and alignment) was achieved. Although the area of search (σ) decreased towards the final generation (Figure 4.6), and metabolic cost decreased during the optimization period, reaching a plateau during the final generations (Figure 4.5), some participants still showed some variation in mean optimization parameter values during these later stages (Figure 4.6). Therefore, improving convergence criteria to stop the optimization process would be meaningful in future research[23].

Another limitation of the current study is the non-rectangular search space of the prosthetic foot. Although the algorithm has shown to be able to deal with the imposed search space and individually optimized settings have been found, it makes it more difficult to draw clear conclusions about which specific parameter values might be advantageous. Therefore, we encourage engineers to take this into account when designing assistive devices with tunable settings.

A fourth limitation is the extensive nature of the protocol of the current study. Some participants had difficulties adapting quickly to the changing prosthetic foot settings during the optimization period. Although participants used a self-selected walking speed and every walking trial was followed by a rest period, some participants seemed fatigued towards the end of their visits. Comparable to other studies [50, 51], this might have resulted in an increase in energy cost that could have affected the outcomes of the optimization process. Therefore, future research should investigate how much time prosthetic users require to adapt to a new prosthetic device. With this information, we could align the duration of optimization to the time scale of human adaptations [23], and the physical strain of the users could be optimally decreased.

Furthermore, it is worth exploring whether alternative optimization criteria could replace the cumbersome metabolic cost measurements. A potential alternative could be perceived comfort (Table 4.1) and experience of the user [52]. Besides that it does not require expensive equipment to obtain [53] and could limit measurement time, it could also engage the user in the process [23].

While we showed that human-in-the-loop optimization resulted in individualized optimal solutions, which reduced the metabolic cost of walking compared to a standard setting, we did not demonstrate whether this process is superior to the current subjective alignment process in prosthetics and orthopedic practice and should be investigated in future research.

4.5. Conclusion

The current study demonstrated that human-in-the-loop optimization can individually tune the stiffness and alignment of a prosthetic foot to lower the metabolic cost of walking for transtibial amputees and provided different optimal settings for each individual participant. The study showed that both optimization of prosthetic components and motor learning of the user contributed to the more than 10% reduction in energy cost, which corroborates that human-in-the-loop optimization could be used to enhance the effectiveness of prosthetic devices.

4.6. Acknowledgments

This work was supported by the European Commission's Horizon 2020 Program as part of the Project MyLeg under Grant 780871. We thank Henk Zijlstra, Chris Bolmer, Sandra Loonen, and Auke Postma (certified prosthetists) of OIM Orthopedie (Haren, the Netherlands) for their help with recruitment of participants and connecting and aligning the tunable prosthetic foot. We thank Chengxiang.Liu (Doctoral candidate at the University of Groningen), Friso van der Bijl and Pim Rive (Bachelor students University of Groningen) for their help with data collection.

4.7. Reference list

[1] J. P. Pell, P. T. Donnan, F. G. Fowkes, and C. V. Ruckley, "Quality of life following lower limb amputation for peripheral arterial disease," European journal of vascular surgery, vol. 7, no. 4, pp. 448-451, Jul, 1993.

[2] J. Gardiner, A. Z. Bari, D. Howard, and L. Kenney, "Transtibial amputee gait efficiency: Energy storage and return versus solid ankle cushioned heel prosthetic feet," Journal of rehabilitation research and development, vol. 53, no. 6, pp. 1133-1138, 2016.

[3] H. Houdijk, E. Pollmann, M. Groenewold, H. Wiggerts, and W. Polomski, "The energy cost for the step-to-step transition in amputee walking," Gait & posture, vol. 30, no. 1, pp. 35-40, Jul, 2009.

[4] S. Ettema, E. Kal, and H. Houdijk, "General estimates of the energy cost of walking in people with different levels and causes of lower-limb amputation: a systematic review and meta-analysis," Prosthetics and orthotics international, vol. 45, no. 5, pp. 417-427, Oct 1, 2021.

[5] C. Grumillier, N. Martinet, J. Paysant, J. M. André, and C. Beyaert, "Compensatory mechanism involving the hip joint of the intact limb during gait in unilateral trans-tibial amputees," Journal of Biomechanics, vol. 41, no. 14, pp. 2926-2931, Oct 20, 2008.

[6] D. C. Morgenroth, A. D. Segal, K. E. Zelik, J. M. Czerniecki, G. K. Klute, P. G. Adamczyk, M. S. Orendurff, M. E. Hahn, S. H. Collins, and A. D. Kuo, "The effect of prosthetic foot push-off on mechanical loading associated with knee osteoarthritis in lower extremity amputees," Gait & posture, vol. 34, no. 4, pp. 502-507, Oct, 2011.

[7] J. M. Casillas, V. Dulieu, M. Cohen, I. Marcer, and J. P. Didier, "Bioenergetic

comparison of a new energy-storing foot and SACH foot in traumatic below-knee vascular amputations," Archives of Physical Medicine and Rehabilitation, vol. 76, no. 1, pp. 39-44, Jan, 1995.

[8] D. H. Nielsen, D. G. Shurr, J. C. Golden, and K. Meier, "Comparison of Energy Cost and Gait Efficiency During Ambulation in Below-Knee Amputees Using Different Prosthetic Feet," The Iowa orthopaedic journal, vol. 8, pp. 95-100, 1988.

[9] G. N. Askew, L. A. McFarlane, A. E. Minetti, and J. G. Buckley, "Energy cost of ambulation in trans-tibial amputees using a dynamic-response foot with hydraulic versus rigid 'ankle': insights from body centre of mass dynamics," Journal of neuroengineering and rehabilitation, vol. 16, no. 1, pp. 019-x, Mar 14, 2019.

[10] N. P. Fey, G. K. Klute, and R. R. Neptune, "The influence of energy storage and return foot stiffness on walking mechanics and muscle activity in below-knee amputees," Clinical Biomechanics, vol. 26, no. 10, pp. 1025-1032, December 2011, 2011.

[11] P. G. Adamczyk, M. Roland, and M. E. Hahn, "Sensitivity of biomechanical outcomes to independent variations of hindfoot and forefoot stiffness in foot prostheses," Human movement science, vol. 54, pp. 154-171, 2017.

[12] E. G. Halsne, J. M. Czerniecki, J. B. Shofer, and D. C. Morgenroth, "The effect of prosthetic foot stiffness on foot-ankle biomechanics and relative foot stiffness perception in people with transtibial amputation," Clinical Biomechanics, vol. 80, pp. 105141, 2020.

[13] M. J. Major, M. Twiste, L. P. J. Kenney, and D. Howard, "The effects of prosthetic ankle stiffness on ankle and knee kinematics, prosthetic limb loading, and net metabolic cost of trans-tibial amputee gait," Clinical Biomechanics, vol. 29, no. 1, pp. 98-104, January 2014, 2014.

[14] E. A. Hedrick, P. Malcolm, J. M. Wilken, and K. Z. Takahashi, "The effects of ankle stiffness on mechanics and energetics of walking with added loads: a prosthetic emulator study," Journal of NeuroEngineering and Rehabilitation, vol. 16, no. 1, pp. 1-15, 2019.

[15] T. Kobayashi, M. S. Orendurff, M. Zhang, and D. A. Boone, "Effect of alignment changes on sagittal and coronal socket reaction moment interactions in transtibial prostheses," Journal of Biomechanics, vol. 46, no. 7, pp. 1343-1350, 2013.

[16] D. H. K. Chow, A. D. Holmes, C. K. L. Lee, and S. W. Sin, "The effect of prosthesis alignment on the symmetry of gait in subjects with unilateral transtibial amputation," Prosthetics and orthotics international, vol. 30, no. 2, pp. 114-128, 2006.

[17] T. Schmalz, S. Blumentritt, and R. Jarasch, "Energy expenditure and biomechanical characteristics of lower limb amputee gait: The influence of prosthetic alignment and different prosthetic components," Gait & posture, vol. 16, no. 3, pp. 255-263, 2002.

[18] L. Fang, X. Jia, and R. Wang, "Modeling and simulation of muscle forces of trans-tibial amputee to study effect of prosthetic alignment," Clinical Biomechanics, vol. 22, no. 10, pp. 1125-1131, 2007.

[19] J. D. Ventura, G. K. Klute, and R. R. Neptune, "The effect of prosthetic ankle energy storage and return properties on muscle activity in below-knee amputee walking," Gait & posture, vol. 33, no. 2, pp. 220-226, Feb, 2011.

[20] R. M. Alexander, "Optimization and gaits in the locomotion of vertebrates," Physiological Reviews, vol. 69, no. 4, pp. 1199-1227, 1989.

[21] J. C. Selinger, S. M. O'Connor, J. D. Wong, and J. M. Donelan, "Humans can continuously optimize energetic cost during walking," Current Biology, vol. 25, no. 18, pp. 2452-2456, 2015.

[22] J. Zhang, P. Fiers, K. A. Witte, R. W. Jackson, K. L. Poggensee, C. G. Atkeson, and S. H. Collins, "Human-in-the-loop optimization of exoskeleton assistance during walking," Science (New York, N.Y.), vol. 356, no. 6344, pp. 1280-1284, Jun 23, 2017.

[23] P. Slade, C. Atkeson, J. M. Donelan, H. Houdijk, K. A. Ingraham, M. Kim, K. Kong, K. L. Poggensee, R. Riener, M. Steinert, J. Zhang, and S. H. Collins, "On human-in-the-loop optimization of human-robot interaction," Nature, vol. 633, no. 8031, pp. 779-788, Sep, 2024.

[24] F. Scotto di Luzio, D. Simonetti, F. Cordella, S. Miccinilli, S. Sterzi, F. Draicchio, and L. Zollo, "Bio-Cooperative Approach for the Human-in-the-Loop Control of an End-Effector Rehabilitation Robot," Frontiers in neurorobotics, vol. 12, pp. 67, Oct 11, 2018.

[25] J. Tabucol, "Study of composite elastic elements for transfemoral prostheses: the MyLeg Project," University of Groningen, 2022.

[26] J. Tabucol, M. Leopaldi, T. M. Brugo, M. Oddsson, and A. Zucchelli, "Design and Mechanical Characterization of a Variable Stiffness ESR Foot

Prosthesis," IEEE Access, vol. 12, pp. 97544-97556, 2024.
[27] M. Leopaldi, T. M. Brugo, J. Tabucol, and A. Zucchelli, "Parametric Design of an Advanced Multi-Axial Energy-Storing-and-Releasing Ankle–Foot Prosthesis," Prosthesis, vol. 6, no. 4, pp. 726-743, 2024.
[28] C. Curtze, A. L. Hof, H. G. van Keeken, J. P. K. Halbertsma, K. Postema, and B. Otten, "Comparative roll-over analysis of prosthetic feet," Journal of Biomechanics, vol. 42, no. 11, pp. 1746-1753, 2009.
[29] A. J. van den Bogert, T. Geijtenbeek, O. Even-Zohar, F. Steenbrink, and E. C. Hardin, "A real-time system for biomechanical analysis of human movement and muscle function," Medical & biological engineering & computing, vol. 51, no. 10, pp. 1069-1077, Oct, 2013.
[30] R. S. Hanspal, K. Fisher, and R. Nieveen, "Prosthetic socket fit comfort score," Disability and rehabilitation, vol. 25, no. 22, pp. 1278-1280, 2003.
[31] N. Hansen, "The CMA evolution strategy: a comparing review," Towards a new evolutionary computation, pp. 75-102, 2006.
[32] C. G. Welker, A. S. Voloshina, V. L. Chiu, and S. H. Collins, "Shortcomings of human-in-the-loop optimization of an ankle-foot prosthesis emulator: a case series," Royal Society open science, vol. 8, no. 5, pp. 202020, 2021.
[33] J. C. Selinger, and J. M. Donelan, "Estimating instantaneous energetic cost during non-steady-state gait," Journal of applied physiology (Bethesda, Md.: 1985), vol. 117, no. 11, pp. 1406-1415, Dec 1, 2014.
[34] M.-A. Brehm, J. Becher, and J. Harlaar, "Reproducibility evaluation of gross and net walking efficiency in children with cerebral palsy," Developmental Medicine & Child Neurology, vol. 49, no. 1, pp. 45-48, 01/01; 2023/08, 2007.
[35] L. Garby, and A. Astrup, "The relationship between the respiratory quotient and the energy equivalent of oxygen during simultaneous glucose and lipid oxidation and lipogenesis," Acta Physiologica Scandinavica, vol. 129, no. 3, pp. 443-444, Mar, 1987.
[36] L. Hak, J. H. van Dieën, P. van der Wurff, and H. Houdijk, "Stepping asymmetry among individuals with unilateral transtibial limb loss might be functional in terms of gait stability," Physical Therapy, vol. 94, no. 10, pp. 1480-1488, Oct, 2014.
[37] J. M. Donelan, R. Kram, and A. D. Kuo, "Simultaneous positive and negative external mechanical work in human walking," Journal of Biomechanics, vol. 35, no. 1, pp. 117-124, Jan, 2002.

[38] T. C. Pataky, “Generalized n-dimensional biomechanical field analysis using statistical parametric mapping,” Journal of Biomechanics, vol. 43, no. 10, pp. 1976-1982, 2010.

[39] H. van der Linde, C. J. Hofstad, A. C. H. Geurts, K. Postema, J. H. B. Geertzen, and J. van Limbeek, “A systematic literature review of the effect of different prosthetic components on human functioning with a lower-limb prosthesis,” Journal of rehabilitation research and development, vol. 41, no. 4, pp. 555-570, Jul, 2004.

[40] J. Kim, B. T. Quinlivan, L.-A. Deprey, D. Arumukhom Revi, A. Eckert-Erdheim, P. Murphy, D. Orzel, and C. J. Walsh, “Reducing the energy cost of walking with low assistance levels through optimized hip flexion assistance from a soft exosuit,” Scientific reports, vol. 12, no. 1, pp. 11004, 2022.

[41] Y. Ding, M. Kim, S. Kuindersma, and C. J. Walsh, “Human-in-the-loop optimization of hip assistance with a soft exosuit during walking,” Science robotics, vol. 3, no. 15, pp. eaar5438., Feb 28, 2018.

[42] C. H. Shea, and R. M. Kohl, “Specificity and variability of practice,” Research quarterly for exercise and sport, vol. 61, no. 2, pp. 169-177, 1990.

[43] G. Wulf, and R. A. Schmidt, “Variability of practice and implicit motor learning,” Journal of Experimental Psychology: Learning, Memory, and Cognition, vol. 23, no. 4, pp. 987, 1997.

[44] K. L. Poggensee, and S. H. Collins, “How adaptation, training, and customization contribute to benefits from exoskeleton assistance,” Science Robotics, vol. 6, no. 58, 2021.

[45] A. D. Kuo, J. M. Donelan, and A. Ruina, “Energetic consequences of walking like an inverted pendulum: step-to-step transitions,” Exercise and sport sciences reviews, vol. 33, no. 2, pp. 88-97, Apr, 2005.

[46] [46] M. Kim, and S. H. Collins, “Once-per-step control of ankle-foot prosthesis push-off work reduces effort associated with balance during walking,” Journal of neuroengineering and rehabilitation, vol. 12, pp. 43-3, May 1, 2015.

[47] H. Houdijk, I. J. Blokland, S. A. Nazier, S. V. Castenmiller, I. van den Heuvel, and T. Ijmker, “Effects of Handrail and Cane Support on Energy Cost of Walking in People With Different Levels and Causes of Lower Limb Amputation,” Archives of Physical Medicine and Rehabilitation, vol. 102, no. 7, pp. 1340-1346.e3, Jul, 2021.

[48] S. M. O'Connor, H. Z. Xu, and A. D. Kuo, "Energetic cost of walking with increased step variability," Gait & posture, vol. 36, no. 1, pp. 102-107, May 2012, 2012.

[49] D. S. Williams, and A. E. Martin, "Gait modification when decreasing double support percentage," Journal of Biomechanics, vol. 92, pp. 76-83, 19 July 2019, 2019.

[50] R. Candau, A. Belli, G. Y. Millet, D. Georges, B. Barbier, and J. D. Rouillon, "Energy cost and running mechanics during a treadmill run to voluntary exhaustion in humans," European journal of applied physiology and occupational physiology, vol. 77, pp. 479-485, 1998.

[51] P.-C. Kao, C. Lomasney, Y. Gu, J. P. Clark, and H. A. Yanco, "Effects of induced motor fatigue on walking mechanics and energetics," Journal of Biomechanics, vol. 156, pp. 111688, July 2023, 2023.

[52] M. A. Diaz, M. Vos, A. Dillen, B. Tassignon, L. Flynn, J. Geeroms, R. Meeusen, T. Verstraten, J. Babic, P. Beckerle, and K. De Pauw, "Human-in-the-Loop Optimization of Wearable Robotic Devices to Improve Human-Robot Interaction: A Systematic Review," IEEE transactions on cybernetics, vol. 53, no. 12, pp. 7483-7496, Dec, 2023.

[53] K. A. Ingraham, M. Tucker, A. D. Ames, E. J. Rouse, and M. K. Shepherd, "Leveraging user preference in the design and evaluation of lower-limb exoskeletons and prostheses," Current Opinion in Biomedical Engineering, pp. 100487, 2023.

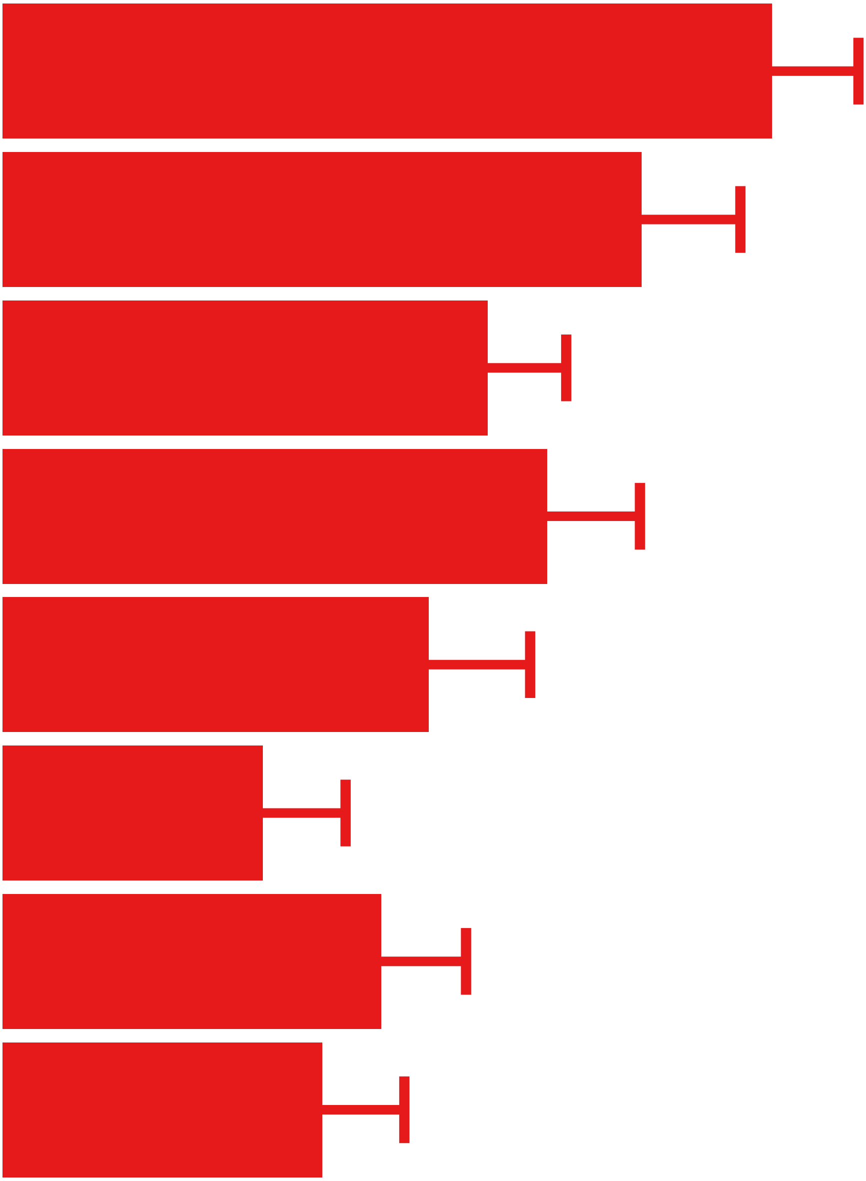

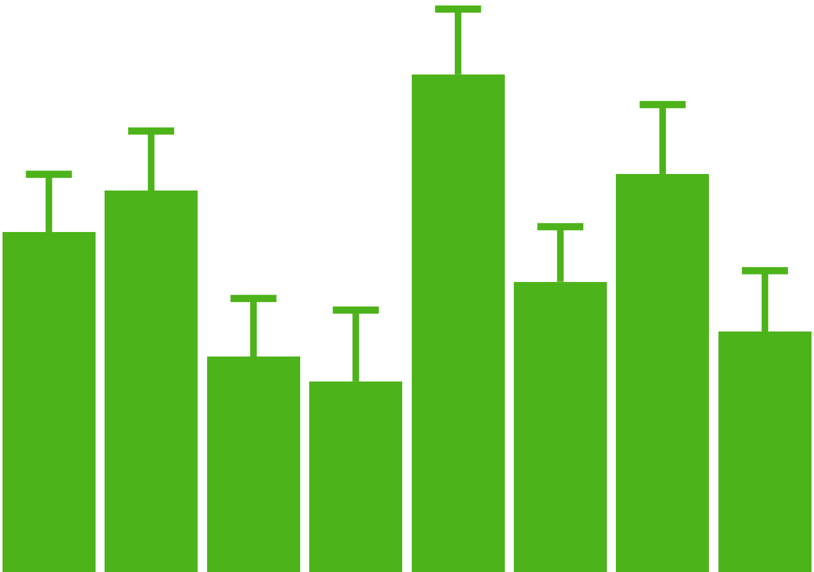

Chapter 5

Time course of motor learning during human-in-the-loop optimization of a prosthetic foot

Thijs Tankink
Juha M. Hijmans
Raffaella Carloni
Han Houdijk

Human Movement Science (2025), 104, 103418.

Abstract

Introduction: People with a lower-limb amputation must undergo a process of co-adaptation with a prosthesis to achieve optimal walking performance. Human-in-the-loop optimization could identify optimal prosthetic settings, while also providing insight into the process of motor learning during prosthetic tuning. The aim of the study was to investigate the time course of motor learning of people with transtibial amputation during the human-in-the-loop optimization process of a prosthetic foot, in which the stiffness and alignment were optimized to minimize metabolic cost. *Methods*: Ten people with a transtibial amputation underwent an optimization protocol while walking on an instrumented treadmill with an experimental prosthetic foot with tuneable stiffness and alignment. We aimed to minimize the metabolic cost of walking by optimizing the stiffness and alignment, using an evolutionary optimization algorithm consisting of six generations of six trials. To monitor motor learning throughout the optimization process, motor learning trials with initial standard settings were repeated after each generation. Occurrence of motor learning over time was assessed by comparing metabolic cost and walking biomechanics during motor learning trials. *Results*: Metabolic cost during the motor learning trials decreased significantly ($\geq$ 6.8%) over time ($p = 0.01$). This reduction in metabolic cost was limited to the first four generations of the optimization process (i.e., 56 min). *Conclusion*: Motor learning of people with a transtibial amputation plays a significant role during prosthetic tuning. Motor learning extended over at least 56 min in our human-in-the-loop optimization experiment. Co-adaptation of the user should therefore be taken into account during tuning of prosthetic devices.

Keywords

Prosthetic foot, transtibial amputation, motor learning, human-in-the-loop optimization, metabolic cost

5.1. Introduction

A lower-limb prosthesis imposes challenges on human movement performance of people with lower-limb amputation. They must undergo a process of co-adaptation with a prosthesis to achieve optimal walking performance. During walking, humans tend to choose the gait pattern that minimizes metabolic energy [1, 2], adopting gait parameters such as step frequency, joint kinetics, or muscle activation patterns accordingly [3-7]. The use of a prosthesis and its mechanical settings can significantly affect the prioritization of optimization criteria (e.g., metabolic cost, balance, prosthetic comfort) [8-10] throughout the adaptation process, and, therefore, affect the adopted gait pattern [11]. This highlights the importance of co-adaptation between the user and prosthesis to enable optimal amputee walking.

To allow optimal co-operation between the user and its prosthesis, optimal prosthetic settings should be found. Previous research already showed that a foot design that matches the activity level of the amputee provides a better match between the user and the prosthesis [12]. Individually adapting prosthetic settings to the specific user's needs could potentially further improve this co-operation [7, 13]. This process, called prosthetic tuning, involves not only adapting prosthetic settings to the user, but also requires motor adaptation of the user. The user needs to continuously adapt to changes made to the prosthetic settings during the tuning process. Alongside these immediate motor adaptations, long-term motor learning also occurs. This is the process by which the user learns how to walk with a new prosthesis, resulting in long-term changes in motor behavior.

5

It remains unclear how the process of motor learning evolves and how it might affect prosthetic tuning. In prosthetic research, the time provided for motor learning to occur, often referred to as accommodation time, varies greatly, ranging from just minutes [7, 14] to several weeks [12, 15, 16]. Various theories about the process of motor learning exist [17]. Abram et al. [18] observed that motor learning involves an initial increase in movement variability, allowing the human to explore and discover different movement executions, followed by a decrease with experience leading to changes in the execution of different gait variables [18, 19]. In contrast, Wurdeman et al. [12] described the motor learning process with a prosthesis as formulated by Bernstein [20], in which the human system initially freezes the different degrees of freedom and becomes more rigid, followed by freeing the degrees of freedom to make the system more flexible and adaptable with experience. Altogether, it remains unknown how people with an amputation learn how to walk with a new prosthesis and how they are capable to adapt to changes in the mechanical settings during the tuning process.

An approach that could be adopted to search for optimal prosthetic settings in the presence of motor learning is human-in-the-loop optimization [21, 22]. During human-in-the-loop optimization, the human is included 'in vivo' in the iterative optimization loop and prosthetic settings are systematically varied during the optimization process using an optimization algorithm in response to measured performance. By using human-in-the-loop optimization during the tuning process, the prosthetic settings can be tuned to the biophysical properties of the user [23], while also taking into account the natural behavior of humans to simultaneously optimize their movement control with respect to walking performance [1].

Besides being an approach to tune prosthetic settings, human-in-the-loop optimization could provide a unique insight into the process of motor learning during prosthetic tuning. It allows to assess motor learning apart from the effects of prosthetic adaptation over the time course of the process. Previous research [24] also showed that human-in-the-loop optimization has the potential to speed up the motor learning process. Its feature of large variation in device settings followed by more refined practice near the optimal solution has been claimed to facilitate motor learning and the capability to adapt to changing settings compared to practice with high or no variation in device settings in the case of exoskeleton optimization [24]. Nevertheless, the process of motor learning is rather context dependent [25], and it remains unclear how motor learning of people with an amputation evolves in the context of prosthetic tuning via human-in-the-loop optimization.

Therefore, the aim of the study is to investigate the time course of motor learning of people with a transtibial amputation during the human-in-the-loop optimization process of a prosthetic foot, in which the stiffness and alignment are optimized to minimize the metabolic cost of walking. Furthermore, we want to explore which underlying neuromechanical adaptations, i.e., changes in movement execution or movement variability, could account for the expected reduction in metabolic cost during the motor learning process. Eventually, the knowledge gathered in this study will provide insight into how motor learning affects the process of prosthetic tuning.

5.2. Method

5.2.1. Participants

10 individuals with a unilateral transtibial amputation participated in this study. Inclusion criteria were: age ≥ 18 years, shoe size 41 – 45, amputation over one year ago, and independent prosthetic walking (MFC-level ≥ K3). Exclusion criteria were: other conditions or drugs affecting balance or gait, use of orthopedic footwear or osseo-integrated prosthesis, or current issues with their prosthesis or socked. The study protocol was approved by the medical ethics committee of the University Medical Center Groningen (protocol number 17321), the Netherlands. All participants were informed about the study and provided written informed consent before the start of the experiments.

5.2.2. The tunable prosthetic foot: MyFlex-η

We used the MyFlex-η, an energy storing and return prosthetic foot prototype [26-28] with manually tunable stiffness and alignment (Figure 5.1), in combination with an Össur foot shell and regular walking shoes (Chris, Dr Comfort, Mequon, WI, USA), with a combined mass of 1.75 kg.

Alignment was defined as the pylon-to-vertical angle while the shoe was flat but unloaded on the ground (range 0 – 10° dorsiflexion; intervals of 1°). Stiffness (range: 3.28 – 5.15 Nm/°) was described by the following equation:

$$k = 1.722 + 0.063 \cdot Dx - 0.09386 \cdot \alpha \qquad (5.1)$$

where k is the stiffness in Nm/°, Dx is the length of the Dx slider in mm (range: 40 – 55 mm; intervals of 1 mm), and α is the alignment expressed in degrees [29].

5.2.3. Experimental set-up

Measurements were performed on the GRAIL system (Gait Realtime Analysis Interactive Lab; Motekforce Link, Amsterdam) of the Department of Rehabilitation Medicine, University Medical Center Groningen, the Netherlands. The GRAIL consists of a 10-camera motion capture system (Vicon Bonita 10, Oxford, United Kingdom; Fs = 100 Hz) tracking 22 markers (diameter = 14 mm) placed according to the lower-limb Human Body Model 2 [30] and a dual-belt treadmill with two separate force plates incorporated (Motekforce Link; Amsterdam; Fs = 1000 Hz). Respiratory

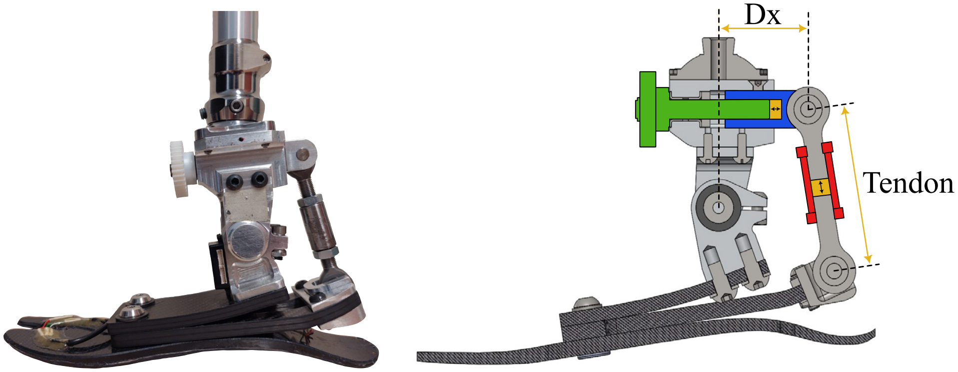

Figure 5.1: Left: The prosthetic foot MyFlex-η with tunable stiffness and tunable alignment [26-28]. Right: a schematic representation. The stiffness and alignment of the prosthetic foot depended on the Dx-length and the tendon length. The Dx-length could be changed by manually turning the knob (green), horizontally translating the position of the Dx-slider (blue) (note that a change in Dx-length affects the alignment as well). The orientation of the foot plate relative to the pylon could be changed by turning the threaded tube adaptor (red) of the tendon link that modifies the tendon length.

data were collected by the portable metabolic analyzer K5 (COSMED, Rome, Italy) in breath-by-breath mode.

5.2.4. Protocol

The protocol (Figure 5.2) consisted of a fitting session and 2 visits to the GRAIL lab. During the fitting session, demographic and body data were collected. A certified prosthetic orthotist fitted the MyFlex-η prosthetic foot to the participant's own prosthetic socket. Participants walked shortly on the prosthetic foot with standard settings (stiffness: 4.24 Nm/°, alignment: 5°; selected as the middle of the stiffness and alignment range) to get familiar with the device.

The first visit at the GRAIL lab consisted of a familiarization period, a pre-test and the first half of the optimization period. The second visit consisted of a warm-up, the second half of the optimization period, and a post-test.

Familiarization period: During the familiarization period, participants chose a self-selected walking speed while using the tunable prosthetic foot with standard settings. The selected speed was maintained during the rest of the protocol.

Pre-test: During the pre-test, participants walked 6 min using the tunable prosthetic foot with standard settings, followed by a 5-min break.

Optimization period: During the optimization period, we aimed to optimize joint stiffness and alignment of the tunable prosthetic foot to minimize metabolic cost. The optimization period consisted of 6 optimization blocks (generations), of 6 trials. The stiffness and alignment of every optimization trial were determined by an evolutionary optimization algorithm [31, 32]. In the first generation, the parameter settings (stiffness and alignment) of the trials were distributed around the middle of the search space of each optimization parameter. After every generation, the 3 trials that resulted in the lowest metabolic cost were used to update the mean and the area of search around this mean, to end up with the optimal stiffness and alignment (Figure 5.2). At the end of each optimization block, a motor learning trial with standard settings was executed to monitor motor learning during the optimization process. Only the results of this motor learning trial, always with the initial standard settings, is reported in this paper. A more detailed description of the optimization protocol and the result on prosthetic foot parameters can be found in the study of Tankink et al. (2025) [29]. In total, participants walked 42 times 120 s on the tunable prosthetic foot with intervening rest periods of 120 s. After every trial, the participant's perceived comfort was determined via the VAS-comfort scale [8] and prosthetic foot settings were adjusted to the imposed stiffness and alignment for the next trial by manually tuning the Dx-length and tendon length.

Post-test: During the post-test, participants walked 3 times 6 min in different foot conditions. 2 times wearing the tunable prosthetic foot with (1) optimal parameter settings found during the optimization period and (2) standard settings in randomized order, followed by (3) a control condition wearing the participant's own prosthetic foot. After every evaluation trial, participants took a 5-min break in which they reported their perceived comfort. Only the post-test using the tunable prosthetic foot with standards settings is reported in this paper.

5.2.5. Data analysis

5.2.5.1. Metabolic cost

To limit measurement time and prevent fatigue in the participants, we used 2-min walking trials and an estimation method [33] to determine metabolic cost. Metabolic cost during the motor learning trials was estimated by fitting a first-order dynamical model with a time constant of 42 s [33] to 120 s of breath-by-breath metabolic

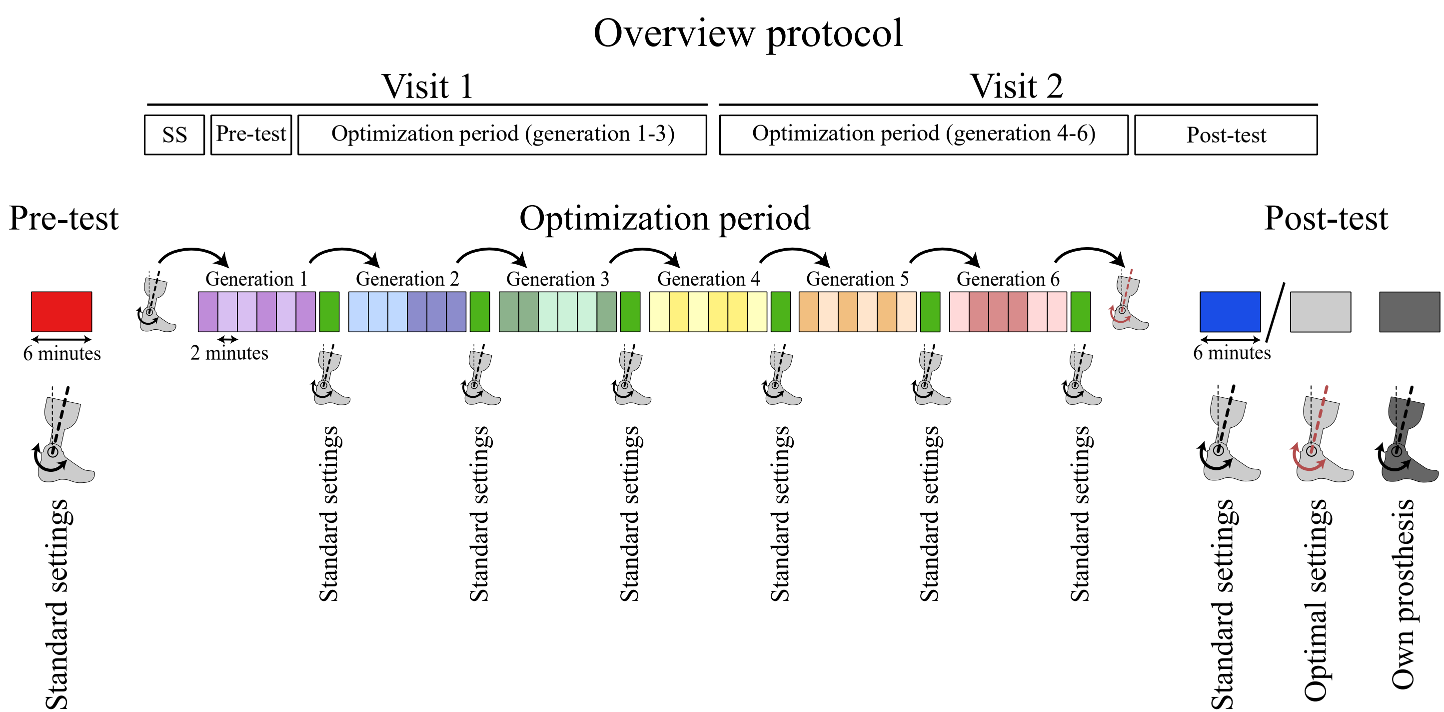

Figure 5.2: Overview of the protocol, consisting of familiarization and determination of self-selected speed (SS), pre-test, optimization period, and post-test. The optimization period consisted of 42 walking trials while walking on the tuneable prosthetic foot with different stiffnesses and alignments. After every generation (6 trials) the 3 trials that resulted in the lowest metabolic cost (darker colours in each generation) were used to determine the prosthetic foot settings of the next generation. Every generation was followed by a motor learning trial (green blocks) with standard settings to monitor motor learning.

measurements [22]. We fitted an exponential curve to the measured O_2 and CO_2 production and used the asymptotes of these fits as an estimate of their steady-state values. During the pre- and post-test, we used the first 120 s of each trial to estimate metabolic cost. Metabolic cost was calculated using the following equation [34]:

$$metabolic\ \ power = 16.04 \cdot \dot{V}O_2 + 4.94 \cdot \dot{V}CO_2 \tag{5.2}$$

where the $metabolic\ \ power$ is in W and $\dot{V}O_2$ and $\dot{V}CO_2$ are expressed in mL/s. Subsequently, we normalized $metabolic\ \ power$ for body mass (W/kg).

Comparing the outcomes of this method with the actual steady-state values during the 6-min evaluation trials, we found a small but systematic overestimation using the estimation method during the pre-test (4.4%) and post-test (4.3%) [35]. As these differences were systematic, we can confidently say that the overall trend in metabolic cost was not affected.

5.2.5.2. Neuromechanical analysis

We used 15 – 120 s of the pre-test, motor learning trials, and post-test for neuromechanical analysis. Kinetic and kinematic data were filtered with a low-pass second-order Butterworth filter with a 6 Hz cut-off frequency. To investigate motor learning on different levels of the whole movement, we calculated step length (variability), step width (variability), and peak ankle power (variability) of the intact leg for every trial. We selected ankle power of the intact leg only, because we anticipated that the intact leg would be most sensitive to motor learning of the user [18] in response to the power produced by the passive prosthetic foot.

We used a custom-made MATLAB (R2023a, MathWorks, Natick, USA) script with a 10 N ground reaction force threshold to detect different steps. Ankle power was extracted from Human Body Model output [30]. To determine average values and variability of step length, step width, and peak ankle power of the intact leg for every trial, we calculated the mean and standard deviation, respectively, over all detected steps.

5.2.6. Statistical analysis

To analyze motor learning over time, we performed repeated measures analyses of variance (ANOVA), in SPSS (version 28.0.1.1, IBM Corp. Armonk, NY, USA), with trial (pre-test, motor learning trial (MLT) 1, MLT 2, MLT 3, MLT 4, MLT 5, MLT 6, post-test) as within-subject factor and metabolic cost as dependent variable. To investigate neuromechanical adaptations over time, we used repeated measures ANOVA with trial (pre-test, MLT 1, MLT 2, MLT 3, MLT 4, MLT 5, MLT 6, post-test) as within-subject factor for step length (variability), step width (variability), and peak ankle power (variability) of the intact leg. To measure perceived comfort, we used repeated measures ANOVA with trial (MLT 1, MLT 2, MLT 3, MLT 4, MLT 5, MLT 6, post-test) as within-subject factor for VAS-comfort score. Participant's own prosthesis comfort scores were presented for reference. For all tests, we used a p-value of 0.05 to indicate statistically significant differences. For post hoc analysis, we used simple contrasts to compare each trial with the pre-test, and Helmert contrasts to compare each trial with the mean of all subsequent trials. If the assumption of sphericity was violated, we used a Greenhouse-Geisser correction.

5.3. Results

5.3.1. Participants

10 people with a transtibial amputation participated in this study. Participant characteristics are presented in Table 5.1.

Table 5.1: Participant characteristics (mean ± standard deviation, n=10).

Reason for amputation[a]	Trauma: 5, Vascular disease: 3, Cancer: 1, Congenital growth disorder: 1
Gender (male : female)[a]	10 : 0
Age (years)	57.2 ± 16.6
Height (cm)	180.0 ± 4.0
Body mass with prosthesis (kg)	85.3 ± 14.6
Time since amputation (years)	16.2 ± 19.7
Shoe size (EU)[b]	42 – 45
Mass personal prosthesis + shoe (kg)	1.34 ± 0.23
Time between lab visits (days)	8.9 ± 8.2
Self-selected walking speed (m/s)	1.02 ± 0.12

[a]Frequencies are given.
[b]Range is given.

5.3.2. Metabolic cost

Metabolic cost differed significantly between trials over the course of the optimization process (Figure 5.3, Table 5.2). Post hoc test with simple contrasts showed that from the fourth motor learning trial (i.e., 56 min of optimization), metabolic cost was significantly reduced compared to the pre-test. The reduction in metabolic cost compared to the pre-test was 10.1% for motor learning trial 4 ($p = 0.02$), 8.3% for motor learning trial 5 ($p = 0.02$), 9.2% for motor learning trial 6 ($p = 0.01$), and 6.8% for the post-test ($p = 0.03$). Helmert contrasts showed that from the third motor learning trial (i.e., 42 min of optimization), metabolic cost did not significantly differ from the mean of all subsequent trials ($p > 0.05$).

5.3.3. Neuromechanical adaptations

Step length and step width differed significantly between trials over the course of the optimization process (Figure 5.4, Table 5.2). Step length during each individual motor learning trial increased compared to the pre-test (Figure 5.4). Step width during

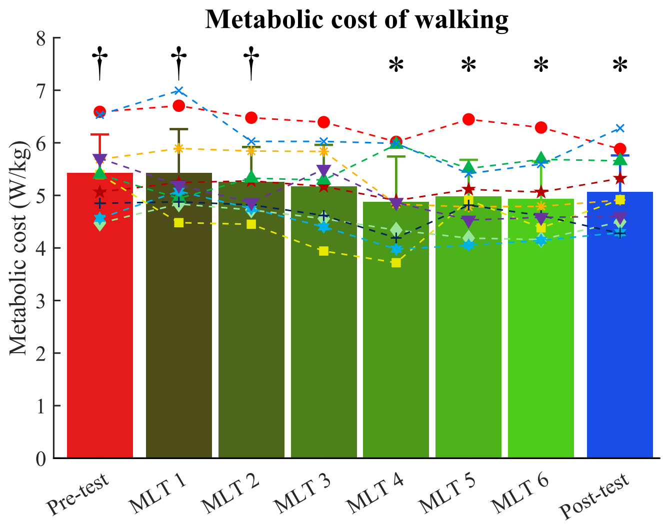

Figure 5.3: Metabolic cost of walking using the tunable prosthetic foot with the standard settings during the pre-test (red), motor learning trials (MLT, green shades), and post-test (blue) (n=10). The colored bars and error bars show mean ± standard deviation. Individual observations are also shown. *Trial is significantly different from pre-test ($p<0.05$). †Trial is significantly different from the mean of all subsequent trials. ($p<0.05$).

Table 5.2: Metabolic cost and different neuromechanical variables during the pre-test, motor learning trial 1-6, and post-test (n=10). Results of the repeated measures analysis of variance for the different variables are also given.

	Pre-test	MLT 1	MLT 2	MLT 3	MLT 4	MLT 5	MLT 6	Post-test	F (7,63)	p	ES[b]
Metabolic cost (W/kg)	5.43 (0.73)	5.43 (0.84)	5.26 (0.66)	5.17 (0.79)	4.88 (0.86)	4.98 (0.70)	4.93 (0.72)	5.06 (0.70)	4.01[a]	**0.014**	0.31
Step length (m)	0.61 (0.07)	0.62 (0.07)	0.62 (0.07)	0.63 (0.07)	0.63 (0.07)	0.63 (0.07)	0.63 (0.07)	0.62 (0.07)	4.09[a]	**0.035**	0.31
Step length variability (mm)	37.9 (17.5)	48.2 (17.9)	48.7 (28.4)	50.4 (23.0)	36.2 (15.6)	37.9 (14.3)	42.3 (16.6)	38.2 (17.2)	1.59[a]	0.228	0.15
Step width (m)	0.15 (0.02)	0.14 (0.02)	0.14 (0.01)	0.13 (0.01)	0.14 (0.02)	0.14 (0.02)	0.14 (0.02)	0.13 (0.02)	3.40[a]	**0.045**	0.27
Step width variability (mm)	34.6 (8.10)	34.2 (5.05)	34.4 (4.18)	35.9 (5.90)	32.3 (3.35)	32.2 (5.20)	33.3 (3.90)	33.1 (6.89)	1.32	0.256	0.13
Peak ankle power (W/kg)	3.97 (1.43)	3.98 (1.17)	4.10 (1.23)	4.01 (1.29)	4.22 (1.36)	4.26 (1.35)	4.17 (1.32)	4.12 (1.31)	1.03[a]	0.391	0.10
Peak ankle power variability (W/kg)	0.59 (0.12)	0.55 (0.14)	0.56 (0.15)	0.60 (0.14)	0.48 (0.11)	0.46 (0.15)	0.52 (0.12)	0.50 (0.11)	3.37[a]	**0.024**	0.27

[a]Greenhouse-Geisser correction was used.
[b]Effect size = partial η^2.

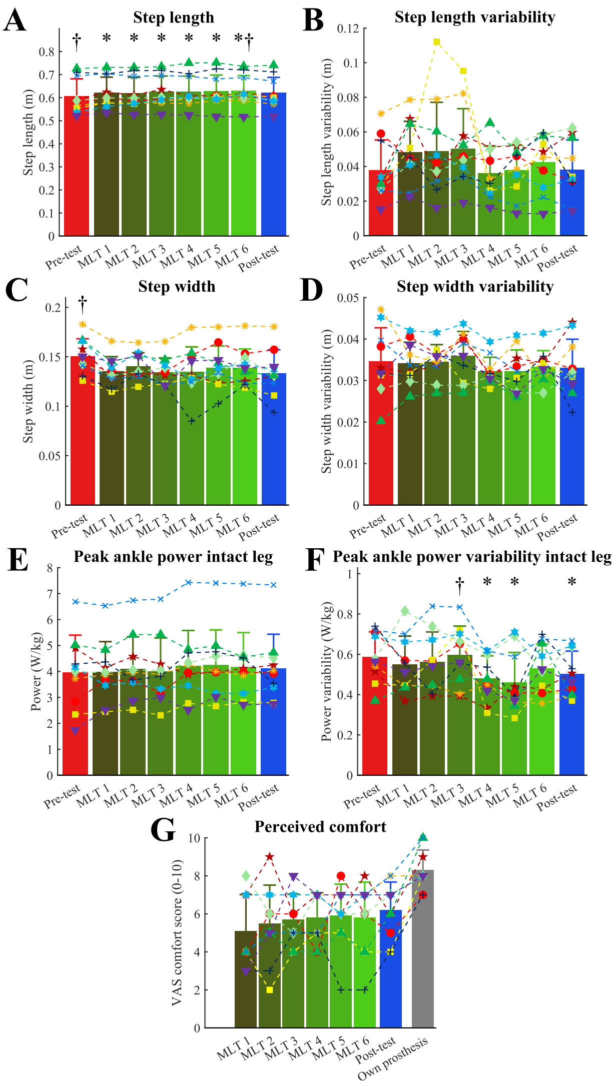

Figure 5.4: Neuromechanical adaptations using the tunable prosthetic foot with the standard settings during the pre-test (red), motor learning trials (MLT, green shades), and post-test (blue) (n=10). A) Step length, B) step length variability, C) step width, D) step width variability, E) peak ankle power of the intact leg, and F) peak ankle power variability of the intact leg are presented. The colored bars and error bars show mean ± standard deviation. Individual observations are also shown. *Trial is significantly different from pre-test ($p<0.05$). †Trial is significantly different from the mean of all subsequent trials. ($p<0.05$). G) Perceived comfort for the motor learning trials, post-test, and own prosthesis (grey) is also presented.

the pre-test was significantly larger (p = 0.002) than the mean of all subsequent trials. Significant differences in step length variability or step width variability were notdfound (Table 5.2). Differences in peak ankle power of the intact leg between trials were not found, but we did find differences in peak ankle power variability (Table 5.2). Peak ankle power variability during motor learning trials 4 and 5, and the post-test was significantly lower than during the pre-test (Figure 5.4).

5.3.4. Perceived comfort

Perceived comfort slowly increased throughout the optimization process, but differences were not significant (F(6,54) = 0.91, p = 0.492; Figure 5.4G).

5.4. Discussion

The aim of this study was to investigate the time course of motor learning of people with a transtibial amputation during human-in-the-loop optimization of prosthetic foot stiffness and alignment to minimize the metabolic cost of walking. Metabolic cost decreased significantly (≥ 6.8%) during the motor learning trials of the optimization process. A reduction in metabolic cost while using the prosthetic foot with standard settings (motor learning trials) was only observed during the first four motor learning trials. This indicates that motor learning had saturated after 28 trials (i.e., 56 min). Thereafter, users appeared adequately accommodated to the new prosthetic device and could further co-adapt with the changing prosthetic foot stiffness and alignment in the context of our human-in-the-loop experiment.

The time frame reported in previous research for people with transtibial amputation to accommodate to a new prosthesis has varied substantially, ranging from just minutes [7, 14] to several weeks [12, 15, 16]. These durations were largely based on subjective assessments or practical experience, and confirmation through systematic measurements was lacking [36, 37]. In people with transfemoral amputation, motor learning of skilled users using a new prosthetic knee saturated within a few hours [36]. Our findings suggest that people with transtibial amputation could accommodate to a new prosthetic foot even faster, i.e., one hour of walking in the context of our experiment, which involved exposure to a wide range of prosthetic settings (i.e., high variability). This variability may have facilitated a faster motor learning process.

Although we did not find clear evidence of underlying neuromechanical adaptations, the trend in movement variability (not all significant) seems to align with the reduction in metabolic cost. During the start of the optimization, we observed a small increase in movement variability, followed by a decrease later in the process (after motor learning had saturated). This could indicate that the human system initially explored new movement executions followed by reduced variability with practice [18, 19], although this did not ultimately lead to adaptive changes in motor behavior.

A neuromechanical adaptation that could account for the reduction in metabolic cost is a shift in strategy of balance control. The shorter and wider steps during the pre-test are characteristic of a gait strategy with generalized anticipatory balance control [38, 39]. The larger step length and smaller step width, combined with the absence of change in step length or step width variability during the end of the optimization process could indicate a shift to the energetically more efficient task-specific reactive control, in which perturbations are handled more on a step-to-step basis [38].

The similarity in trends between perceived comfort score and metabolic cost throughout the motor learning trials of the optimization process supports the potential of user preference as optimization criterion [40]. In the current set-up, only one single cost function (metabolic cost) is used to optimize device parameters, which could overlook other important optimization criteria like stability or pain. Besides that user preference could incorporate different user specific criteria simultaneously [41], the increase in perceived comfort score during the motor learning trials while using the prosthetic foot with standard settings, indicates that user preference also takes motor learning into account.

5.4.1. Limitations

A first limitation of the current study is the number of available steps to determine movement variability. According to Riva et al. [35], the minimum required number of steps to determine variability is 125. In the current study, we used 78 – 178 steps per trial to determine variability. However, this is in line with the study by Abrams et al. [18], who used a minimum of 80 and found that outcomes were not affected.

Another limitation is the extensiveness of the current protocol. Although participants walked on preferred walking speed and walking trial were always followed by a rest period, some participants indicated some fatigue towards the end of their visits. This might have affected metabolic cost [42, 43]. Future studies could control for this by collecting the level of fatigue throughout the protocol

Finally, the motor learning process is known to be context dependent [24, 25]. Therefore, the generalizability of the current course of motor learning to the optimization of devices with varying complexity and adaptability should be approached with caution.

5.5. Conclusion

This study shows that motor learning of people with a transtibial amputation plays a significant role during prosthetic tuning. Motor learning extended over at least 28 optimization trials (i.e., 56 min of optimization) in the context of our human-in-the-loop optimization experiment on metabolic cost. Motor learning should therefore be taken into account when optimizing prosthetic devices, also when human-in-the-loop optimization is not used. More extensive motor learning periods might be included during prosthetic tuning in clinical practice to allow users to accommodate to the different settings.

5.6. Acknowledgments

This work was supported by the European Commission's Horizon 2020 Program as part of the Project MyLeg under Grant 780871. We gratefully acknowledge Johnnidel Tabucol and Marco Leopaldi, the developers of the prototype tuneable prosthetic foot MyFlex-η, for their help throughout the project. We thank Henk Zijlstra, Chris Bolmer, Sandra Loonen, and Auke Postma (certified prosthetists) of OIM Orthopedie (Haren, the Netherlands) for their help with recruitment of participants and connecting and aligning the tunable prosthetic foot. We thank Chengxiang Liu (Doctoral candidate at the University of Groningen), Friso van der Bijl and Pim Rive (Bachelor students University of Groningen) for their help with data collection.

5.7. Reference list

[1] R. M. Alexander, "Optimization and gaits in the locomotion of vertebrates," Physiological Reviews, vol. 69, no. 4, pp. 1199-1227, 1989.

[2] J. E. Bertram, "Constrained optimization in human walking: cost minimization and gait plasticity," Journal of experimental biology, vol. 208, no. 6, pp. 979-991, 2005.

[3] S. J. Abram, J. C. Selinger, and J. M. Donelan, "Energy optimization is a major objective in the real-time control of step width in human walking," Journal of Biomechanics, vol. 91, pp. 85-91, 25 June 2019, 2019.

[4] J. M. Finley, A. J. Bastian, and J. S. Gottschall, "Learning to be economical: the energy cost of walking tracks motor adaptation," The Journal of physiology, vol. 591, no. 4, pp. 1081-1095, 2013.

[5] N. L. Pieper, S. T. Baudendistel, C. J. Hass, G. B. Diaz, R. L. Krupenevich, and J. R. Franz, "The metabolic and mechanical consequences of altered propulsive force generation in walking," Journal of Biomechanics, vol. 122, pp. 110447, Jun 9, 2021.

[6] J. C. Selinger, S. M. O'Connor, J. D. Wong, and J. M. Donelan, "Humans can continuously optimize energetic cost during walking," Current Biology, vol. 25, no. 18, pp. 2452-2456, 2015.

[7] J. D. Ventura, G. K. Klute, and R. R. Neptune, "The effect of prosthetic ankle energy storage and return properties on muscle activity in below-knee amputee walking," Gait & posture, vol. 33, no. 2, pp. 220-226, Feb, 2011.

[8] R. S. Hanspal, K. Fisher, and R. Nieveen, "Prosthetic socket fit comfort

5

score," Disability and rehabilitation, vol. 25, no. 22, pp. 1278-1280, 2003.

[9] C. Kendell, E. D. Lemaire, N. L. Dudek, and J. Kofman, "Indicators of dynamic stability in transtibial prosthesis users," Gait & posture, vol. 31, no. 3, pp. 375-379, Mar, 2010.

[10] L. Hak, J. H. van Dieën, P. van der Wurff, M. R. Prins, A. Mert, P. J. Beek, and H. Houdijk, "Walking in an unstable environment: strategies used by transtibial amputees to prevent falling during gait," Archives of Physical Medicine and Rehabilitation, vol. 94, no. 11, pp. 2186-2193, Nov, 2013.

[11] S. R. Wurdeman, S. A. Myers, A. L. Jacobsen, and N. Stergiou, "Prosthesis preference is related to stride-to-stride fluctuations at the prosthetic ankle," 2013.

[12] S. R. Wurdeman, S. A. Myers, A. L. Jacobsen, and N. Stergiou, "Adaptation and prosthesis effects on stride-to-stride fluctuations in amputee gait," PloS one, vol. 9, no. 6, pp. e100125, 2014.

[13] M. K. Shepherd, A. M. Simon, J. Zisk, and L. J. Hargrove, "Patient-preferred prosthetic ankle-foot alignment for ramps and level-ground walking," IEEE Transactions on Neural Systems and Rehabilitation Engineering, vol. 29, pp. 52-59, 2020.

[14] N. P. Fey, G. K. Klute, and R. R. Neptune, "The influence of energy storage and return foot stiffness on walking mechanics and muscle activity in below-knee amputees," Clinical Biomechanics, vol. 26, no. 10, pp. 1025-1032, December 2011, 2011.

[15] S. F. Ray, S. R. Wurdeman, and K. Z. Takahashi, "Prosthetic energy return during walking increases after 3 weeks of adaptation to a new device," Journal of neuroengineering and rehabilitation, vol. 15, no. 1, pp. 6-1, Jan 27, 2018.

[16] G. K. Klute, J. S. Berge, M. S. Orendurff, R. M. Williams, and J. M. Czerniecki, "Prosthetic intervention effects on activity of lower-extremity amputees," Archives of physical medicine and rehabilitation, vol. 87, no. 5, pp. 717-722, 2006.

[17] R. Cano-de-la-Cuerda, A. Molero-Sánchez, M. Carratalá-Tejada, I. M. Alguacil-Diego, F. Molina-Rueda, J. C. Miangolarra-Page, and D. Torricelli, "Theories and control models and motor learning: Clinical applications in neurorehabilitation," Neurología (English Edition), vol. 30, no. 1, pp. 32-41, January–February 2015, 2015.

[18] S. J. Abram, K. L. Poggensee, N. Sánchez, S. N. Simha, J. M. Finley, S. H. Collins, and J. M. Donelan, "General variability leads to specific adaptation toward optimal movement policies," Current Biology, vol. 32, no. 10, pp. 2222-2232. e5, 2022.

[19] A. K. Dhawale, M. A. Smith, and B. P. Ölveczky, "The role of variability in motor learning," Annual Review of Neuroscience, vol. 40, no. 1, pp. 479-498, 2017.

[20] N. A. Bernstein, "The co-ordination and regulation of movements," 1967.

[21] P. Slade, C. Atkeson, J. M. Donelan, H. Houdijk, K. A. Ingraham, M. Kim, K. Kong, K. L. Poggensee, R. Riener, M. Steinert, J. Zhang, and S. H. Collins, "On human-in-the-loop optimization of human-robot interaction," Nature, vol. 633, no. 8031, pp. 779-788, Sep, 2024.

[22] J. Zhang, P. Fiers, K. A. Witte, R. W. Jackson, K. L. Poggensee, C. G. Atkeson, and S. H. Collins, "Human-in-the-loop optimization of exoskeleton assistance during walking," Science (New York, N.Y.), vol. 356, no. 6344, pp. 1280-1284, Jun 23, 2017.

[23] F. Scotto di Luzio, D. Simonetti, F. Cordella, S. Miccinilli, S. Sterzi, F. Draicchio, and L. Zollo, "Bio-Cooperative Approach for the Human-in-the-Loop Control of an End-Effector Rehabilitation Robot," Frontiers in neurorobotics, vol. 12, pp. 67, Oct 11, 2018.

[24] K. L. Poggensee, and S. H. Collins, "How adaptation, training, and customization contribute to benefits from exoskeleton assistance," Science Robotics, vol. 6, no. 58, 2021.

[25] D. M. Wolpert, and J. R. Flanagan, "Computations underlying sensorimotor learning," Current opinion in neurobiology, vol. 37, pp. 7-11, 2016.

[26] J. Tabucol, M. Leopaldi, T. M. Brugo, M. Oddsson, and A. Zucchelli, "Design and Mechanical Characterization of a Variable Stiffness ESR Foot Prosthesis," IEEE Access, vol. 12, pp. 97544-97556, 2024.

[27] M. Leopaldi, T. M. Brugo, J. Tabucol, and A. Zucchelli, "Parametric Design of an Advanced Multi-Axial Energy-Storing-and-Releasing Ankle–Foot Prosthesis," Prosthesis, vol. 6, no. 4, pp. 726-743, 2024.

[28] J. Tabucol, V. G. M. Kooiman, M. Leopaldi, R. Leijendekkers, G. Selleri, M. Mellini, N. Verdonschot, M. Oddsson, R. Carloni, A. Zucchelli, and T. M. Brugo, "The MyFlex-ζ Foot: a Variable Stiffness ESR Ankle-Foot Prosthesis," IEEE Transactions on Neural Systems and Rehabilitation

5

Engineering, pp. 1, 2025.

[29] T. Tankink, H. Houdijk, J. Tabucol, M. Leopaldi, J. M. Hijmans, and R. Carloni, "Human-in-the-Loop Optimization of the Stiffness and Alignment of a Prosthetic Foot to Reduce the Metabolic Cost of Walking," IEEE Transactions on Neural Systems and Rehabilitation Engineering, 2025.

[30] A. J. van den Bogert, T. Geijtenbeek, O. Even-Zohar, F. Steenbrink, and E. C. Hardin, "A real-time system for biomechanical analysis of human movement and muscle function," Medical & biological engineering & computing, vol. 51, no. 10, pp. 1069-1077, Oct, 2013.

[31] N. Hansen, "The CMA evolution strategy: a comparing review," Towards a new evolutionary computation, pp. 75-102, 2006.

[32] C. G. Welker, A. S. Voloshina, V. L. Chiu, and S. H. Collins, "Shortcomings of human-in-the-loop optimization of an ankle-foot prosthesis emulator: a case series," Royal Society open science, vol. 8, no. 5, pp. 202020, 2021.

[33] J. C. Selinger, and J. M. Donelan, "Estimating instantaneous energetic cost during non-steady-state gait," Journal of applied physiology (Bethesda, Md.: 1985), vol. 117, no. 11, pp. 1406-1415, Dec 1, 2014.

[34] L. Garby, and A. Astrup, "The relationship between the respiratory quotient and the energy equivalent of oxygen during simultaneous glucose and lipid oxidation and lipogenesis," Acta Physiologica Scandinavica, vol. 129, no. 3, pp. 443-444, Mar, 1987.

[35] F. Riva, M. C. Bisi, and R. Stagni, "Gait variability and stability measures: Minimum number of strides and within-session reliability," Computers in biology and medicine, vol. 50, pp. 9-13, 2014.

[36] T. Schmalz, M. Bellmann, E. Proebsting, and S. Blumentritt, "Effects of adaptation to a functionally new prosthetic lower-limb component: Results of biomechanical tests immediately after fitting and after 3 months of use," JPO: Journal of Prosthetics and Orthotics, vol. 26, no. 3, pp. 134-143, 2014.

[37] N. Olaya-Mira, L. M. Gómez-Hernández, C. Viloria-Barragán, and I. C. Soto-Cardona, "Methods to assess lower limb prosthetic adaptation: a systematic review," Journal of NeuroEngineering and Rehabilitation, vol. 22, no. 1, pp. 100, 2025.

[38] S. Ahuja, and J. R. Franz, "The metabolic cost of walking balance control and adaptation in young adults," Gait & posture, vol. 96, pp. 190-194, July 2022, 2022.

[39] S. M. O'Connor, H. Z. Xu, and A. D. Kuo, "Energetic cost of walking with increased step variability," Gait & posture, vol. 36, no. 1, pp. 102-107, May, 2012.

[40] K. A. Ingraham, M. Tucker, A. D. Ames, E. J. Rouse, and M. K. Shepherd, "Leveraging user preference in the design and evaluation of lower-limb exoskeletons and prostheses," Current Opinion in Biomedical Engineering, pp. 100487, 2023.

[41] K. A. Ingraham, C. D. Remy, and E. J. Rouse, "The role of user preference in the customized control of robotic exoskeletons," Science robotics, vol. 7, no. 64, pp. eabj3487, 2022.

[42] R. Candau, A. Belli, G. Y. Millet, D. Georges, B. Barbier, and J. D. Rouillon, "Energy cost and running mechanics during a treadmill run to voluntary exhaustion in humans," European journal of applied physiology and occupational physiology, vol. 77, pp. 479-485, 1998.

[43] P.-C. Kao, C. Lomasney, Y. Gu, J. P. Clark, and H. A. Yanco, "Effects of induced motor fatigue on walking mechanics and energetics," Journal of Biomechanics, vol. 156, pp. 111688, July 2023, 2023.

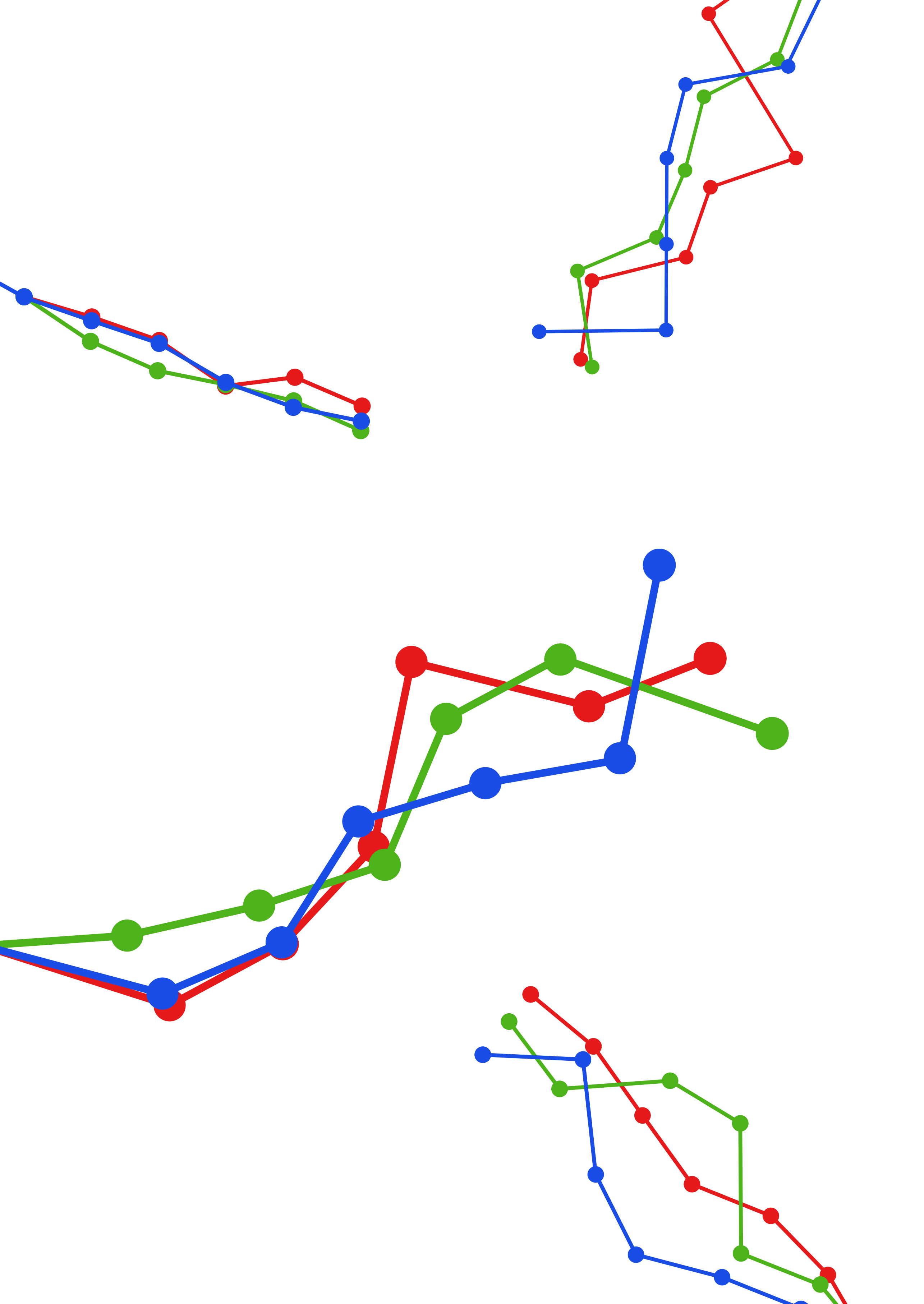

Chapter 6

Effects of walking speed on human-in-the-loop optimized settings and performance of a prosthetic foot: a case-series

Thijs Tankink
Juha M. Hijmans
Han Houdijk
Raffaella Carloni

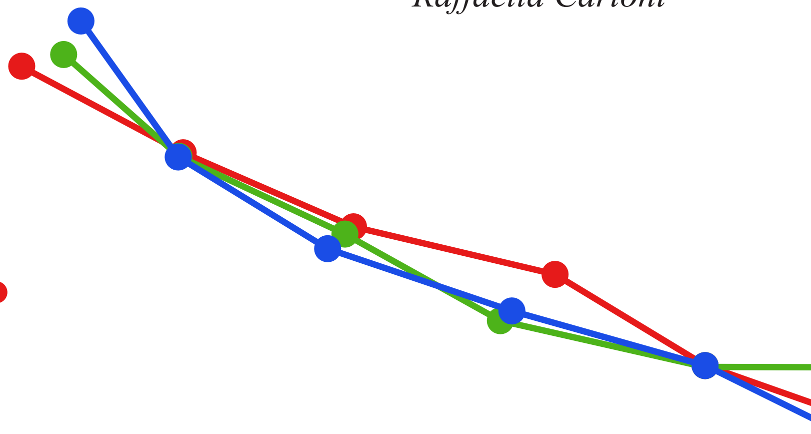

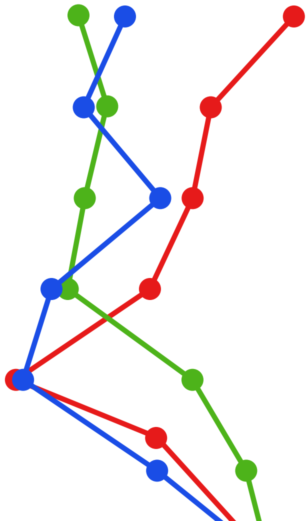

Submitted for publication.

Abstract

Prosthetic prescription for people with a lower-limb amputation involves selecting and tuning prosthetic settings that allow optimal co-operation between the user and the prosthesis. A standardized approach for determining individually optimized prosthetic settings is provided by human-in-the-loop optimization, which is typically performed at a fixed comfortable walking speed. However, to allow optimal gait performance at different walking speeds, different prosthetic settings might be required. The aim of the current study is to explore whether optimal prosthetic foot settings (stiffness and alignment) obtained via human-in-the-loop optimization with the aim of reducing the metabolic cost of walking of transtibial amputees, depend on the walking speed. Three transtibial amputees using an experimental prosthetic foot with tunable stiffness and alignment underwent human-in-the-loop optimization protocols using different walking speeds (self-selected speed and 120% self-selected speed). We aimed to minimize the metabolic cost of walking by optimizing the stiffness and alignment at different walking speeds, using an evolutionary optimization algorithm. The metabolic cost while walking with both optimal settings was compared at both self-selected speed and 120% self-selected speed. We found small differences in optimal prosthetic foot settings between walking speeds, but the direction of change differed between participants. The differences in optimal settings did not result in a clear trend or meaningful change in metabolic cost of walking (range: -2.7 – +4.8%), which suggests that prosthetic foot settings optimized for self-selected walking speed could be used effectively across a broader range of walking speeds.

Keywords

Prosthetic foot, human-in-the-loop optimization, metabolic cost, gait, transtibial amputation

6.1. Introduction

Prosthetic prescription for people with a lower-limb amputation involves selecting and tuning prosthetic settings, e.g., stiffness, alignment or roll-over shape, that allow optimal co-operation between the user and the prosthesis [1]. In current practice, the process of prosthetic tuning is primarily performed by trial and error based on subjective observations and empirical knowledge of the clinical specialist involved [2]. However, this subjective approach lacks solid evidence base and is getting more complex as the number of tunable prosthetic components and their variety in settings continue to grow.

A standardized approach for determining individualized optimal prosthetic settings, that could also handle their growing complexity, is provided by human-in-the-loop optimization [3, 4]. In this method, the human is included 'in vivo' in the iterative optimization loop, and the prosthetic settings are systematically varied during the optimization process using an optimization algorithm in response to a measured performance. By using human-in-the-loop optimization during the tuning process, the prosthetic settings can be tuned to the biophysical properties of the user [5], while also taking into account the natural adaptive behavior of the human, as they simultaneously optimize their movement control in response to changes in device settings to enhance the gait performance [6].

To enable accurate comparison between different prosthetic settings, human-in-the-loop optimization is typically performed in controlled conditions, e.g., at a fixed walking speed [7-9], which might result in optimal settings that are quite condition dependent. However, the use of a fixed walking speed is the exception rather than the norm during real-world walking [10, 11]. In daily life, people continuously adapt walking speed due to different intentions and environmental constraints.

To allow optimal gait performance at these different walking speeds, different prosthetic settings might be required. Previous research has shown that user preference of prosthetic alignment while walking on level-ground and ramps was speed dependent [12]. Additionally, user preference of prosthetic stiffness was found to differ between walking speeds [13, 14]. Moreover, prosthetic settings tuned for a specific walking speed have shown to be able to enhance user performance [15]. A variable-stiffness prosthesis has shown to increase push-off power and energy return at a range of walking speeds compared to a passive device of a fixed stiffness, with a higher stiffness being more beneficial for higher walking speeds [15]. It could hence be hypothesized that individually tuned prosthetic settings using human-in-the-loop optimization are speed dependent. However, it remains unknown whether human-in-the-loop optimization will result in different optimal settings at different walking speeds and to what extent optimizing prosthetic settings for each different speed is necessary.

In a previous study, we have shown that human-in-the-loop optimization of the stiffness and alignment of a prosthetic foot was able to reduce the metabolic cost of walking of transtibial amputees by 10% [8]. The current study builds upon previous work and aims to explore whether optimal prosthetic foot settings, i.e., stiffness and alignment, obtained via human-in-the-loop optimization depend on the walking speed. We were interested to see whether optimal prosthetic stiffness and alignment differ between walking speeds, and to what extent these potentially different settings affect metabolic cost of walking during these walking speeds.

6.2. Method

6.2.1. Participants

This study was conducted as an extension of the study of Tankink et al. (2025) [8], in which ten individuals with a unilateral transtibial amputation participated. Given the extended protocol required optimization at high walking speed (120% of self-selected walking speed), only the most physically fit and adaptive participants were considered capable completing the protocol at higher walking speed and were invited to participate in this follow-up study. The study protocol was approved by the medical ethics committee of the University Medical Center Groningen (protocol number 17321), the Netherlands. All participants were informed about the study and provided written informed consent before the start of the experiments.

6.2.2. The tunable prosthetic foot: MyFlex-η

In this study, we used the MyFlex-η, an energy storing and return prosthetic foot prototype [16-18] (Figure 6.1) with tunable stiffness and tunable alignment, in combination with an Össur foot shell and regular walking shoes (Chris, Dr Comfort, Mequon, WI, USA), with a combined mass of 1.75 kg.

Alignment was defined as the pylon-to-vertical angle while the shoe was flat but unloaded on the ground (range 0 – 10° dorsiflexion; intervals of 1°). Stiffness (range: 3.28 – 5.15 Nm/°) was described by the following equation:

$$k = 1.722 + 0.063 \cdot Dx - 0.09386 \cdot \alpha \tag{6.1}$$

where k is the stiffness in Nm/°, Dx is the length of the Dx slider in mm (range: 40 – 55 mm; intervals of 1 mm), and α is the alignment expressed in degrees [8].

6.2.3. Experimental set-up

Measurements were performed using the GRAIL system (Gait Realtime Analysis Interactive Lab; Motekforce Link, Amsterdam) of the Department of Rehabilitation Medicine, University Medical Center Groningen, the Netherlands. The GRAIL consists of ten-camera motion capture system (Vicon Bonita 10 during visit 1 and 2, and Vicon Vero during visit 3 and 4; Oxford, United Kingdom; Fs = 100 Hz) that registered the marker trajectories of 22 markers (diameter = 14 mm) placed according to the lower-limb Human Body Model 2 [19] and a dual-belt treadmill with two separate force plates incorporated in the treadmill (Motekforce Link; Amsterdam; Fs

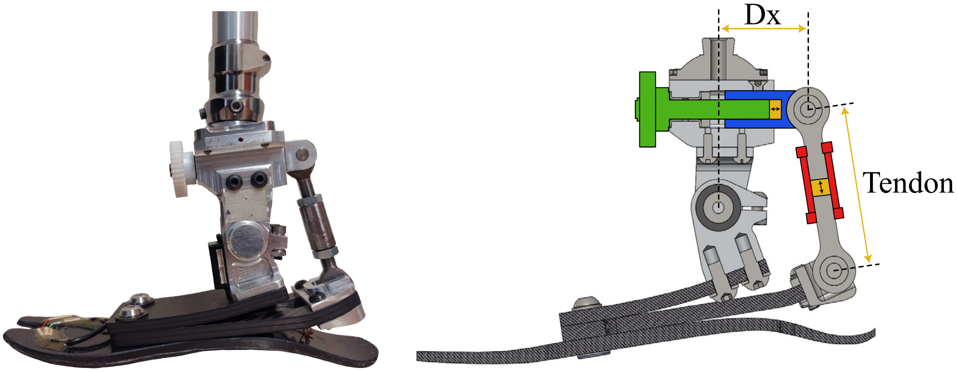

Figure 6.1: Left: The prosthetic foot MyFlex-η with tunable stiffness and tunable alignment [14, 17, 18]. Right: A schematic representation. The stiffness and alignment of the prosthetic foot depended on the Dx-length and the tendon length. The Dx-length could be changed by manually turning the knob (green), horizontally translating the position of the Dx-slider (blue) (note that a change in Dx-length affects the alignment as well). The orientation of the foot plate relative to the pylon could be changed by turning the threaded tube adaptor (red) of the tendon link that modifies the tendon length.

= 1000 Hz). Respiratory data were collected by the portable metabolic analyzer K5 (COSMED, Rome, Italy) in breath-by-breath mode, i.e. integrating continuous flow and gas signals over every breathing cycle. Measurement systems were calibrated according to the recommended calibration protocols of the manufacturers.

6.2.4. Protocol

The protocol consisted of a fitting session and four visits to the GRAIL lab. The first two visits were part of the original protocol and described in more detail in Tankink et al. (2025) [8].

During the fitting session, demographic and anthropometric data were collected. A certified prosthetic orthotist fitted the MyFlex-η prosthetic foot to the participant's own prosthetic socket. Participants walked shortly on the prosthetic foot with standard settings (stiffness: 4.24 Nm/°, alignment: 5°; selected as the middle of the stiffness and alignment range) to get familiar with the device. Participants used the tunable prosthetic foot during the rest of the protocol. The first visit to the GRAIL lab consisted of a familiarization period, in which participants chose a self-selected walking speed while using the tunable prosthetic foot with standard settings. In addition, the first half of the optimization trials at self-selected speed were performed. The second visit consisted of a warm-up at self-selected walking speed, and the second half of the optimization trials at self-selected speed. The third visit consisted of a warm-up at high walking speed (120% self-selected speed), and the first part of the optimization trials at high walking speed. The fourth visit consisted of a warm-up at high walking speed, the second part of the optimization trials at high walking speed, and an evaluation period.

Optimization periods: During the optimization periods, we aimed to optimize joint stiffness and alignment of the tunable prosthetic foot to minimize the metabolic cost of walking. The optimization period at self-selected speed consisted of 36 walking trials (6 optimization blocks of 6 trials) [8]. The optimization period at high walking speed consisted of 30 walking trials (5 optimization blocks of 6 trials). The optimization period at high speed was reduced with 1 block, because we could start with a better guess of initial settings (see section *6.2.5. Optimization algorithm*) and to prevent fatigue due to the higher walking speed. Every walking trial of 120 s was followed by a rest period of 120 s. The foot stiffness and alignment of every optimization trial were determined by an evolutionary optimization algorithm (see section *6.2.5. Optimization algorithm*). After every trial, the prosthetic foot settings were adjusted to the imposed stiffness and alignment for the next trial by manually tuning the Dx-length and tendon length.

Evaluation period: During the evaluation period, participants walked 4 times 6 min using the tunable prosthetic foot in 2 different speed conditions; self-selected speed and high speed. At each speed, participants used the prosthetic foot with optimal parameter settings found during the optimization period at self-selected speed, and the prosthetic foot with optimal settings found during the optimization period at high walking speed. Every trial was followed by a rest period of 5 min. The order of conditions was randomized.

6.2.5. Optimization algorithm

We used a covariance matrix adaptation evolution strategy (CMA-ES) [20] to optimize the stiffness and alignment of the prosthetic foot. The calculated values of the metabolic cost during the different walking trials were used as input for the optimization algorithm. The algorithm used a predetermined number of measurements, forming 1 generation, to determine the parameter values of the next generation. Every generation consisted of 6 trials [7, 20]. During the optimization period at self-selected walking speed, we chose to explore 6 generations with a generation size of 6, and the parameter settings (stiffness & alignment) of the trials in the first generation were distributed around the middle of the search space of each optimization parameter, i.e., the standard settings of the prosthetic foot [8]. The area of the search space was determined by σ, i.e., the standard deviation of parameter values within every generation ($\sigma_{initial}$ = 0.50 after standardization of each optimization parameter). After every generation, the settings of the 3 trials that resulted in the lowest metabolic cost were used to update the mean of the search space of the next generation, which represented the best estimate of the optimal parameter values, and the area of search (σ) around this mean to end up with the optimal joint stiffness and alignment. Eventually, the mean calculated after the final generation presented the best estimate of the optimal settings and were used as optimal parameter values for self-selected speed.

During the optimization period at high walking speed, we chose to explore 5 generations, and the parameter settings of the trials in the first generation were distributed around the optimal parameter values found during the optimization period at self-selected speed ($\sigma_{initial}$ = 0.50 after standardization of each optimization parameter). Eventually, the mean calculated after the final generation presented the best estimate of the optimal settings and were used as optimal parameter values for high walking speed.

6.2.6. Data analysis

Metabolic cost during the optimization trials was estimated by fitting a first-order dynamical model with a time constant of 42 s [11] to 120 s of breath-by-breath metabolic measurements, because it has shown to provide a good balance between limiting estimation errors and trial duration [4]. We fitted an exponential curve to the measured $\dot{V}O_2$ consumption and $\dot{V}CO_2$ production and used the asymptotes of these fits as an estimate of their steady state values. During the evaluation trials, we determined the steady state $\dot{V}O_2$ and $\dot{V}CO_2$ based on their mean values over the last 2 min of each trial to calculate metabolic cost of walking. Gross energy consumption was used to account for variations in resting energy consumption between measurement days [21]. Metabolic cost was calculated using the equation the equation of Garby and Astrup [22]:

$$metabolic\ \ power = 16.04 \cdot \dot{V}O_2 + 4.94 \cdot \dot{V}CO_2 \tag{6.2}$$

where the $metabolic\ \ power$ is in W and $\dot{V}O_2$ and $\dot{V}CO_2$ are expressed in mL/s. Subsequently, we normalized $metabolic\ \ power$ for body mass (W/kg).

6.2.7. Data presentation

6.2.7.1. Optimization period

The progression of stiffness and alignment settings, and their corresponding metabolic cost of walking, were investigated throughout the optimization period at self-selected and high walking speed. We fitted a linear regression equation to the measured metabolic cost to determine its slope as function of time.

Optimal prosthetic foot stiffness and alignment settings obtained during the optimization period at the different walking speeds (self-selected and high) were reported and compared between speeds for every participant.

6.2.7.2. Evaluation period

Metabolic cost of walking for the four different walking conditions during the evaluation period for every participant were reported and compared:

1. Self-selected speed foot (prosthetic foot settings optimal for self-selected speed at self-selected walking speed
2. Self-selected speed foot (prosthetic foot settings optimal for self-selected speed) at high walking speed
3. High-speed foot (prosthetic foot settings optimal for high speed) at self-selected walking speed
4. High-speed foot (prosthetic foot settings optimal for high speed) at high walking speed

6.3. Results

6.3.1. Study population characteristics

5 out of 10 participants were invited to participate in this follow-up study [8]. 2 participants could not participate due to sickness and prosthetic socket problems. Therefore, 3 individuals with a unilateral transtibial amputation participated in this study. Participant characteristics are presented in Table 6.1. The first visit of the follow-up study, i.e., visit 3, took place 279, 288, and 292 days after visit 2 for participant 1, 2, and 3, respectively. No important changes to the prothesis and participants walking ability occurred between visits.

6.3.2. Optimization period

An overview of the optimization period at self-selected and high walking speed for every participant is presented in Figure 6.2. The prosthetic foot settings of every

Table 6.1: Participant characteristics (n=3).

	Participant 1	Participant 2	Participant 3
Gender	Male	Male	Male
Age (year)	55	23	60
Height (cm)	183	178	175
Body mass with prosthesis (kg)	103.0	58.0	75.9
Reason for amputation	Trauma	CGD	Trauma
Side of amputation	Left	Right	Left
Shoe size (EU)	42	42	42
Self-selected walking speed (m/s)	1.00	1.20	1.20
120% self-selected walking speed (m/s)	1.20	1.44	1.44

CGD = Congenital growth disorder.

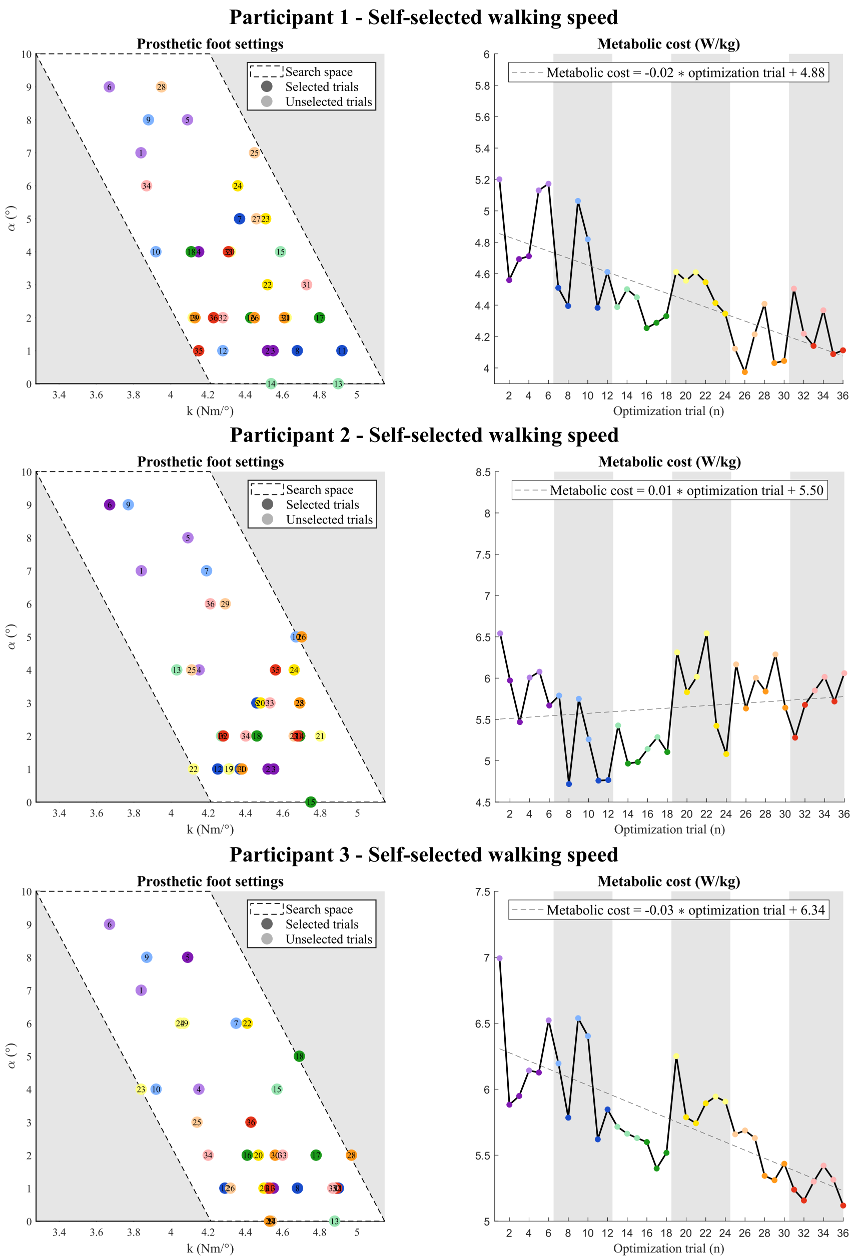

Figure 6.2: Overview of the optimization period at self-selected speed (page 130) and high walking speed (page 131) for every participant. In each subfigure, prosthetic foot stiffness and alignment for every trial (left side of subfigures) and corresponding metabolic cost of walking (right side of subfigures) are presented. The different colors indicate the different generations, which are also indicated by the...

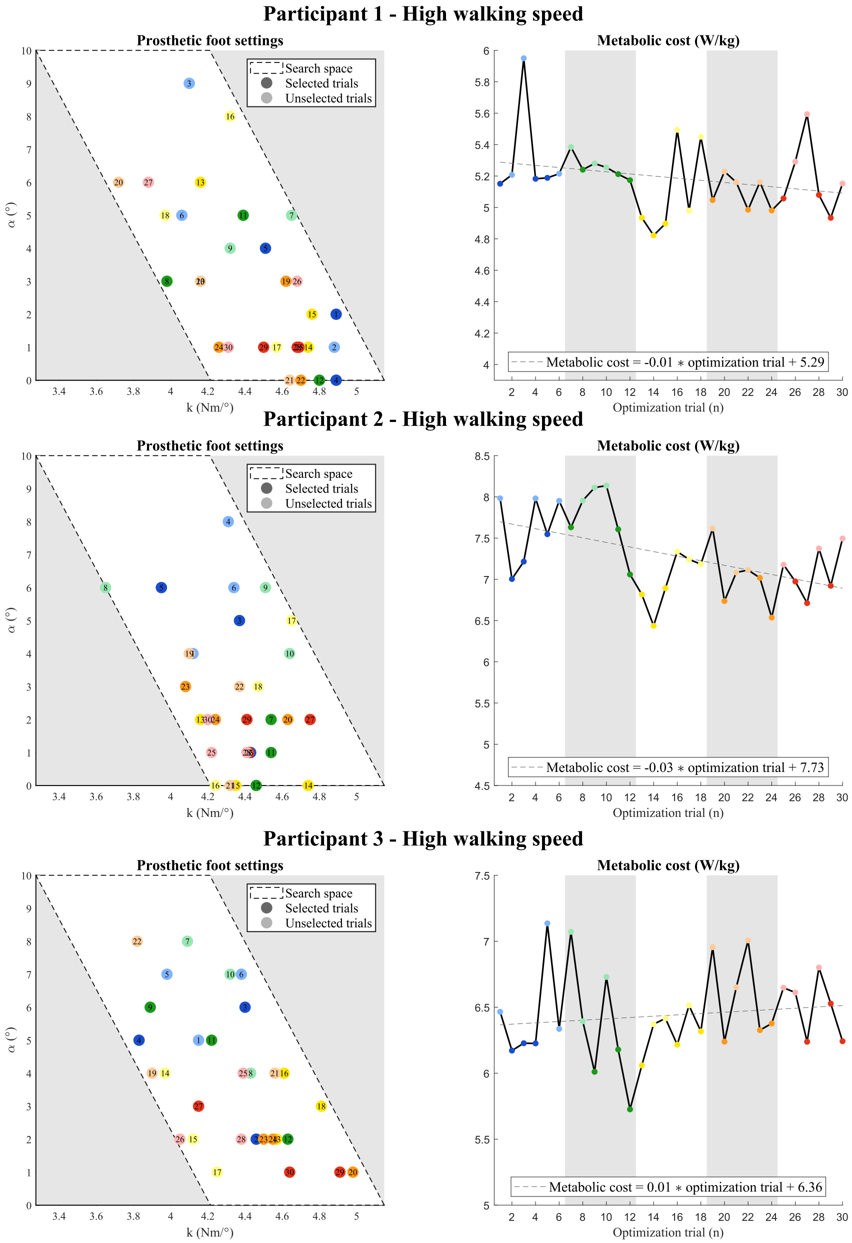

Figure 6.2 (continued): ... shaded areas in the background.The darker colored circles in every generation indicate the trials that resulted in the lowest metabolic cost and were selected by the algorithm. The dashed grey line presents the regression line of the metabolic cost during the optimization period (right side of subfigures).

optimization trial and corresponding metabolic cost of walking are presented. The slopes of the linear regression equation to the measured metabolic cost were -0.02 W/kg, 0.01 W/kg, and -0.03 W/kg at self-selected speed, and -0.01 W/kg, -0.03 W/kg, and 0.01 W/kg at high walking speed for participants 1, 2, and 3, respectively (Figure 6.2).

The progression of the optimization algorithm parameters (prosthetic foot stiffness and alignment, and search space σ) throughout the optimization period at self-selected speed and high walking speed are presented in Figure 6.3. The area of search of stiffness and alignment landscape (σ) decreased towards the final generation during optimization at both self-selected speed and high speed (range σ_{final} all optimization periods: 0.23 – 0.29; Figure 6.3), which is indicative of convergence.

Optimization at high walking speed only brought relatively small changes (≤

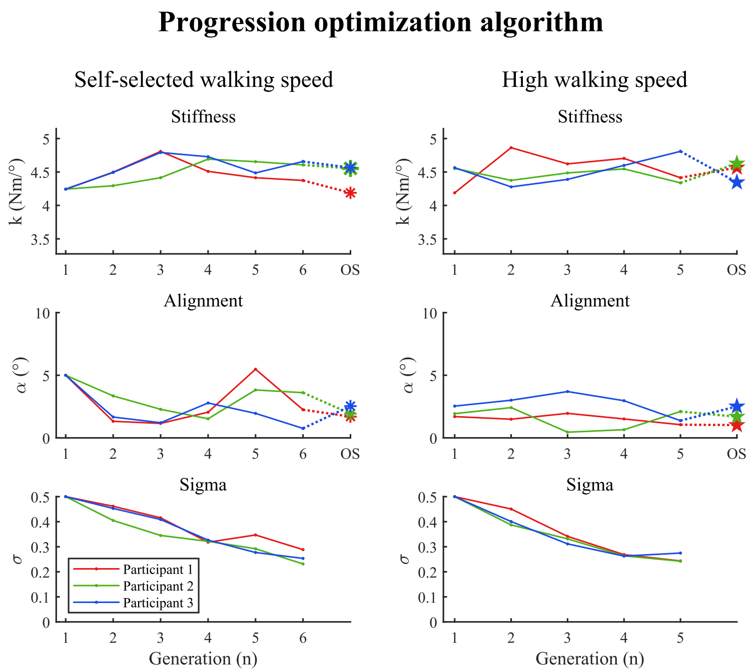

Figure 6.3: Progression of the optimization parameters during the optimization period at self-selected walking speed (left) and high walking speed (right). Mean parameter values (stiffness and alignment) and search space (σ) are presented for every generation. The progression for every individual participant (n=3) is given. Optimal stiffness and alignment values (OS) for self-selected speed (asterisks) and high walking speed (pentagrams) are also given.

1°) in optimal prosthetic foot alignment (range: 1 – 3°) compared to optimization at self-selected walking speed (range 2 – 3°; Figure 6.3 and Figure 6.4). The differences in optimal alignment between high walking speed and self-selected walking speed were -1°, 0°, and 0°, for participant 1, 2, and 3, respectively. We found differences in optimal stiffness values for high walking speed (range: 4.35 – 4.63 Nm/°) compared to self-selected walking speed (range: 4.19 – 4.60 Nm/°), but the direction of change differed between participants (Figure 6.3 and Figure 6.4). The differences in optimal stiffness between high walking speed and self-selected walking speed were 0.38 Nm/°, 0.08 Nm/°, and -0.25 Nm/° for participant 1, 2, and 3, respectively.

6.3.3. Evaluation period

During the evaluation trials at self-selected walking speed, using the self-selected speed foot resulted in lower metabolic cost of walking compared to using the high-speed foot in 2 of the 3 participants (Figure 6.5). Averaged over the 3 participants,

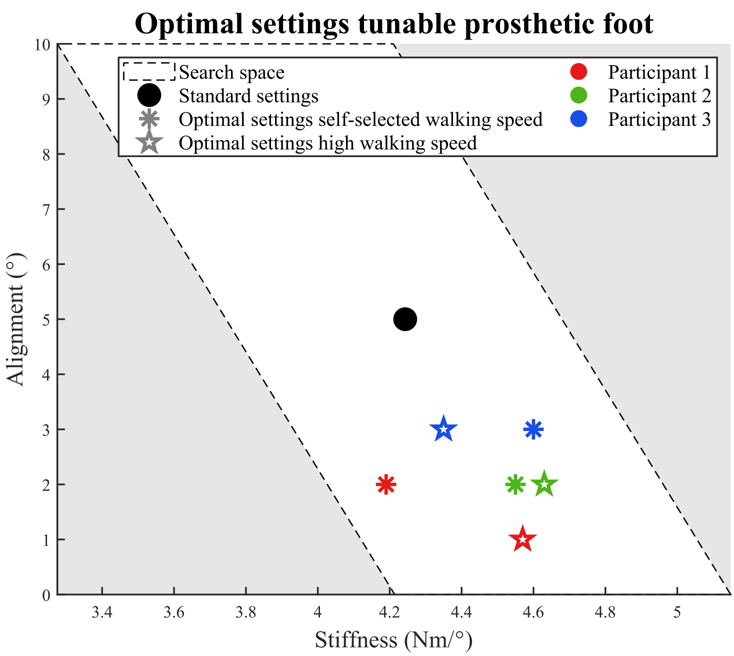

Figure 6.4: Optimal stiffness and alignment settings for every participant (n=3) within the search space of the tunable prosthetic foot (white area). Optimal settings for both self-selected walking speed (asterisks) and high walking speed (pentagrams), and standard settings (black dot) are given.

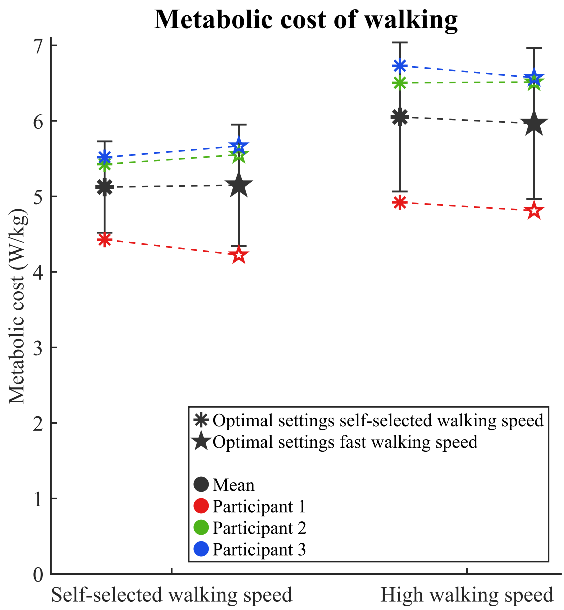

Figure 6.5: Metabolic cost of walking using the tunable prosthetic foot with optimal settings for self-selected walking speed (asterisks) and high walking speed (pentagrams) while walking at self-selected walking speed (left) and high walking speed (right). Mean ± standard deviation and individual observations are given (n=3).

metabolic cost was 0.47% lower with the self-selected speed foot (range: -2.65 – +4.83%).

During the evaluation trials at high walking speed, using the high-speed foot also resulted in a lower metabolic cost compared to using the self-selected speed foot in 2 of the 3 cases (Figure 6.5). On average metabolic was 1.43% lower with the high-speed foot (range: -2.36 – +0.12%).

6.4. Discussion

The aim of the present study was to explore whether human-in-the-loop optimization of prosthetic foot settings (stiffness and alignment) at different walking speeds (self-selected walking speed and 120% self-selected walking speed) resulted in different optimal prosthetic foot settings for each speed. Differences in optimal prosthetic foot alignment settings obtained during optimization to lower the metabolic cost of transtibial amputees at different walking speeds were only marginal (≤ 1°). We found small differences in optimal prosthetic foot stiffness (range: -0.25 – +0.38 Nm/°), but the direction of change was not consistent between participants.

The differences in optimal settings did not result in a clear trend or a meaningful change [23] in metabolic cost of walking (range: -2.7 – +4.8%) when using speed specific prosthetic foot settings of either self-selected or fast walking speed. Although participants 1 and 3 showed the largest change in optimal stiffness (Figure 6.4), they did not consistently show the largest change in metabolic cost between speeds and settings (Figure 6.5). While previous research showed that speed-specific prosthetic stiffness could enhance walking biomechanics compared to standard device settings [15], the current findings suggest energy cost might be quite robust to small differences in prosthetic foot settings. This could imply that on an individual level not all circumstances require speed-specific optimized prosthetic settings to enhance walking energetics, and individually optimized prosthetic settings remain effective across a broader range of walking speeds.

While the sample size of this study might seem small, the current human-in-the-loop design has advantage over traditional study designs to investigate the relation between prosthetic settings and walking speed. These traditional designs typically test two or three fixed settings at different speeds across a group of individuals [15, 24]. This does not take into account that different people might have different optimal settings at a given speed, causing differences in optimal settings between participants to appear as noise in the experiments. During our human-in-the-loop optimization experiment, participants used the prosthetic foot across a wide variety of stiffness and alignment combinations to identify speed-specific optimal settings for every individual. This optimization approach could provide more personalized speed-specific settings than traditional study designs, and shows that even when speed specific optimization is used, the effect of these settings on metabolic cost at different walking speeds is minimal.

The current results seem to indicate that prosthetic settings optimized at self-selected walking speed remain effective at high walking speed. Self-selected walking speed likely reflects a balance of multiple criteria, such as metabolic cost and comfort [25], and closely aligns with the speed that minimizes metabolic cost [26] and muscle fatigue [27]. Although real-world walking requires frequent adjustments in speed to match environmental demands [10, 11], settings optimized at self-selected speed remain effective across a range of walking speeds. Therefore, self-selected walking speed might be an appropriate condition for prosthetic tuning when metabolic cost minimization is the target of intervention.

A critical consideration emerging from the current results is whether the human-in-the-loop optimization procedure, using metabolic cost as cost function, is sufficiently sensitive to find different optimal prosthetic settings between speeds. This was further substantiated by the slopes of the linear regression equation to the measured metabolic cost (Figure 6.2). We had expected a larger negative slope during optimization at self-selected speed, compared to a smaller or plateauing slope at high walking speed, due to the better guess of initial settings. However, this was not the case for participant two, who instead showed a positive slope during optimization at self-selected speed. This means that over the course of optimization no clear decrease in metabolic cost was found. Interestingly, this participant did show the largest slope during optimization at high speed. Consequently, it remains questionable whether variation in optimal settings between speeds occurred as an effect of speed or as an effect of limited accuracy in our human-in-the-loop optimization procedure.

6.4.1. Limitations

We showed that human-in-the-loop optimization at different walking speeds resulted in small differences in optimal prosthetic foot settings between speed conditions that did not affect metabolic cost consistently, despite the difference in energetic demand between the speeds (Figure 6.5). Nevertheless, we should acknowledge that the difference in walking speed between optimization protocols was relatively small (20%), and the study was conducted on a treadmill in a controlled lab environment with a rather small set of participants. Therefore, the generalizability to the real world can be debated.

6.5. Conclusion

This study on human-in-the-loop optimization of prosthetic foot settings (stiffness and alignment) to minimize the metabolic cost at different walking speeds demonstrated that differences in optimal prosthetic settings between walking speeds did not lead to improved walking energetics at both self-selected and fast walking speed. These findings suggest that prosthetic foot settings optimized for self-selected walking speed could be used effectively across a broader range of walking speeds, and therefore, self-selected walking speed could serve as a practical basis for prosthetic tuning in clinical practice.

6.6. Acknowledgments

This work was supported by the European Commission's Horizon 2020 Program as part of the project MyLeg under grant agreement n. 780871.

We gratefully acknowledge Johnnidel Tabucol and Marco Leopaldi, the developers of the prototype tunable prosthetic foot MyFlex-η, for their help throughout the project. We thank Henk Zijlstra, Chris Bolmer, Sandra Loonen, and Auke Postma (certified prosthetists) of OIM Orthopedie (Haren, the Netherlands) for their help with recruitment of participants and connecting and aligning the tunable prosthetic foot. We thank Foeke van Minnen and Julie van der Tempel (Bachelor students at the University of Groningen) for their help with data collection.

6.7. Reference list

[1] A. Cortes, E. Viosca, J. Hoyos, J. Prat, and J. Sanchez-Lacuesta, "Optimisation of the prescription for trans-tibial (TT) amputees," Prosthetics and orthotics international, vol. 21, no. 3, pp. 168-174, 1997.

[2] C. J. Hofstad, H. van der Linde, J. Van Limbeek, and K. Postema, "Prescription of prosthetic ankle-foot mechanisms after lower limb amputation," Cochrane Database of Systematic Reviews, no. 1, 2004.

[3] P. Slade, C. Atkeson, J. M. Donelan, H. Houdijk, K. A. Ingraham, M. Kim, K. Kong, K. L. Poggensee, R. Riener, M. Steinert, J. Zhang, and S. H. Collins, "On human-in-the-loop optimization of human-robot interaction," Nature, vol. 633, no. 8031, pp. 779-788, Sep, 2024.

[4] J. Zhang, P. Fiers, K. A. Witte, R. W. Jackson, K. L. Poggensee, C. G. Atkeson, and S. H. Collins, "Human-in-the-loop optimization of exoskeleton assistance during walking," Science (New York, N.Y.), vol. 356, no. 6344, pp. 1280-1284, Jun 23, 2017.

[5] F. Scotto di Luzio, D. Simonetti, F. Cordella, S. Miccinilli, S. Sterzi, F. Draicchio, and L. Zollo, "Bio-Cooperative Approach for the Human-in-the-Loop Control of an End-Effector Rehabilitation Robot," Frontiers in neurorobotics, vol. 12, pp. 67, Oct 11, 2018.

[6] R. M. Alexander, "Optimization and gaits in the locomotion of vertebrates," Physiological Reviews, vol. 69, no. 4, pp. 1199-1227, 1989.

[7] C. G. Welker, A. S. Voloshina, V. L. Chiu, and S. H. Collins, "Shortcomings of human-in-the-loop optimization of an ankle-foot prosthesis emulator: a

6

case series," Royal Society open science, vol. 8, no. 5, pp. 202020, 2021.
[8] T. Tankink, H. Houdijk, J. Tabucol, M. Leopaldi, J. M. Hijmans, and R. Carloni, "Human-in-the-Loop Optimization of the Stiffness and Alignment of a Prosthetic Foot to Reduce the Metabolic Cost of Walking," IEEE Transactions on Neural Systems and Rehabilitation Engineering, 2025.
[9] S. C. Senatore, K. Z. Takahashi, and P. Malcolm, "Using human-in-the-loop optimization for guiding manual prosthesis adjustments: a proof-of-concept study," Frontiers in Robotics and AI, vol. 10, pp. 1183170, 2023.
[10] M. S. Orendurff, J. A. Schoen, G. C. Bernatz, A. V. Segal, and G. K. Klute, "How humans walk: bout duration, steps per bout, and rest duration," Journal of Rehabilitation Research & Development, vol. 45, no. 7, 2008.
[11] J. C. Selinger, and J. M. Donelan, "Estimating instantaneous energetic cost during non-steady-state gait," Journal of applied physiology (Bethesda, Md.: 1985), vol. 117, no. 11, pp. 1406-1415, Dec 1, 2014.
[12] M. K. Shepherd, A. M. Simon, J. Zisk, and L. J. Hargrove, "Patient-preferred prosthetic ankle-foot alignment for ramps and level-ground walking," IEEE Transactions on Neural Systems and Rehabilitation Engineering, vol. 29, pp. 52-59, 2020.
[13] T. R. Clites, M. K. Shepherd, K. A. Ingraham, L. Wontorcik, and E. J. Rouse, "Understanding patient preference in prosthetic ankle stiffness," Journal of neuroengineering and rehabilitation, vol. 18, no. 1, pp. 128, 2021.
[14] J. Tabucol, V. G. M. Kooiman, M. Leopaldi, R. Leijendekkers, G. Selleri, M. Mellini, N. Verdonschot, M. Oddsson, R. Carloni, A. Zucchelli, and T. M. Brugo, "The MyFlex-ζ Foot: a Variable Stiffness ESR Ankle-Foot Prosthesis," IEEE Transactions on Neural Systems and Rehabilitation Engineering, pp. 1, 2025.
[15] E. Rogers-Bradley, S. H. Yeon, C. Landis, D. R. Lee, and H. M. Herr, "Variable-stiffness prosthesis improves biomechanics of walking across speeds compared to a passive device," Scientific Reports, vol. 14, no. 1, pp. 16521, 2024.
[16] J. Tabucol, "Study of composite elastic elements for transfemoral prostheses: the MyLeg Project," University of Groningen, 2022.
[17] J. Tabucol, M. Leopaldi, T. M. Brugo, M. Oddsson, and A. Zucchelli, "Design and Mechanical Characterization of a Variable Stiffness ESR Foot Prosthesis," IEEE Access, vol. 12, pp. 97544-97556, 2024.

[18] M. Leopaldi, T. M. Brugo, J. Tabucol, and A. Zucchelli, "Parametric Design of an Advanced Multi-Axial Energy-Storing-and-Releasing Ankle–Foot Prosthesis," Prosthesis, vol. 6, no. 4, pp. 726-743, 2024.

[19] A. J. van den Bogert, T. Geijtenbeek, O. Even-Zohar, F. Steenbrink, and E. C. Hardin, "A real-time system for biomechanical analysis of human movement and muscle function," Medical & biological engineering & computing, vol. 51, no. 10, pp. 1069-1077, Oct, 2013.

[20] N. Hansen, "The CMA evolution strategy: a comparing review," Towards a new evolutionary computation, pp. 75-102, 2006.

[21] M.-A. Brehm, J. Becher, and J. Harlaar, "Reproducibility evaluation of gross and net walking efficiency in children with cerebral palsy," Developmental Medicine & Child Neurology, vol. 49, no. 1, pp. 45-48, 01/01; 2023/08, 2007.

[22] L. Garby, and A. Astrup, "The relationship between the respiratory quotient and the energy equivalent of oxygen during simultaneous glucose and lipid oxidation and lipogenesis," Acta Physiologica Scandinavica, vol. 129, no. 3, pp. 443-444, Mar, 1987.

[23] B. J. Darter, K. M. Rodriguez, and J. M. Wilken, "Test–retest reliability and minimum detectable change using the k4b2: oxygen consumption, gait efficiency, and heart rate for healthy adults during submaximal walking," Research quarterly for exercise and sport, vol. 84, no. 2, pp. 223-231, 2013.

[24] S. D'Andrea, N. Wilhelm, A. K. Silverman, and A. M. Grabowski, "Does Use of a Powered Ankle-foot Prosthesis Restore Whole-body Angular Momentum During Walking at Different Speeds?," Clinical Orthopaedics and Related Research®, vol. 472, no. 10, pp. 3044-3054, 2014.

[25] S. Song, H. Choi, and S. H. Collins, "Using force data to self-pace an instrumented treadmill and measure self-selected walking speed," Journal of NeuroEngineering and Rehabilitation, vol. 17, no. 1, pp. 68, 2020.

[26] H. J. Ralston, "Energy-speed relation and optimal speed during level walking," Internationale Zeitschrift für Angewandte Physiologie Einschliesslich Arbeitsphysiologie, vol. 17, no. 4, pp. 277-283, 1958.

[27] S. Song, and H. Geyer, "Predictive neuromechanical simulations indicate why walking performance declines with ageing," The Journal of physiology, vol. 596, no. 7, pp. 1199-1210, 2018.

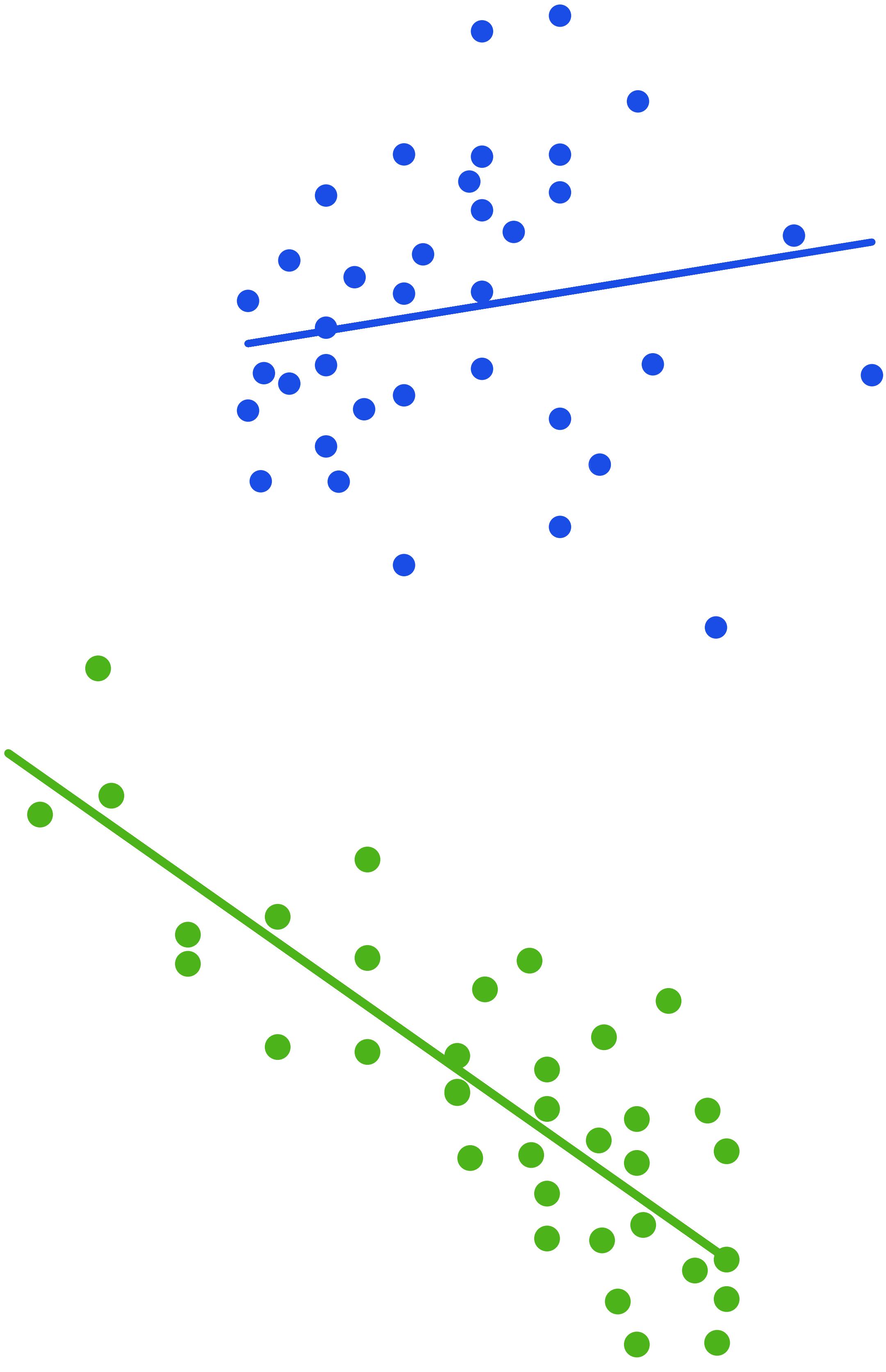

Chapter 7

Correlation between metabolic cost and perceived comfort during human-in-the-loop optimization of a prosthetic foot

Thijs Tankink
Han Houdijk
Raffaella Carloni
Juha M. Hijmans

Gait & Posture, 110111.

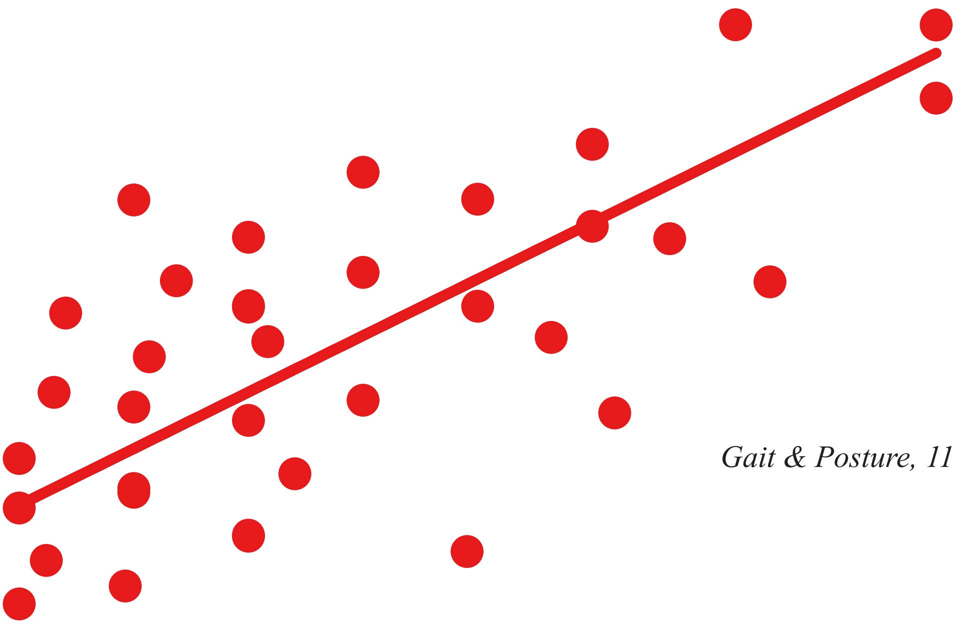

Abstract

Background: Human-in-the-loop optimization provides a standardized approach to enhance the effectiveness of assistive technology for gait by tuning devices to the needs of the individual user. Metabolic cost is frequently used as optimization objective. However, the assessment of metabolic cost requires relatively long-lasting physiological steady-state conditions. Subjective user preference could be an interesting alternative optimization objective that could shorten trial duration. We aim to explore whether the measured metabolic cost of walking correlates with the perceived comfort of the user during human-in-the-loop optimization process. *Methods*: Ten transtibial amputees underwent an optimization protocol while walking on a treadmill with an experimental prosthetic foot with tuneable stiffness and alignment. We used human-in-the-loop optimization to minimize the metabolic cost of walking by optimizing the stiffness and alignment of the prosthetic foot, using an evolutionary optimization algorithm. The participant's perceived comfort of every optimization trial was determined via the visual analogue comfort scale. To determine the association between metabolic cost and perceived comfort during the optimization period, we performed a repeated measures correlation and a separate Pearson correlation for every individual. *Results*: Results showed a moderate negative correlation between metabolic cost and perceived comfort. On an individual level a significant correlation was found in six out of ten cases. *Significance*: Perceived comfort allows people to prioritize different optimization objectives simultaneously, and apparently, metabolic cost is prioritized to varying extents.

Keywords

Metabolic cost, user preference, prosthetic foot, transtibial amputation, human-in-the-loop optimization

7.1. Introduction

Human-in-the-loop optimization provides a standardized approach to enhance the effectiveness of assistive technology for gait by tuning devices to the needs of the individual user [1]. To individually optimize device settings, human-in-the-loop optimization requires an optimization objective that should be meaningful for the user and could be measured directly and reliably throughout the optimization process [1]. Metabolic cost is frequently used as optimization objective [2, 3], as often assistive devices are developed with the intention to reduce the energetic effort of the user [4]. However, the assessment of metabolic cost requires relatively long-lasting physiological steady-state conditions [5, 6]. Although newly developed methods are able to estimate metabolic cost within two-min trials [6, 7], thereby significantly reducing measurement time, human-in-the-loop optimization protocols remain lengthy as a combination of trial length and the high number of iterations involved.

To reduce the time of optimization, an alternative optimization objective could be explored. As conclusive results about what users really aim to optimize are still lacking, subjective user preference has been put forward as an interesting candidate [8]. User preference, i.e., perceived comfort in the current study, refers to an internal cost function, in which users can implicitly prioritise different metrics at the same time [4]. In addition to shortening the optimization process, perceived comfort does not require advanced data capture systems or controlled conditions to be measured. However, it is unknown whether perceived comfort has potential as optimization objective within the context of human-in-the-loop optimization and to what extent perceived comfort assesses the same or different gait performance metric(s) as metabolic cost.

People with lower-limb amputation could benefit from human-in-the-loop optimization, as the walking ability of this heterogeneous group is affected by an increased metabolic cost of walking [9, 10]. In a previous study, we have shown that human-in-the-loop optimization of the stiffness and alignment of a prosthetic foot was able to reduce the metabolic cost of walking of people using a transtibial prosthesis by 10% [11]. In the current study, we aim to explore whether the measured metabolic cost of walking during human-in-the-loop optimization process correlates with the perceived comfort of the user, and whether perceived comfort might be a relevant optimization objective to use during the tuning of assistive devices as a proxy for metabolic cost.

7.2. Method

7.2.1. Participants

For this study we used data of our previously published study [11]. 10 individuals with a unilateral transtibial amputation participated in this study. Inclusion criteria were: age ≥ 18 years, shoe size 41 – 45, amputation over 1 year ago, and MFC-level ≥ K3. Exclusion criteria were: other conditions affecting balance or gait, use of orthopaedic footwear or osseo-integrated prosthesis, or current issues with their prosthesis or socked. The study protocol was approved by the medical ethics committee of the University Medical Center Groningen (under protocol number 17321), the Netherlands. All participants were informed about the study and provided written informed consent before the start of the experiments.

7.2.2. Experimental set-up

We used the MyFlex-η, an energy storing and return prosthetic foot [12-14] with manually tuneable stiffness and alignment (Figure 7.1), with an Össur foot shell and regular walking shoes (Chris, Dr Comfort, Mequon, WI, USA), with a combined mass

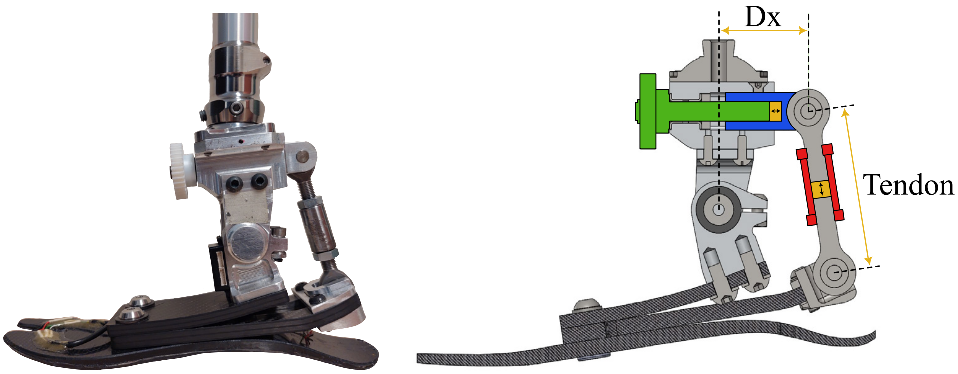

Figure 7.1: Left: The prosthetic foot MyFlex-η with tunable stiffness and tunable alignment [10-12]. Right: A schematic representation. The stiffness and alignment of the prosthetic foot depend on the Dx-length and the tendon length. The Dx-length could be changed by manually turning the knob (green), horizontally translating the position of the Dx-slider (blue) (note that a change in Dx-length affects the alignment as well). The orientation of the foot plate relative to the pylon could be changed by turning the threaded tube adaptor (red) of the tendon link that modifies the tendon length.

of 1.75 kg. Alignment was defined as the pylon-to-vertical angle while the shoe was flat but unloaded on the ground [11]. Measurements were performed on the dual-belt treadmill of the GRAIL system (Gait Realtime Analysis Interactive Lab; Motekforce Link, Amsterdam) of the Department of Rehabilitation Medicine, University Medical Center Groningen, the Netherlands. Respiratory data were collected by the portable metabolic analyser K5 (COSMED, Rome, Italy) in breath-by-breath mode.

7.2.3. Protocol

The protocol (Fig. 2) consisted of a fitting session and two visits to the GRAIL lab in which the optimization at predetermined constant self-selected speed was conducted [11]. During the fitting session, demographic and antropometric data were collected. A certified prosthetic orthotist fitted the MyFlex-η prosthetic foot to the participant's own prosthetic socket.

During the optimization period, we aimed to optimize stiffness and alignment of the prosthetic foot to minimize metabolic cost. The stiffness and alignment of every optimization trial were determined by an evolutionary optimization algorithm [11, 15, 16]. The optimization period consisted of 36 optimization trials (6 generations of 6 trials) of 120 s with intervening rest periods. After every trial, the participant's perceived comfort was determined via the visual analogue comfort scale (range: 0-10) [17]. The specific question that we asked was: "On a scale from 0 to 10, what is the perceived comfort of the prosthetic foot with the settings that were just used?"

7.2.4. Data analysis

Metabolic cost during the optimization trials was estimated by fitting a first-order dynamical model with a time constant of 42 seconds [6] to 120 s of breath-by-breath metabolic measurements, because it has shown provide a good balance between limiting estimation errors (4.3%) and trial duration [2]. We fitted an exponential curve to the measured $\dot{V}O_2$ consumption and $\dot{V}CO_2$ production and used the asymptotes of these fits as an estimate of their steady state values. Gross energy consumption was used to account for variations in resting energy consumption between measurement days [18]. Metabolic power was calculated using the following equation [19]:

$$metabolic\ \ power = 16.04 \cdot \dot{V}O_2 + 4.94 \cdot \dot{V}CO_2 \tag{7.1}$$

where the $metabolic\ \ power$ is in Watts and $\dot{V}O_2$ and $\dot{V}CO_2$ are expressed in mL/s.

7

Subsequently, we normalized *metabolic power* for body mass (W/kg).

7.2.5. Statistical analysis

To determine the association between metabolic cost and perceived comfort during the optimization period, we performed a repeated measures correlation [20] using custom-made MATLAB (R2024b, MathWorks, Natick, USA) scripts. In addition, we performed a separate Pearson correlation between metabolic cost and perceived comfort for every individual. We used a p-value of 0.05 to indicate statistically significant correlations.

7.3. Results

7.3.1. Participant characteristics

10 people with a transtibial amputation participated in this study. Participant characteristics are presented in Table 7.1.

7.3.2. Correlation metabolic power and perceived comfort

We found significant moderate negative correlation between metabolic cost of walking and perceived comfort ($r = -0.35$, $p < 0.001$; Figure 7.2). On an individual level, we found significant negative Pearson correlation coefficients in 6 out of 10 participants (Figure 7.2).

Table 7.1: Participant characteristics (mean ± standard deviation, n=10).

Reason for amputationa	Trauma: 5, Vascular disease: 3, Cancer: 1, Congenital growth disorder: 1
Side of amputation (left : right)[a]	5 : 5
Gender (male : female)[a]	10 : 0
Age (years)	57.2 ± 16.6
Height (cm)	180.0 ± 4.0
Body mass with prosthesis (kg)	85.3 ± 14.6
Shoe size (EU)b	42 – 45
Mass personal prosthesis + shoe (kg)	1.34 ± 0.23
Time between lab visits (days)	8.9 ± 8.2
Self-selected walking speed (m/s)	1.02 ± 0.12

[a]Frequencies are given.
[b]Range is given.

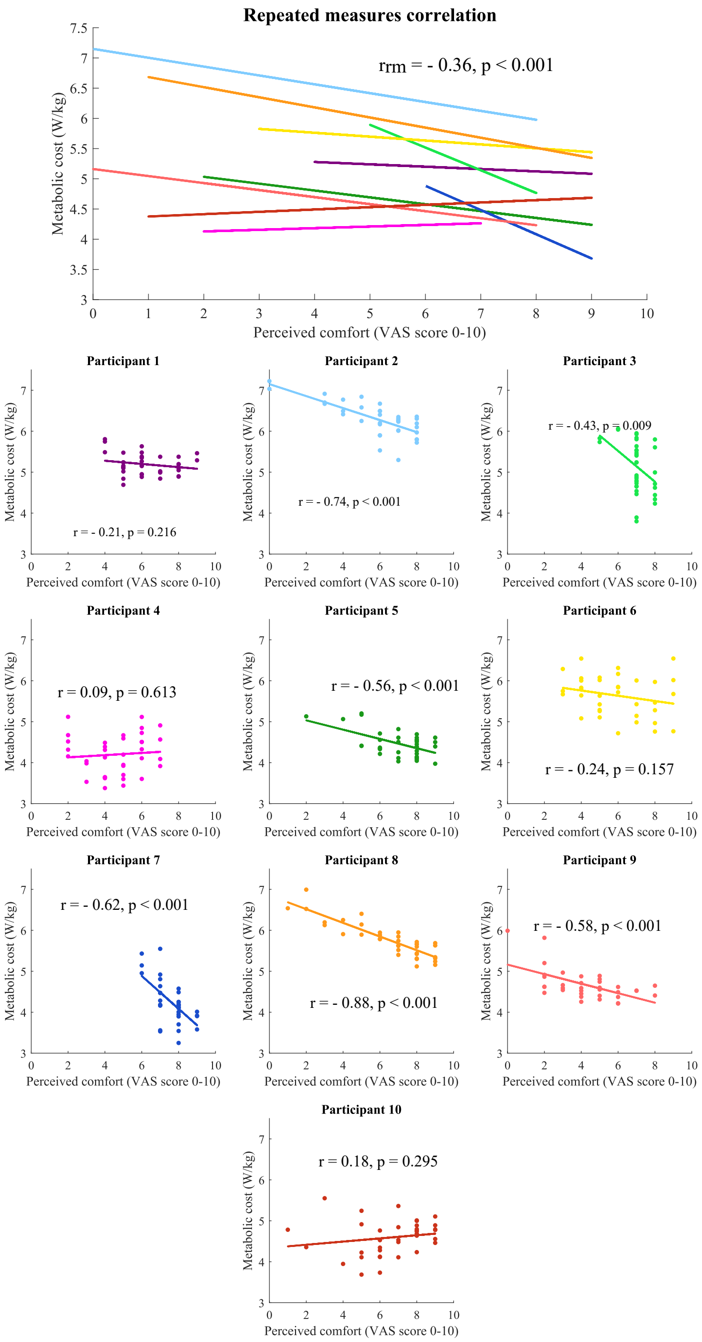

Figure 7.2: Correlation between metabolic cost and perceived comfort during the optimization period. Both results for repeated measures correlation (top, n=10) and individual Pearson correlations (bottom) are presented.

7.4. Discussion

The aim of the study was to explore the correlation between metabolic cost of walking and the perceived comfort of transtibial amputees during human-in-the-loop optimization of the stiffness and alignment of a prosthetic foot. The current results showed an overall significant negative correlation between metabolic cost and perceived comfort, with significant correlation on an individual level in six out of ten cases. The lack of correlation between metabolic cost and perceived comfort in some individuals shows that these metrics do not always measure the same aspect of gait performance. Perceived comfort allows people to prioritize different optimization objectives simultaneously [4] during the optimization of an assistive device, and apparently, metabolic cost is to varying extents prioritized for the perceived comfort score.

Perceived comfort as an optimization objective, has the potential to substantially reduce trial duration and limit the time required to complete the optimization protocol, as participants in the current study reported that they were generally able to score new prosthetic settings within just a few steps. Although further research on the required time to determine perceived comfort is needed, this indicates that it could reduce trial duration, e.g., to 30 s [8]. Moreover, this optimization objective can be obtained without the need of a controlled lab environment or advance measurement systems, and can actively involve the user in the tuning process [1, 21]. Previous research has already shown that subjective measures as user preference could be a reliable source of information during the tuning of assistive devices [8], covering different optimization objectives including metabolic cost. Therefore, perceived comfort represents an interesting optimization objective that could accelerate the implementation of human-in-the-loop optimization in clinical practice to enhance the effectiveness of assistive technology for gait although cannot be seen as a proxy for metabolic cost as primary cost function.

7.5. Acknowledgments

This work was supported by the European Commission's Horizon 2020 Program as part of the project MyLeg under grant agreement n. 780871.

We gratefully acknowledge Johnnidel Tabucol and Marco Leopaldi, the developers of the prototype tunable prosthetic foot MyFlex-η, for their help throughout the project. We thank Henk Zijlstra, Chris Bolmer, Sandra Loonen, and Auke Postma (certified prosthetists) of OIM Orthopedie (Haren, the Netherlands) for their help with recruitment of participants and connecting and aligning the tunable prosthetic foot. We thank Chengxiang Liu (Doctoral Candidate at the University of Groningen), Friso van der Bijl and Pim Rive (Bachelor students University of Groningen) for their help with data collection.

7.6. Reference list

[1] P. Slade, C. Atkeson, J. M. Donelan, H. Houdijk, K. A. Ingraham, M. Kim, K. Kong, K. L. Poggensee, R. Riener, M. Steinert, J. Zhang, and S. H. Collins, "On human-in-the-loop optimization of human-robot interaction," Nature, vol. 633, no. 8031, pp. 779-788, Sep, 2024.

[2] J. Zhang, P. Fiers, K. A. Witte, R. W. Jackson, K. L. Poggensee, C. G. Atkeson, and S. H. Collins, "Human-in-the-loop optimization of exoskeleton assistance during walking," Science (New York, N.Y.), vol. 356, no. 6344, pp. 1280-1284, Jun 23, 2017.

[3] J. Kim, B. T. Quinlivan, L.-A. Deprey, D. Arumukhom Revi, A. Eckert-Erdheim, P. Murphy, D. Orzel, and C. J. Walsh, "Reducing the energy cost of walking with low assistance levels through optimized hip flexion assistance from a soft exosuit," Scientific reports, vol. 12, no. 1, pp. 11004, 2022.

[4] M. A. Diaz, M. Vos, A. Dillen, B. Tassignon, L. Flynn, J. Geeroms, R. Meeusen, T. Verstraten, J. Babic, P. Beckerle, and K. De Pauw, "Human-in-the-Loop Optimization of Wearable Robotic Devices to Improve Human-Robot Interaction: A Systematic Review," IEEE transactions on cybernetics, vol. 53, no. 12, pp. 7483-7496, Dec, 2023.

[5] I. J. Blokland, J. J. De Koning, T. Van Kan, C. A. Van Bennekom, J. H. Van Dieen, and H. Houdijk, "Estimation of metabolic energy expenditure during short walking bouts," International Journal of Sports Medicine, vol. 42, no. 12, pp. 1098-1104, 2021.

[6] J. C. Selinger, and J. M. Donelan, "Estimating instantaneous energetic cost during non-steady-state gait," Journal of applied physiology (Bethesda, Md.: 1985), vol. 117, no. 11, pp. 1406-1415, Dec 1, 2014.

[7] A. J. Ries, M. N. Pitts, K. M. Steele, J. M. Donelan, and M. H. Schwartz, "Accurate steady-state VO2 estimation with less metabolic data using calibrated patient-specific Bayesian regression models," Gait & Posture, vol. 121, pp. 192-193, 2025.

[8] K. A. Ingraham, C. D. Remy, and E. J. Rouse, "The role of user preference in the customized control of robotic exoskeletons," Science robotics, vol. 7, no. 64, pp. eabj3487, 2022.

[9] D. Wezenberg, L. H. van der Woude, W. X. Faber, A. de Haan, and H. Houdijk, "Relation between aerobic capacity and walking ability in older adults with a lower-limb amputation," Archives of physical medicine and rehabilitation, vol. 94, no. 9, pp. 1714-1720, 2013.

[10] S. Ettema, E. Kal, and H. Houdijk, "General estimates of the energy cost of walking in people with different levels and causes of lower-limb amputation: a systematic review and meta-analysis," Prosthetics and orthotics international, vol. 45, no. 5, pp. 417-427, Oct 1, 2021.

[11] T. Tankink, H. Houdijk, J. Tabucol, M. Leopaldi, J. M. Hijmans, and R. Carloni, "Human-in-the-Loop Optimization of the Stiffness and Alignment of a Prosthetic Foot to Reduce the Metabolic Cost of Walking," IEEE Transactions on Neural Systems and Rehabilitation Engineering, 2025.

[12] J. Tabucol, M. Leopaldi, T. M. Brugo, M. Oddsson, and A. Zucchelli, "Design and Mechanical Characterization of a Variable Stiffness ESR Foot Prosthesis," IEEE Access, vol. 12, pp. 97544-97556, 2024.

[13] M. Leopaldi, T. M. Brugo, J. Tabucol, and A. Zucchelli, "Parametric Design of an Advanced Multi-Axial Energy-Storing-and-Releasing Ankle–Foot Prosthesis," Prosthesis, vol. 6, no. 4, pp. 726-743, 2024.

[14] J. Tabucol, V. G. M. Kooiman, M. Leopaldi, R. Leijendekkers, G. Selleri, M. Mellini, N. Verdonschot, M. Oddsson, R. Carloni, A. Zucchelli, and T. M. Brugo, "The MyFlex-ζ Foot: a Variable Stiffness ESR Ankle-Foot Prosthesis," IEEE Transactions on Neural Systems and Rehabilitation Engineering, pp. 1, 2025.

[15] N. Hansen, "The CMA evolution strategy: a comparing review," Towards a new evolutionary computation, pp. 75-102, 2006.

[16] C. G. Welker, A. S. Voloshina, V. L. Chiu, and S. H. Collins, "Shortcomings of human-in-the-loop optimization of an ankle-foot prosthesis emulator: a case series," Royal Society open science, vol. 8, no. 5, pp. 202020, 2021.

[17] R. S. Hanspal, K. Fisher, and R. Nieveen, "Prosthetic socket fit comfort score," Disability and rehabilitation, vol. 25, no. 22, pp. 1278-1280, 2003.

[18] M.-A. Brehm, J. Becher, and J. Harlaar, "Reproducibility evaluation of gross and net walking efficiency in children with cerebral palsy," Developmental Medicine & Child Neurology, vol. 49, no. 1, pp. 45-48, 01/01; 2023/08, 2007.

[19] L. Garby, and A. Astrup, "The relationship between the respiratory quotient and the energy equivalent of oxygen during simultaneous glucose and lipid oxidation and lipogenesis," Acta Physiologica Scandinavica, vol. 129, no. 3, pp. 443-444, Mar, 1987.

[20] J. Z. Bakdash, and L. R. Marusich, "Repeated measures correlation," Frontiers in psychology, vol. 8, pp. 456, 2017.

[21] K. A. Ingraham, M. Tucker, A. D. Ames, E. J. Rouse, and M. K. Shepherd, "Leveraging user preference in the design and evaluation of lower-limb exoskeletons and prostheses," Current Opinion in Biomedical Engineering, pp. 100487, 2023.

7

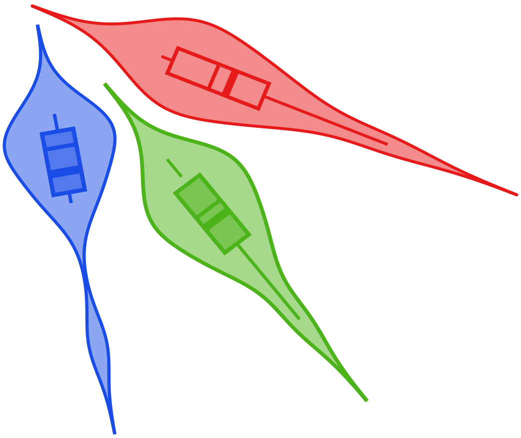

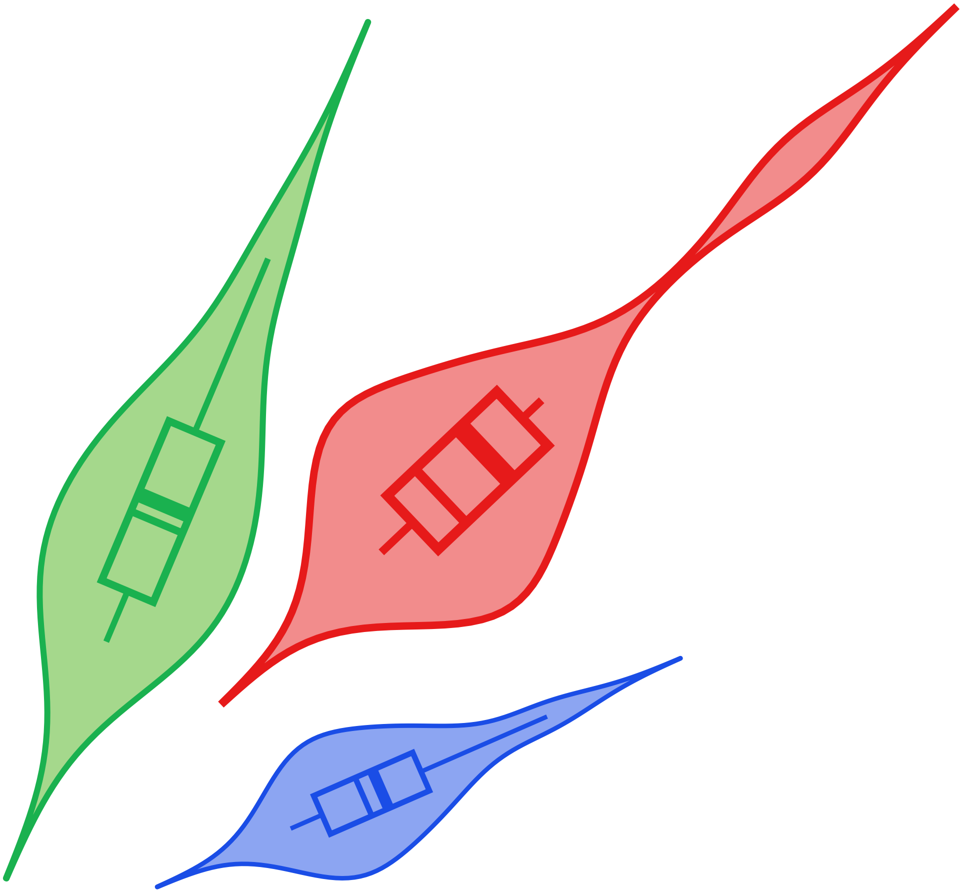

Chapter 8

General discussion

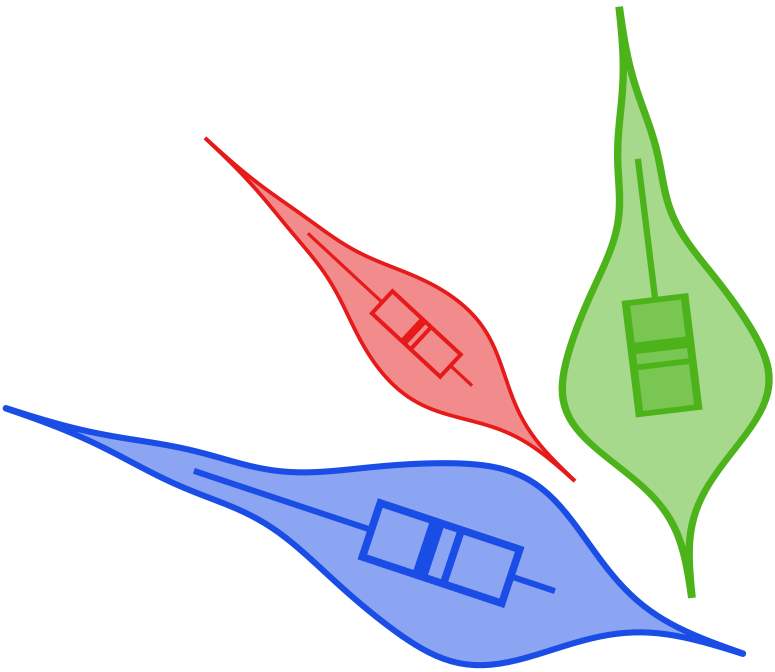

8.1. Aim of this thesis

Assistive technology for gait, such as footwear, ankle-foot orthoses, or prosthetic devices, could be used to enhance gait energetics, biomechanics, or stability to a user's maximum. However, despite all innovations, the effectiveness of current state-of-the-art assistive technology lags behind expectations. Human-in-the-loop optimization could overcome current challenges with regard to the tuning process of such sophisticated devices and help us find individually optimized settings. Therefore, the goal of the current thesis was to explore human-in-the-loop optimization protocols for assistive technology to augment gait performance. The broader goal of this thesis was to address open questions within the human-in-the-loop paradigm, develop knowledge that could enhance the process of tuning assistive technology to the individual end-user, and explore the potential of human-in-the-loop optimization within clinical practice and beyond.

In this general discussion, we reflect on how factors, such as cost-function selection, optimization algorithm settings, and context affect the optimization of an assistive device. Furthermore, we elaborate on the process of co-adaptation between user and device, i.e., adaptations of the device and adaptations of the user, to achieve optimal gait performance. Finally, the discussion considers the implications of these findings, highlights directions for future research within the human-in-the-loop optimization paradigm, and explores its potential to enhance assistive technology in clinical practice and beyond.

8.2. Cost function

An important consideration with regard to human-in-the-loop optimization is the selection of an appropriate cost function. **Chapter 3** showed that human-in-the-loop optimization via different cost functions resulted in different optimal device settings, i.e., rocker profiles, and showed that the optimal solution depends on the selected cost function. Moreover, the responsiveness of these cost functions to changes in rocker profiles differed, and not all optimizations resulted in improved performance. For instance, a broad range of rocker profiles resulted in similar step distance variability, preventing the optimization algorithm from converging to an optimum and improving gait stability. These findings emphasize the importance of selecting a cost function that matches the intended optimization domain of the user and is sufficiently sensitive and robust to the device parameters being tuned, to allow the optimization algorithm to converge to the desired optimum.

The importance of cost function selection was also substantiated in **Chapters 2** and **7**. In **Chapter 2**, we tested whether a proxy could be used to optimize the cost function of interest. Specifically, we used human-in-the-loop optimization to optimize the apex position and apex angle of running shoes with the aim to maximize positive ankle work (proxy) in order to improve running economy (cost function of interest). Although the study showed that human-in-the-loop optimization successfully increased positive ankle work and redistributed the share of positive work generated around the lower-limb joints (hip: decreased, knee: decreased, and ankle: increased), the hypothesized improvement in running economy was not observed. While positive mechanical ankle power has been correlated with energy cost [1, 2], maximizing one does not necessarily minimize the other.

Chapter 7 additionally showed that the correlation between metabolic cost and perceived comfort score varied across individuals. Perceived comfort, or user preference [3], allows users to implicitly weight different cost functions at the same time [4], and it seems that metabolic cost is weighted to varying extents for the perceived comfort score.

Apparently, there are more factors that determine metabolic cost than the biomechanical (**Chapters 2**, **3**, and **4**) and comfort (**Chapter 7**) factors that were investigated in the current thesis, of which the effect on metabolic cost could also differ between individuals. Optimizing a proxy of the cost function of interest, without first testing its validity with respect to the cost function of interest, undermines the main advantage of human-in-the-loop optimization, i.e., its capability to capture the full complexity of the human-device system [5]. To capture the full complexity of the system, optimizing the actual cost function of interest would be recommended. Nevertheless, it remains somewhat of a mystery what people are actually trying to optimize when they walk, i.e., what their (potentially multidimensional) cost function is. Tackling that question might be the largest challenge in optimizing assistive technology.

Another consideration regarding cost function selection is the practical feasibility of measuring a given construct over the full duration of the protocol. Different cost functions require different data capture systems and/or conditions to be measured. For example, the assessment of external mechanical power requires advanced motion capture systems and instrumented treadmills [6], whereas metabolic cost requires long-lasting steady-state conditions [7, 8]. Consequently, the measurement of a chosen cost function should be feasible within the available time and resources, e.g., the capabilities of the available measurement systems and the physical capacity of the end-user.

8.3. Optimization algorithm

Another key aspect of human-in-the-loop optimization is the selection of an optimization algorithm, e.g., evolutionary algorithm, Bayesian optimization, gradient-based methods [9], along with its configurations. Human-in-the-loop optimization requires a clever algorithm that rapidly and effectively explores the noisy and dynamic search landscape (Figure 8.1) [5]. First, the algorithm should be robust to the noise inherent in human physiological signals and avoid getting trapped in local optima that do not represent the global optimum. Second, the algorithm should be adaptive to a changing landscape, as people might optimize their movement strategy throughout the optimization process, resulting in an evolving search landscape. Third, the algorithm should be sample efficient, limiting the time required to converge to the optimal device settings.

Gradient-based methods have been used for human-in-the-loop optimization [10, 11], but have been shown to be vulnerable to the effect of measurement noise, and getting trapped in local optima. While estimating the gradient over a bigger interval could overcome this problem, it would reduce sample efficiency and is therefore undesirable [5]. Bayesian optimization has been shown to reduce convergence time compared to traditional approaches [12, 13], and achieve greater improvements in reducing muscle activity (cost function) using a portable hip exoskeleton compared to an evolutionary algorithm [14]. However, Bayesian optimization is less adaptive to a changing parameter landscape due to human adaptations (Figure 8.1). In contrast, the covariance matrix adaptation evolution strategy (CMA-ES) [15] has been shown to be both sample efficient and robust against measurement noise and human adaptations [5]. Consequently, CMA-ES is well suited to address the challenges inherent in the human-in-the-loop optimization process [16-18]. Therefore, all studies in the current thesis used this CMA-ES evolutionary algorithm [15].

Adjusting the algorithm's configuration can affect its convergence time and outcomes. Based on experiences from the current thesis, we recommend standardizing the optimization parameters during optimization, i.e., scale every optimization parameter over their range of settings, and start with a sufficiently large standard

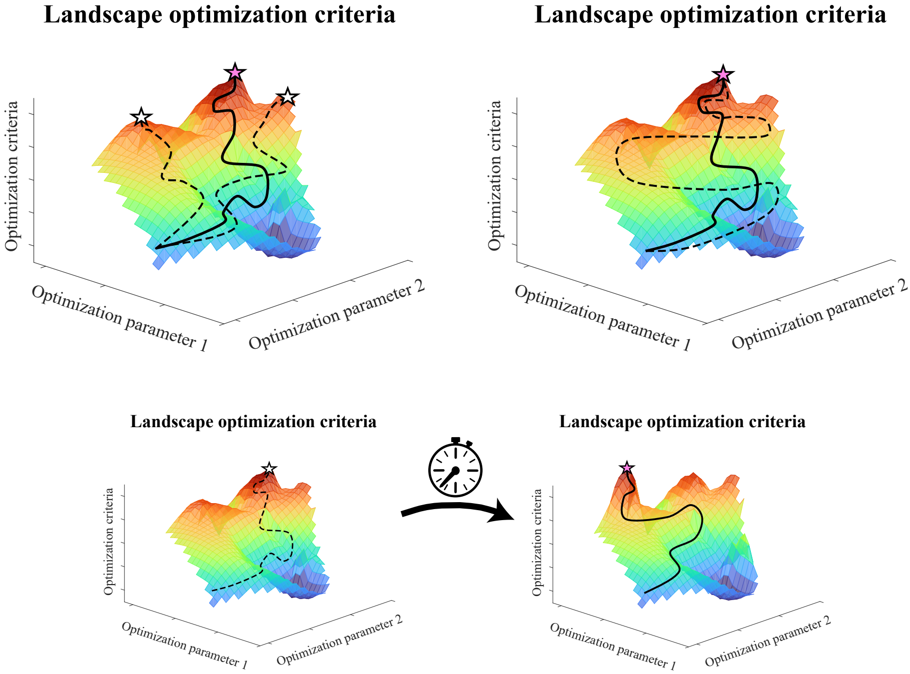

Figure 8.1: Human-in-the-loop optimization requires a clever algorithm that rapidly and effectively explores the noisy and changing search landscape. The algorithm should be able to deal with local optima (top left), converge in a sample or time efficient manner (top right), and be adaptive to a changing parameter landscape over time due to human adaptations (bottom: left vs. right).

deviation of optimization parameter values (σ), which determines the area of search during the optimization process. Standardization of the optimization parameters and a large $\sigma_{initial}$ ensure that the whole search space, i.e., full range of every optimization parameter, is explored (visually presented in **Chapter 6**).

Another configuration that could influence the outcome of the optimization process is the way the algorithm handles parameter values that fall outside the search space. The algorithm could either regenerate these values or set these values to the boundary of the search space. These choices influence whether optimization parameters are biased away from or drawn toward boundaries, respectively. In the current thesis, the optimization algorithm regenerated parameter values that fell outside the search space, and optimal solutions did not reach the boundaries. Using tunable devices with a wide parameter space could ensure that the global optimum is located well within the boundaries of the search space, and increase the certainty that the true optimum is found.

An open question within the human-in-the-loop paradigm is when to end the optimization process. In the current thesis, we ended optimization after a fixed number of trials (30, 32, and 36 in **Chapters 3** and **6**, **Chapter 2**, and **Chapters 4**, **5**, **6**, and **7**, respectively), primarily for practical reasons and to limit the physical strain of the participants. In **Chapter 2**, we observed relatively high variance in parameter values at the final generation, indicating that convergence had not always been achieved. This was likely due to the relatively high generation size of eight used for the two optimization parameters. Although a larger generation size improves global search capability and robustness of the algorithm, it reduces convergence speed [15]. Therefore, later studies used a smaller generation size of six, which is more appropriate for optimizing two parameters [15, 19]. In **Chapter 3**, we observed that convergence depended on the cost function being used, with the responsive cost functions (metabolic cost and collision work) reaching a plateau at the end of the optimization process, which is indicative of convergence. In addition to the plateauing of metabolic cost in **Chapters 4**, **5**, **6**, and **7**, the convergence to the optimal settings in these studies was further confirmed by stabilization of the optimization parameters and a decreased σ at the end of optimization (**Chapters 4** and **6**). Although these results show that the current number of trials allowed convergence in most of our studies, more evidence-based stopping criteria, e.g., convergence of the optimization parameters or the cost function reaching a performance plateau, are desired.

Another algorithm configuration that we changed throughout this thesis was the selection of optimal parameter settings at the end of the optimization phase. In **Chapters 2** and **3**, the device settings that resulted in the best cost function outcome across all optimization trials were selected as optimal settings. Although this choice is less vulnerable to local optima, it can be sensitive to the noise that human measurements entail, and could overlook the effect of human adaptations. The settings generated by the algorithm after the final optimization trial are less sensitive to noise and take into account the evolving parameter landscape. Therefore, the final settings generated by the algorithm represent the best estimation of the global optimum and are recommended for use as optimal settings (**Chapters 4** and **6**).

8.4. Context

In **Chapter 6**, we explored whether optimal device settings depend on the activity performed during the optimization process, i.e., optimization of prosthetic foot stiffness and alignment at self-selected walking speed and 120% of self-selected walking speed. Although optimal prosthetic foot settings differed between walking speeds, these different optimal settings did not result in a meaningful change [20] in metabolic cost, i.e., the cost function of interest. These findings suggest that prosthetic foot settings individually optimized for self-selected walking speed remain effective across a broader range of walking speeds. Apparently, optimal device settings vary independently individually, but not all circumstances require optimized settings. This suggests that self-selected walking speed might be an appropriate condition to use for optimizing assistive technology within the context of walking [21, 22]. It should be noted that this aspect has received limited attention. Therefore, the generalizability of optimal settings to contexts beyond the controlled treadmill environment should be explored in much more detail in the future.

8.5. Co-adaptation

8.5.1. Device adaptations

Previous research already showed that assistive technology design that matches the activity level of the user enables better co-operation between the user and their device to achieve optimal gait performance [23]. This implies that individualized optimal device settings should be found.

This thesis showed that optimal device settings, e.g., rocker profiles for running shoes (**Chapter 2**) and regular walking shoes (**Chapter 3**) or stiffness and alignment for prosthetic feet (**Chapters 4** and **6**), vary across individuals. Optimal device settings can differ substantially between individuals (**Chapter 3**), while even small differences in settings can already affect the cost function on an individual level (**Chapter 4**). This highlights the complexity and unpredictability of the user-device system and emphasizes the importance of individually optimizing assistive technology [24].

8.5.2. Human adaptations

Alongside these device adaptations, the tuning process of a device also involves motor adaptations of the user, which can account for more than 50% of the improvement in performance (**Chapter 5**) [25]. During the tuning process, the user needs to continuously adapt their motor strategies to the changing device settings.

Alongside these immediate motor adaptations, long-term motor learning also occurs. This is the process by which the user learns how to walk with the new device, resulting in long-term changes in motor behavior. This process was demonstrated in **Chapter 5**, in which transtibial amputees used a prosthetic foot with initial standard settings throughout the optimization process, resulting in a decrease in metabolic cost over time. Although **Chapter 5** showed that motor learning extended over 56 min in the context of our optimization experiment, the time for motor learning to saturate has been shown to be really context dependent. It has been suggested that it could range from less than one hour to a couple of hours [25, 26]. Therefore, the generalizability of these results to other devices with varying complexity and adaptability should be approached with caution.

Despite its context dependent nature, human-in-the-loop optimization could be used to accelerate motor learning (**Chapter 5**) [25, 27]. By exposing users to a wide range of device settings, human-in-the-loop optimization allows users to explore and refine their motor strategies. Subsequently, users can further co-adapt with the more targeted changes in device settings towards the optimal solution (**Chapter 5**) [25].

8.6. Implications and future directions

This thesis demonstrated that human-in-the-loop optimization can individually optimize device settings across different devices, tasks, and optimization criteria. By using human-in-the-loop optimization during the tuning process of assistive technology, device settings could be tuned to the biophysical properties of the user while simultaneously tuning the user to the device, thereby enhancing the effectiveness of this technology.

In order to achieve effective optimization, it is important to pay attention to the selection of a suitable device, cost function, and optimization algorithm. The selected cost function should be sufficiently sensitive and robust to the device parameters being tuned, match the intended optimization domain of the user, and capture the full complexity of the user-device system. The optimization algorithm should be sample efficient and robust against both measurement noise and the evolving search landscape due to human adaptation. To further improve the effectiveness of human-in-the-loop optimization protocols, future research should explore what algorithm configurations, and evidence-based stopping criteria (e.g., convergence of the optimization parameters or the cost function reaching a performance plateau) are most effective. In the following sections, we discuss applications of human-in-the-loop optimization, both within the context of research and its potential to be used in clinical practice and beyond.

8.6.1. Research purposes

Human-in-the-loop optimization represents an interesting research paradigm for investigating the complex interaction between user and device during the tuning process of assistive technologies. Unlike traditional experimental designs, where only two or three fixed device settings are tested across a group of participants, this method enables the identification of personalized optimal device settings for a given task. Such an individualized approach can reveal more meaningful insights into how specific device parameters influence performance and, ultimately, how assistive technology can augment human gait.

The importance of this individual approach was confirmed in this thesis. On a group level we did not find a clear biomechanical mechanism that could account for the changes in metabolic cost (**Chapters 2**, **3**, and **4**). In-depth data analysis on an individual level might reveal new mechanisms that remain hidden on a group level and is therefore recommended for future research.

Furthermore, human-in-the-loop optimization could be used as a research paradigm to investigate motor learning in assistive device users (**Chapter 5**). Future research should investigate whether differences exist in people's ability to use a new device and to immediately adapt to changing settings during the tuning process. Differences in the extent and speed of adaptation across individuals could provide clarity on whether human-in-the-loop optimization is beneficial for all people, i.e., responders vs. non-responders.

8.6.2. Clinical practice and beyond

This thesis showed the potential of an individual approach to enhance the effectiveness of assistive gait technology and improve performance. Human-in-the-loop optimization was able to achieve clinically relevant effects, e.g., reducing the metabolic cost of walking of transtibial amputees by more than 10 percent (**Chapter 4**) [20]. We showed that optimal device settings differed substantially between participants, demonstrating the necessity for individual tuning (**Chapter 3**). Moreover, human-in-the-loop optimization can identify optimal settings that are beyond the range reported in the existing literature [28] and that might not have been found in regular practice (**Chapter 2**). Although general guidelines could be a good starting point for tuning assistive technology and might be sufficient for some individuals and circumstances, this thesis highlights that a one-size-fits-all approach is not sufficient, and that tuning assistive technology to the individual end-user via human-in-the-loop optimization could enhance its effectiveness.

To find these individually optimized settings, tunable devices are required. Therefore, we encourage engineers and companies to develop tunable emulators with a wide range of parameter settings that could be integrated into the sport specific or clinical setting, e.g., the Open-Source Leg [29]. For these devices to be successfully integrated, it is important that their settings are easy and fast to tune, either manually or automatically, and that the different parameters can be tuned independently of each other. Such features will simplify the tuning and optimization process of these parameters, and the interpretation of specialists involved.

The use of tunable devices and human-in-the-loop optimization could enhance the co-adaptation process between user and device in two ways. First, it provides a standardized and efficient method to explore the search space of the device and find optimal settings, which can subsequently inform the design and fabrication of personalized devices. Second, it could facilitate motor learning of the user (**Chapter 5**) during the tuning process. Together, this could enhance co-adaptation between user and device and eventually improve the prescription and customization of assistive technology compared to current standards [5].

Although human-in-the-loop optimization could be feasible in contexts where time and resources are sufficiently available, e.g., elite sports, its clinical feasibility remains questionable in its current state. Many existing protocols require prolonged use of advanced measurement systems or exceed the physical capacity of the end-user. Incorporating user preference (**Chapter 7**) into these protocols has the potential to overcome these challenges. Participants in the current thesis reported that they could score new device settings within just a few steps, which could drastically reduce trial duration to, e.g., 30 s (**Chapter 7**). Moreover, this optimization objective allows people to prioritize different cost functions (e.g., metabolic cost, comfort, or stability) simultaneously [4] and can actively involve the user in the tuning process [5, 30]. However, further research is required to determine whether user preference is a suitable cost function before such approaches can be implemented into clinical practice.

However, although the current thesis showed that human-in-the-loop optimization is able to find individually optimal solutions of these devices, we did not directly compare the effect of human-in-the-loop optimization with the current subjective device tuning performed by specialists. Consequently, it remains unknown whether human-in-the-loop optimization is superior to current standards, which should be investigated in future research.

8.7. Conclusion

In this thesis, we explored human-in-the-loop optimization protocols for assistive technology to augment gait performance. We demonstrated that optimal device settings differ substantially between individuals, while even small differences in settings can already affect gait performance on an individual level. This highlights the need to tune assistive technology to the individual end-user. Human-in-the-loop optimization can identify optimal device settings while fostering motor learning, enabling co-adaptation between the user and device to optimize gait performance. Although clinical feasibility remains questionable in its present state, current limitations could be addressed, and human-in-the-loop optimization has the potential to enhance the effectiveness of state-of-the-art assistive gait technology.

8.8. Reference list

[1] D. E. Miller, G. R. Tan, E. M. Farina, A. L. Sheets-Singer, and S. H. Collins, “Characterizing the relationship between peak assistance torque and metabolic cost reduction during running with ankle exoskeletons,” Journal of neuroengineering and rehabilitation, vol. 19, no. 1, pp. 46, 2022.

[2] M. Sanno, S. Willwacher, G. Epro, and G. P. Brüggemann, “Positive Work Contribution Shifts from Distal to Proximal Joints during a Prolonged Run,” Medicine and science in sports and exercise, vol. 50, no. 12, pp. 2507-2517, Dec, 2018.

[3] K. A. Ingraham, C. D. Remy, and E. J. Rouse, “The role of user preference in the customized control of robotic exoskeletons,” Science robotics, vol. 7, no. 64, pp. eabj3487, 2022.

[4] M. A. Diaz, M. Vos, A. Dillen, B. Tassignon, L. Flynn, J. Geeroms, R. Meeusen, T. Verstraten, J. Babic, P. Beckerle, and K. De Pauw, “Human-in-the-Loop Optimization of Wearable Robotic Devices to Improve Human-Robot Interaction: A Systematic Review,” IEEE transactions on cybernetics, vol. 53, no. 12, pp. 7483-7496, Dec, 2023.

[5] P. Slade, C. Atkeson, J. M. Donelan, H. Houdijk, K. A. Ingraham, M. Kim, K. Kong, K. L. Poggensee, R. Riener, M. Steinert, J. Zhang, and S. H. Collins, “On human-in-the-loop optimization of human-robot interaction,” Nature, vol. 633, no. 8031, pp. 779-788, Sep, 2024.

[6] J. M. Donelan, R. Kram, and A. D. Kuo, “Simultaneous positive and negative external mechanical work in human walking,” Journal of Biomechanics, vol. 35, no. 1, pp. 117-124, Jan, 2002.

[7] I. J. Blokland, J. J. De Koning, T. Van Kan, C. A. Van Bennekom, J. H. Van Dieen, and H. Houdijk, “Estimation of metabolic energy expenditure during short walking bouts,” International Journal of Sports Medicine, vol. 42, no. 12, pp. 1098-1104, 2021.

[8] J. C. Selinger, and J. M. Donelan, “Estimating instantaneous energetic cost during non-steady-state gait,” Journal of applied physiology (Bethesda, Md.: 1985), vol. 117, no. 11, pp. 1406-1415, Dec 1, 2014.

[9] S. C. Senatore, K. Z. Takahashi, and P. Malcolm, “Using human-in-the-loop optimization for guiding manual prosthesis adjustments: a proof-of-concept study,” Frontiers in Robotics and AI, vol. 10, pp. 1183170, 2023.

[10] W. Felt, J. C. Selinger, J. M. Donelan, and C. D. Remy, ““‘Body-In-The-

Loop": Optimizing device parameters using measures of instantaneous energetic cost," PloS one, vol. 10, no. 8, pp. e0135342, 2015.

[11] R. Garcia-Rosas, Y. Tan, D. Oetomo, C. Manzie, and P. Choong, "Personalized online adaptation of kinematic synergies for human-prosthesis interfaces," IEEE transactions on cybernetics, vol. 51, no. 2, pp. 1070-1084, 2019.

[12] Y. Ding, M. Kim, S. Kuindersma, and C. J. Walsh, "Human-in-the-loop optimization of hip assistance with a soft exosuit during walking," Science robotics, vol. 3, no. 15, pp. eaar5438., Feb 28, 2018.

[13] M. Kim, Y. Ding, P. Malcolm, J. Speeckaert, C. J. Siviy, C. J. Walsh, and S. Kuindersma, "Human-in-the-loop Bayesian optimization of wearable device parameters," PloS one, vol. 12, no. 9, pp. e0184054, 2017.

[14] L. Xu, X. Liu, Y. Chen, L. Yu, Z. Yan, C. Yang, C. Zhou, and W. Yang, "Reducing the muscle activity of walking using a portable hip exoskeleton based on human-in-the-loop optimization," Frontiers in Bioengineering and Biotechnology, vol. 11, pp. 1006326, 2023.

[15] N. Hansen, "The CMA evolution strategy: a comparing review," Towards a new evolutionary computation, pp. 75-102, 2006.

[16] J. Zhang, P. Fiers, K. A. Witte, R. W. Jackson, K. L. Poggensee, C. G. Atkeson, and S. H. Collins, "Human-in-the-loop optimization of exoskeleton assistance during walking," Science (New York, N.Y.), vol. 356, no. 6344, pp. 1280-1284, Jun 23, 2017.

[17] P. Slade, M. J. Kochenderfer, S. L. Delp, and S. H. Collins, "Personalizing exoskeleton assistance while walking in the real world," Nature, vol. 610, no. 7931, pp. 277-282, 2022.

[18] J. Kim, B. T. Quinlivan, L.-A. Deprey, D. Arumukhom Revi, A. Eckert-Erdheim, P. Murphy, D. Orzel, and C. J. Walsh, "Reducing the energy cost of walking with low assistance levels through optimized hip flexion assistance from a soft exosuit," Scientific reports, vol. 12, no. 1, pp. 11004, 2022.

[19] C. G. Welker, A. S. Voloshina, V. L. Chiu, and S. H. Collins, "Shortcomings of human-in-the-loop optimization of an ankle-foot prosthesis emulator: a case series," Royal Society open science, vol. 8, no. 5, pp. 202020, 2021.

[20] B. J. Darter, K. M. Rodriguez, and J. M. Wilken, "Test–retest reliability and minimum detectable change using the k4b2: oxygen consumption, gait efficiency, and heart rate for healthy adults during submaximal walking," Research quarterly for exercise and sport, vol. 84, no. 2, pp. 223-231, 2013.

[21] H. J. Ralston, “Energy-speed relation and optimal speed during level walking,” Internationale Zeitschrift für Angewandte Physiologie Einschliesslich Arbeitsphysiologie, vol. 17, no. 4, pp. 277-283, 1958.

[22] S. Song, and H. Geyer, “Predictive neuromechanical simulations indicate why walking performance declines with ageing,” The Journal of physiology, vol. 596, no. 7, pp. 1199-1210, 2018.

[23] S. R. Wurdeman, S. A. Myers, A. L. Jacobsen, and N. Stergiou, “Adaptation and prosthesis effects on stride-to-stride fluctuations in amputee gait,” PloS one, vol. 9, no. 6, pp. e100125, 2014.

[24] J. D. Ventura, G. K. Klute, and R. R. Neptune, “The effect of prosthetic ankle energy storage and return properties on muscle activity in below-knee amputee walking,” Gait & posture, vol. 33, no. 2, pp. 220-226, Feb, 2011.

[25] K. L. Poggensee, and S. H. Collins, “How adaptation, training, and customization contribute to benefits from exoskeleton assistance,” Science Robotics, vol. 6, no. 58, 2021.

[26] T. Schmalz, M. Bellmann, E. Proebsting, and S. Blumentritt, “Effects of adaptation to a functionally new prosthetic lower-limb component: Results of biomechanical tests immediately after fitting and after 3 months of use,” JPO: Journal of Prosthetics and Orthotics, vol. 26, no. 3, pp. 134-143, 2014.

[27] A. K. Dhawale, M. A. Smith, and B. P. Ölveczky, “The role of variability in motor learning,” Annual Review of Neuroscience, vol. 40, no. 1, pp. 479-498, 2017.

[28] Y. Watanabe, N. Kawabe, and K. Mito, “The apex angle of the rocker sole affects the posture and gait stability of healthy individuals,” Gait & posture, vol. 86, pp. 303-310, May, 2021.

[29] A. F. Azocar, L. M. Mooney, J.-F. Duval, A. M. Simon, L. J. Hargrove, and E. J. Rouse, “Design and clinical implementation of an open-source bionic leg,” Nature biomedical engineering, vol. 4, no. 10, pp. 941-953, 2020.

[30] K. A. Ingraham, M. Tucker, A. D. Ames, E. J. Rouse, and M. K. Shepherd, “Leveraging user preference in the design and evaluation of lower-limb exoskeletons and prostheses,” Current Opinion in Biomedical Engineering, pp. 100487, 2023.

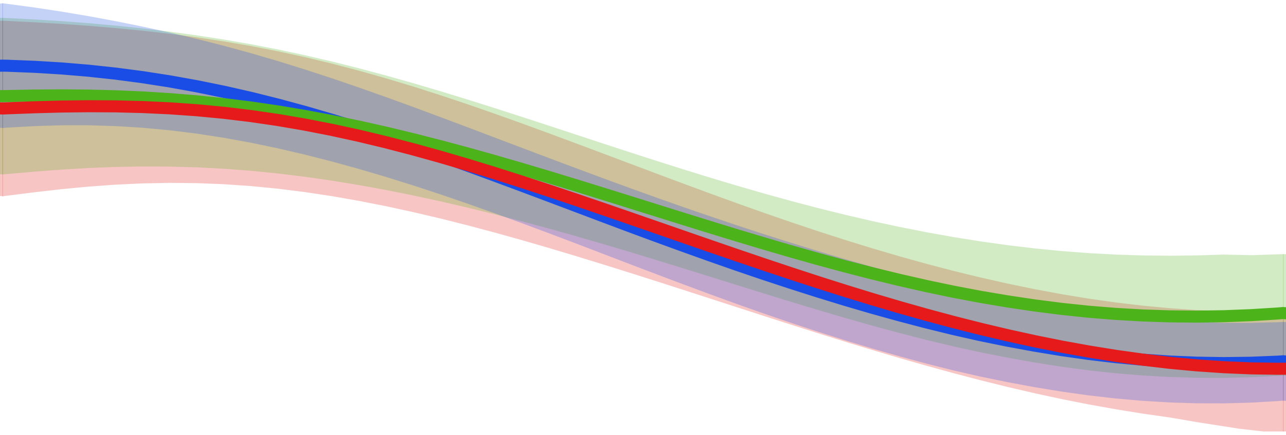

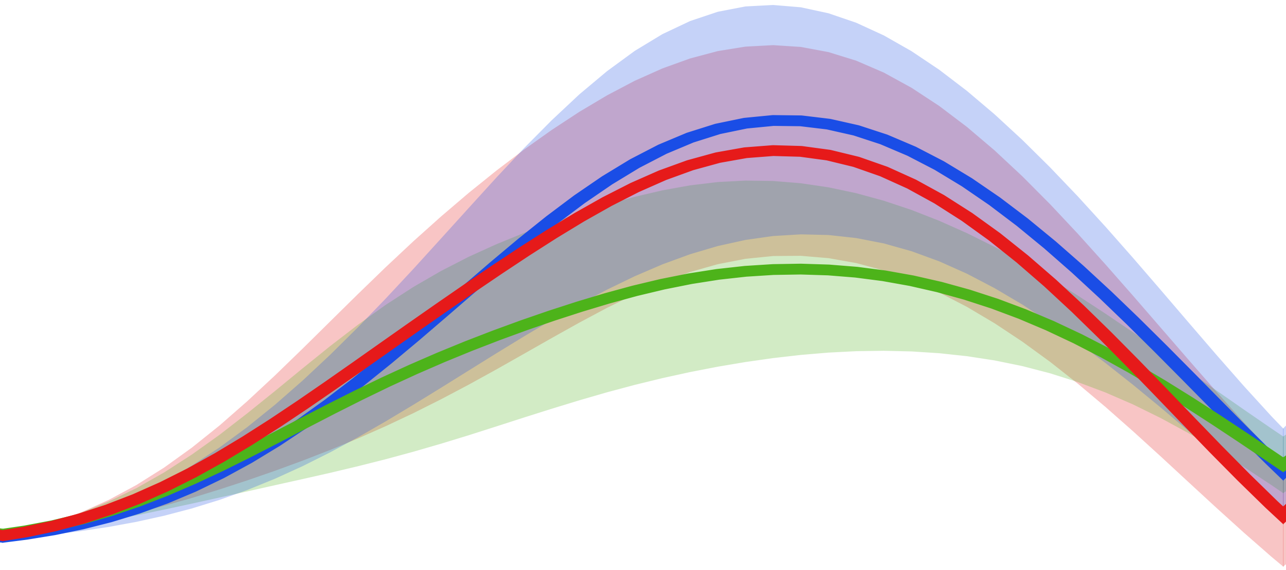

Appendix

Summary
Samenvatting
Author contributions
Dankwoord
About the author
Scientific output

Summary

In this thesis, we aimed to explore the human-in-the-loop optimization paradigm for enhancing gait performance using different types of assistive technology for the foot and ankle, spanning from footwear to prosthetic ankle-foot devices.

The important role of the foot-ankle system during human gait was introduced in **Chapter 1**. The foot and ankle continuously adjust their alignment and function to achieve the desired movement, e.g., by adjusting the support surface to enhance stability or acting as a lever system to enhance propulsion and gait economy. Assistive technology for gait such as footwear, ankle-foot orthoses, or prosthetic devices can be used to support, augment or replace the physiological foot-ankle system to enhance the user's performance. However, the effectiveness of current state-of-the-art assistive gait technology lags behind expectations. This may be due to the properties or behavior of these devices being insufficiently adjusted to the individual user. A promising method that could address current challenges and improve the efficacy of assistive gait technology is human-in-the-loop optimization. By means of human-in-the-loop optimization, device parameters of assistive technology could be tuned to the biological properties of the user while also taking into account the natural behavior of humans to simultaneously optimize their gait performance.

In **Chapter 2**, we aimed to individually optimize the rollover profile of rocker shoes to increase the efficiency at which muscles generate mechanical power during running, by reducing muscle fiber shortening velocities and enhancing energy storing and return of mechanical power. In particular, the Triceps Surae contain morphologies suitable for these processes. Optimizing the gear ratio of the Triceps Surae at the ankle via optimization of a rocker shoe rollover profile could fully utilize these properties. Therefore, we aimed to individually optimize the rollover profile of rocker shoes via human-in-the-loop optimization to maximize positive ankle work, redistribute joint work from the hip and knee to the ankle, and ultimately improve running economy. A total of ten runners ran on a treadmill with experimental rocker shoes in which the apex position and angle were optimized to maximize ankle work. Optimal apex settings differed considerably between participants. Using optimal settings resulted in higher positive ankle work and a higher proportional share of the ankle in the total positive lower-limb work compared to using standard apex settings. The study showed that human-in-the-loop optimization could improve the effectiveness of footwear with respect to the selected optimization objective on an individual level. However, an expected difference in running economy between these conditions was

not found.

The importance of cost function selection was further explored in **Chapter 3**. The outcome of the human-in-the-loop optimization process likely depends on the selected cost function and its responsiveness to the device parameters being tuned. In this study, we aimed to explore whether and how human-in-the-loop optimization via different cost functions (i.e., metabolic cost, collision work as measure for external mechanical work, and step distance variability as measure for gait stability) affects the optimal apex position and angle of a rocker shoe differently for individuals during walking. Ten healthy individuals walked on a treadmill with experimental rocker shoes in which the apex position and angle were optimized via human-in-the-loop optimization using different cost functions. Optimal apex parameters differed substantially between participants, and optimal apex positions differed between cost functions. Moreover, the responsiveness to changes in apex parameters differed between cost functions. Collision work was the only cost function that resulted in a significant improvement in its performance criteria. Significant improvements in metabolic cost or step distance variability were not found after optimization. This study shows that cost function selection is important when human-in-the-loop optimization is used, because different cost functions lead to different optimal settings. Therefore, it is important to select a cost function that is sufficiently sensitive and robust to the device parameters being tuned and simultaneously results in an outcome that matches the intended optimization domain of the user, to allow conversion to an optimum that suits the individual.

Subsequently, we aimed to make the next step towards clinical practice, introducing human-in-the-loop optimization as a method that could be useful in rehabilitation care. Therefore, we tested human-in-the-loop optimization in a population of people with a transtibial amputation using a non-commercial energy storing and return prosthetic foot in **Chapters 4**, **5**, **6**, and **7**.

In **Chapter 4**, we used human-in-the-loop optimization to individually optimize the stiffness and alignment of a prosthetic foot to decrease the metabolic cost of walking. Ten individuals with a transtibial amputation underwent an optimization protocol while walking on a treadmill with an experimental prosthetic foot with tunable stiffness and tunable alignment. Optimized stiffness and alignment settings differed between participants. Walking on the prosthetic foot with optimized settings (after the optimization process) resulted in a more than 10% reduction in metabolic cost compared to walking on the prosthetic foot with standard settings before optimization. This seemed partly due to changes in stiffness and alignment settings of the prosthetic foot, but also partly due to motor adaptations of the user. This study indicates that both optimization of prosthetic components and motor adaptation of the user contribute to the reduction in metabolic cost.

In **Chapter 5**, we further explored the effect of motor learning of the user throughout the optimization process, as people with a lower-limb amputation must undergo a process of co-adaptation with a prosthesis to achieve optimal walking performance. During the tuning process, the user is assumed to continuously adapt their motor strategies to the changing device settings. Alongside these immediate motor adaptations, long-term motor learning also occurs. This study aimed to investigate the time course of motor learning of individuals with a transtibial amputation during the human-in-the-loop optimization process of a prosthetic foot, in which the stiffness and alignment were optimized to minimize the metabolic cost of walking. Motor learning was monitored by repeatedly walking on the experimental prosthetic foot with the initial standard settings throughout the optimization process. Metabolic cost of walking with the initial standard settings decreased significantly over time. This decrease extended over at least 56 minutes in our human-in-the-loop optimization experiment. This shows that motor learning plays a significant role during prosthetic tuning, and co-adaptation should be taken into account during the tuning of prosthetic devices, even when human-in-the-loop optimization is not used.

In **Chapter 6**, we explored the context-dependence of optimized device settings. Human-in-the-loop optimization is typically performed at a fixed walking speed, which might result in optimal settings that are quite speed-dependent. We aimed to explore whether optimal prosthetic settings (stiffness and alignment) of the experimental prosthetic foot obtained via human-in-the-loop optimization depend on the walking speed (self-selected walking speed and 120% self-selected walking speed), and to what extent these potentially different settings affect the metabolic cost of walking at these speeds. In a case series experiment with three participants, we found small differences in optimal prosthetic foot settings between walking speeds, but the direction of change in optimal settings differed between participants. The differences in optimal settings did not result in a clear trend or meaningful change in metabolic cost. However, this suggests that prosthetic foot settings individually optimized for self-selected walking speed might be used effectively across a broader range of walking speeds.

In **Chapter 7**, we explored the correlation between metabolic cost and perceived comfort during the human-in-the-loop optimization process. Perceived comfort could be an interesting alternative optimization objective, either as a proxy for metabolic cost or to capture alternative objectives of the individual. Perceived comfort does not require advanced data capture systems to be measured and could shorten trial duration. This study aimed to explore whether the measured metabolic cost of walking correlates with the perceived comfort of the user during the human-in-the-loop optimization process of a prosthetic foot, and whether perceived comfort might be a relevant optimization objective to use during the tuning of assistive devices as a proxy for metabolic cost. Results showed a moderate negative correlation between metabolic cost and perceived comfort. On an individual level, a significant negative correlation was found in six out of the ten participants. The lack of correlation between metabolic cost and perceived comfort in some individuals shows that these metrics do not always measure the same aspect of gait performance. Perceived comfort allows users to prioritize different optimization objectives simultaneously during the optimization of an assistive device, and apparently, metabolic cost is, to varying extents, prioritized for the perceived comfort score.

Finally, in **Chapter 8**, we provided a general discussion of the findings in this thesis. We demonstrated that optimal device settings differ substantially between individuals, while even small differences in settings can already affect gait performance on an individual level. This highlights the need to tune assistive technology to the individual end-user. Human-in-the-loop optimization can identify optimal device settings while fostering motor learning, enabling co-adaptation between the user and device to optimize gait performance. Key factors influencing human-in-the-loop optimization include the choice of cost function, the design of the optimization algorithm, and contextual conditions. Human-in-the-loop optimization requires careful cost function selection to ensure meaningful optimization, alongside a clever optimization algorithm capable of rapidly and effectively exploring the noisy and dynamic search landscape. We also demonstrated that optimal device settings tend to remain effective across a broader range of activities, and not every circumstance requires fully optimized settings. Although the clinical feasibility of human-in-the-loop optimization remains uncertain in its present state, current barriers to implementation could be addressed, and human-in-the-loop optimization therefore has the potential to enhance the effectiveness of state-of-the-art assistive gait technology.

Samenvatting

In dit proefschrift hebben we het human-in-the-loop-optimalisatieparadigma onderzocht voor het verbeteren van de loopprestatie door gebruik te maken van verschillende soorten technologische hulpmiddelen, variërend van orthopedische schoenen tot enkel-voetprothesen.

Het belang van de voet en enkel tijdens het menselijk lopen werd geïntroduceerd in **Hoofdstuk 1**. De voet en enkel passen hun stand en functie telkens aan om de gewenste beweging tot stand te laten komen. Zo kunnen ze het steunoppervlak aanpassen om balans te verbeteren of functioneren als een hefboom om de afzet en loopefficiëntie te verbeteren. Technologische hulpmiddelen voor het lopen, zoals schoenen, enkel-voetorthesen of prothesen, kunnen worden gebruikt om het biologische voet-enkelsysteem te ondersteunen, te versterken, of te vervangen en de loopprestatie van de gebruiker te verbeteren. Echter, de effectiviteit van geavanceerde technologische hulpmiddelen voldoet nog niet aan de verwachtingen. Een mogelijke oorzaak hiervoor is dat de eigenschappen of het gedrag van deze hulpmiddelen onvoldoende zijn afgestemd op de individuele gebruiker. Een veelbelovende methode, die de huidige uitdagingen kan aanpakken en de doeltreffendheid van technologische hulpmiddelen kan verbeteren, is human-in-the-loop-optimalisatie. Door middel van human-in-the-loop-optimalisatie kunnen de instellingen van deze hulpmiddelen worden afgestemd op de biologische eigenschappen van de gebruiker, terwijl ook rekening wordt gehouden met het natuurlijke gedrag van mensen om gelijktijdig hun looppatroon aan te passen aan het hulpmiddel.

Ons doel in **Hoofdstuk 2** was om het afwikkelprofiel van rockerschoenen individueel te optimaliseren om hardloopefficiëntie te verbeteren. Dit zouden we kunnen bereiken door de efficiëntie waarmee spieren mechanisch vermogen leverden te verhogen door de verkortingssnelheid van spiervezels te verlagen en de opslag en teruggave van mechanische energie te verbeteren. Met name de mm. Triceps Surae hebben eigenschappen die hiervoor geschikt zijn. Door het optimaliseren van de verhouding tussen de interne en externe momentarm van spier- en grondreactiekracht rond het enkelgewricht door aanpassing van het afwikkelprofiel van een rockerschoen kunnen deze eigenschappen maximaal worden benut. Het doel van deze studie was het afwikkelprofiel van rockerschoenen individueel te optimaliseren via human-in-the-loop-optimalisatie om de positieve enkelarbeid te maximaliseren, gewrichtsarbeid van de heup en knie naar de enkel te herverdelen en zo de hardloopefficiëntie te verbeteren. Tien hardlopers liepen op een loopband met experimentele

rockerschoenen, waarvan de apexpositie en apexhoek werden geoptimaliseerd om positieve enkelarbeid te maximaliseren. Optimale apexinstellingen verschilden substantieel tussen proefpersonen. Het gebruik van de optimale apexinstellingen resulteerde in hogere positieve enkelarbeid en een hoger proportioneel aandeel van de enkel in de totale positieve arbeid gegenereerd rond de gewrichten van de onderste ledematen vergeleken met het gebruik van de standaard apexinstellingen. Hoewel het verwachte verschil in hardloopefficiëntie niet werd gevonden, toonde deze studie aan dat human-in-the-loop-optimalisatie de effectiviteit van schoenen ten opzichte van het gekozen optimalisatiecriterium op individueel niveau kan verbeteren.

Het belang van de keuze van het optimalisatiecriterium hebben we verder onderzocht in **Hoofdstuk 3**. De uitkomst van het human-in-the-loop-optimalisatieproces is waarschijnlijk afhankelijk van het gekozen optimalisatiecriterium (gerepresenteerd in een kostfunctie) en zijn gevoeligheid voor de verstelbare parameters van het hulpmiddel. In deze studie onderzochten we hoe human-in-the-loop-optimalisatie via verschillende kostfuncties (metabole kosten, impactarbeid als maat voor externe mechanische arbeid en stapvariabiliteit als maat voor loopstabiliteit) de optimale apexpositie en apexhoek van rockerschoenen verschillend beïnvloed bij individuen tijdens het wandelen. Tien gezonde proefpersonen wandelden op een loopband met experimentele rockerschoenen, waarbij apexpositie en apexhoek werden geoptimaliseerd via human-in-the-loop-optimalisatie met verschillende kostfuncties. De optimale apexparameters verschilden aanzienlijk tussen de proefpersonen en de optimale apexposities verschilden tussen de kostfuncties. Bovendien verschilde de gevoeligheid voor veranderingen in apexparameters tussen de kostfuncties. Impactarbeid was de enige kostfunctie die bij gebruik van de optimale apexparameters resulteerde in een significante verbetering van zijn optimalisatiecriterium. Het gebruik van apexparameters geoptimaliseerd voor metabole kosten of stapvariabiliteit resulteerde niet in verbeteringen in respectievelijk metabole kosten of stapvariabiliteit. Deze studie toont aan dat de keuze van kostfunctie van belang is bij het gebruik van human-in-the-loop-optimalisatie, want verschillende kostfuncties leiden tot verschillende optimale instellingen. Het is daarom van belang om een kostfunctie te selecteren die voldoende gevoelig en robuust is voor de verstelbare hulpmiddelparameters die worden geoptimaliseerd, en gelijktijdig resulteert in een uitkomst die past bij het beoogde optimalisatiedoel van de gebruiker, zodat convergentie naar het gewenste optimum van de gebruiker kan plaatsvinden.

Vervolgens hebben we de volgende stap richting klinische toepassing gezet door human-in-the-loop-optimalisatie te introduceren als een bruikbare methode in de revalidatie. Hiervoor hebben we human-in-the-loop-optimalisatie voor een niet-commerciële ‘Energy Storing and Return’ (ESAR) prothesevoet getest in een populatie van mensen met een transtibiale amputatie in **Hoofdstuk 4**, **5**, **6** en **7**.

In **Hoofdstuk 4** gebruikten we human-in-the-loop-optimalisatie voor het individueel optimaliseren van de stijfheid en uitlijning van een prothesevoet om de metabole kosten van het wandelen te verlagen. Tien deelnemers met een transtibiale amputatie ondergingen een optimalisatieprotocol terwijl ze liepen op een loopband met de experimentele prothesevoet met verstelbare stijfheid en uitlijning. Optimale instellingen voor stijfheid en uitlijning verschilden tussen proefpersonen. Lopen op de prothesevoet met geoptimaliseerde instellingen (na het optimalisatieproces) resulteerde in een afname in metabole kosten van meer dan 10% vergeleken met lopen op de prothesevoet met de standaard instellingen. Deze afname leek gedeeltelijk te worden veroorzaakt door optimalisatie van de stijfheid en uitlijning van de prothesevoet en gedeeltelijk door motorische adaptaties van de gebruiker. Deze studie wijst erop dat zowel optimalisatie van onderdelen van de prothesevoet als motorische adaptaties van de gebruiker bijdragen aan de afname in metabole kosten.

In **Hoofdstuk 5** hebben we het effect van motorisch leren van de gebruiker gedurende het optimalisatieproces verder onderzocht. Mensen met een beenamputatie ondergaan een proces van co-adaptatie met hun prothese om het looppatroon te optimaliseren. Tijdens het aanmeetproces van een prothese wordt verondersteld dat de gebruiker zijn of haar motorische strategieën continu aanpast aan de veranderende instellingen van het hulpmiddel. Naast deze directe motorische adaptaties vindt gelijktijdig ook motorisch leren op de lange termijn plaats. Het doel van deze studie was om het tijdsverloop van motorisch leren bij mensen met een transtibiale amputatie te onderzoeken tijdens het human-in-the-loop-optimalisatieproces van een prothesevoet, waarbij de stijfheid en uitlijning werden geoptimaliseerd om de metabole kosten van het wandelen te minimaliseren. Motorisch leren werd gemonitord door gedurende het optimalisatieproces deelnemers herhaaldelijk te laten lopen op de experimentele prothesevoet met initiële standaardinstellingen. Metabole kosten tijdens het lopen op de initiële standaardinstellingen namen significant af in de loop van de tijd. Tijdens ons human-in-the-loop-optimalisatie experiment hield deze afname gedurende 56 minuten aan. Dit laat zien dat motorisch leren een significante rol speelt tijdens het aanmeetproces van prothesen. Ook wanneer er geen gebruik wordt gemaakt van human-in-the-loop-optimalisatie tijdens het aanmeten van prothesen, moet co-adaptatie in acht genomen worden.

In **Hoofdstuk 6** onderzochten we de contextafhankelijkheid van geoptimaliseerde instellingen van technologische hulpmiddelen. Human-in-the-loop-optimalisatie vindt doorgaans plaats op een constante loopsnelheid. Dit zou mogelijk kunnen resulteren in optimale instellingen die snelheidsspecifiek zijn. Tijdens deze studie onderzochten we of optimale prothese-instellingen (stijfheid en uitlijning) van de experimentele prothesevoet, verkregen via human-in-the-loop-optimalisatie, afhangen van de loopsnelheid (voorkeurssnelheid en 120% voorkeurssnelheid) en in welke mate deze mogelijk verschillende instellingen de metabole kosten van het lopen op deze snelheden beïnvloeden. In een case-series experiment met drie deelnemers met een transtibiale amputatie, vonden we kleine verschillen in optimale prothese-instellingen tussen de loopsnelheden, maar de richting van deze verandering verschilde tussen deelnemers. De verschillende optimale instellingen tussen snelheden resulteerden niet in een duidelijk trend of betekenisvolle veranderingen in metabole kosten. Dit zou erop kunnen duiden dat prothesevoetinstellingen, individueel geoptimaliseerd voor de voorkeursloopsnelheid, effectief gebruikt kunnen worden over een groter bereik van loopsnelheden.

In **Hoofdstuk 7** onderzochten we de correlatie tussen metabole kosten en ervaren comfort tijdens het human-in-the-loop-optimalisatieproces. Ervaren comfort is mogelijk een interessant alternatief optimalisatiecriterium, ofwel als proxy voor metabole kosten of als alternatief optimalisatiecriterium voor het individu. Ervaren comfort vereist geen geavanceerde meetsystemen om te bepalen en zou daarnaast de tijdsduur van experimenten kunnen verkorten. Tijdens deze studie onderzochten we of de gemeten metabole kosten van het lopen correleren met het ervaren comfort van de gebruiker tijdens het human-in-the-loop-optimalisatieproces van een prothesevoet en of ervaren comfort mogelijk een relevant optimalisatiecriterium is om te gebruiken als proxy voor metabole kosten tijdens het aanmeten van technologische hulpmiddelen. De resultaten lieten een matige negatieve correlatie zien tussen metabole kosten en ervaren comfort. Op individueel niveau werd een significante negatieve correlatie gevonden bij zes van de tien proefpersonen. Het ontbreken van een significante correlatie tussen metabole kosten en ervaren comfort laat zien dat deze constructen niet altijd hetzelfde aspect van de loopprestatie meten. Ervaren comfort stelt mensen in staat om tijdens het optimalisatieproces van een hulpmiddel verschillende optimalisatiecriteria gelijktijdig te prioriteren en blijkbaar worden metabole kosten in verschillende mate geprioriteerd in het ervaren comfort.

Tot slot bediscussieerden we in **Hoofdstuk 8** de bevindingen in dit proefschrift. We lieten zien dat optimale instellingen van technologische hulpmiddelen substantieel verschillen tussen individuen, waarbij zelfs kleine verschillen in instellingen de loopprestatie op individueel niveau al kunnen beïnvloeden. Dit benadrukt de noodzaak om hulpmiddelen af te stemmen op de individuele eindgebruiker. Human-in-the-loop-optimalisatie is in staat deze optimale instellingen te identificeren terwijl het gelijktijdig het motorisch leren van de gebruiker faciliteert en hiermee co-adaptie tussen gebruiker en hulpmiddel om de loopprestatie te verbeteren bevordert. Sleutelfactoren die het human-in-the-loop-optimalisatieproces beïnvloeden zijn de gekozen kostfunctie, het ontwerp van het optimalisatiealgoritme en de contextuele omstandigheden. Human-in-the-loop-optimalisatie vereist een zorgvuldig gekozen kostfunctie die betekenisvolle optimalisatie waarborgt, samen met een slim algoritme dat in staat is om snel en efficiënt het ruisachtige en dynamische zoeklandschap te verkennen. We hebben ook laten zien dat optimale hulpmiddelinstellingen effectief lijken te blijven bij een breder bereik van activiteiten en dat mogelijk niet iedere omstandigheid volledig geoptimaliseerde instellingen vereist. Hoewel de klinische haalbaarheid van human-in-the-loop-optimalisatie in de huidige vorm nog niet verzekerd is, zijn huidige obstakels tot implementatie te overbruggen en heeft human-in-the-loop-optimalisatie de potentie om de effectiviteit van geavanceerde technologische hulpmiddelen voor lopen te verbeteren.

Author contributions

The contributions of the PhD candidate, Thijs Tankink, to this thesis are detailed below for each chapter, using the Contributor Role Taxonomy (CRediT). Contributions are listed according to role definitions as established by the CRediT system.

Chapter 1: General introduction.
Conceptualization, visualization, writing – original draft preparation

Chapter 2: Human-in-the-loop optimized rocker profile of running shoes to enhance ankle work and running economy. Tankink, T., Houdijk, H., & Hijmans, J. M. (2024). *European Journal of Sport Science, 24 (1), 164-173*.
Conceptualization, formal analysis, investigation, methodology, visualization, writing – original draft preparation

Chapter 3: Human-in-the-loop optimization of rocker shoes via different cost functions during walking. Tankink, T., Hijmans, J. M., Carloni, R., & Houdijk, H. (2024). *Journal of Biomechanics, 166, 112028*.
Conceptualization, formal analysis, investigation, methodology, visualization, writing – original draft preparation

Chapter 4: Human-in-the-loop optimization of the stiffness and alignment of a prosthetic foot to reduce the metabolic cost of walking. Tankink, T., Houdijk, H., Tabucol, J., Leopaldi, M., Hijmans, J. M., & Carloni, R. (2025). *IEEE Transactions on Neural Systems and Rehabilitation Engineering, 33, 2823-2833*.
Conceptualization, formal analysis, investigation, methodology, visualization, writing – original draft preparation

Chapter 5: Time course of motor learning during human-in-the-loop optimization of a prosthetic foot. Tankink, T., Hijmans, J. M., Carloni, R., & Houdijk, H. (2025). *Human Movement Science, 104, 103418*.
Conceptualization, formal analysis, investigation, methodology, visualization, writing – original draft preparation

Chapter 6: Effects of walking speed on human-in-the-loop optimized settings and performance of a prosthetic foot: a case-series. Tankink, T., Hijmans, J. M., Houdijk, H., & Carloni, R. (2025).
Conceptualization, formal analysis, investigation, methodology, visualization, writing – original draft preparation

Chapter 7: Correlation between metabolic cost and perceived comfort during human-in-the-loop optimization of a prosthetic foot. Tankink, T., Houdijk, H., Carloni, R., & Hijmans, J. M. (2025). *Gait & Posture, 110111*.
Conceptualization, formal analysis, investigation, methodology, visualization, writing – original draft preparation

Chapter 8: General discussion.
Conceptualization, visualization, writing – original draft preparation

Dankwoord

Onderzoek doe je nooit alleen. Dit proefschrift had er dan ook niet gelegen zonder de mensen die me de afgelopen jaren, op wat voor manier dan ook, hebben geholpen. Mijn dank is groot!

Hierbij wil ik natuurlijk graag een aantal mensen in het bijzonder bedanken, te beginnen bij mijn promotieteam. **Han**, **Juha** & **Raffaella**, dank voor de fijne begeleiding en samenwerking de afgelopen jaren. Door jullie openheid, constructieve feedback, de geboden kansen en het vertrouwen dat jullie me gaven, heb ik me enorm kunnen ontwikkelen.

Han, na je komst in Groningen kwamen we in contact via de cursus Inleiding Neuromechanica, waar ik als student-assistent een rol mocht vervullen. Je persoonlijke begeleiding, waarin je vriendelijke persoonlijkheid direct naar voren kwam, beviel me zo goed dat ik voor mijn review en masterafstudeerproject opnieuw bij je uitkwam. Zo kwam het balletje aan het rollen. Ik waardeer het dat je, ondanks je bomvolle agenda, altijd de tijd neemt om te horen hoe het met me gaat.
Of het nu gaat om een 'eenvoudig' wandelexperiment of de (steeds bijna werkende) Open-Source Leg, je nieuwsgierigheid naar de biomechanica van het menselijk bewegen en je enthousiasme om dit beter te begrijpen zijn aanstekelijk. Het samenwerken is na al die jaren dan ook nooit gaan vervelen, en ik ben blij dat we er nog een paar jaar aan vast kunnen plakken.

Juha, je kwam aan het begin van mijn masterafstudeerproject in beeld en je begeleiding, to the point, zonder dat dit ten koste gaat van diepgang of persoonlijke aandacht, is mij ontzettend bevallen. Je soms pragmatische houding heeft er de afgelopen jaren voor gezorgd dat belangrijke beslissingen niet te lang werden uitgesteld en projecten geen onnodige vertraging opliepen.
Je telefoontje toen ik in Stanford zat, met de vraag of ik het zag zitten om mijn promotietraject te combineren met werken als labtechnicus bij de GRAIL in Beatrixoord, kwam als een grote verrassing en staat me nog goed bij. Dank voor het bieden van deze kans. Naast het feit dat ik er ontzettend veel van heb geleerd, heeft het ook veel deuren geopend en mijn promotietraject een flinke boost gegeven. Ik ben ontzettend blij dat we onze samenwerking kunnen voortzetten tijdens de postdoc.

Raffaella, you joined the team last, during the writing process of the MSc-PhD application. Your technical background and expertise were a valuable addition to the team. By involving me in the MyLeg project early in my PhD, you helped me develop my technical knowledge of prosthetics and gave me insight into how engineers approach such assistive devices, which proved extremely useful in later projects. Working from your lab and helping with supervision was a welcome change from my other duties at Human Movement Sciences. Thank you very much for the great supervision and collaboration.

Dear members of the reading committee, **Herman van der Kooij**, **Rienk Dekker**, and **Steve Collins**, thank you very much for reading and assessing my thesis. I am grateful for your feedback and for attending the defense ceremony. **Steve** & **Russell**, thank you so much for hosting me during my research internship. My time in the United States was a truly unique experience, and without the knowledge and insights I gained at Stanford, this thesis would not have been possible.

Ik wil ook graag alle partners bedanken die hebben bijgedragen aan de projecten. OIM Orthopedie: **Henk**, **Chris**, **Sandra**, **Auke** & **Lysanne**, dankjewel voor het meedenken bij de opzet van de projecten, het werven van de proefpersonen en het aanmeten van de verstelbare prothesevoet! Jullie flexibiliteit, wanneer ik weer eens onverwacht of ongeduldig de kantine of werkplaats kwam binnenvallen, en bijdrage tijdens de metingen waren onmisbaar! University of Bologna: **Johnnidel** & **Marco**, thank you for the smooth collaboration and technical support regarding the tunable prosthetic foot MyFlex-η.

Technische Dienst: **Anniek**, **Dirk**, **Emiel** & **Wim**, dank voor jullie ondersteuning en het meedenken bij de verschillende projecten. Petje af voor hoe jullie altijd direct voor iedereen klaarstaan en helpen om problemen op te lossen.

Ook wil ik graag alle studenten bedanken die hebben geholpen bij de verschillende onderzoeken. **Daan**, **Sanne**, **Denise**, **Iris**, **Twan**, **Friso**, **Pim**, **Foeke**, **Julie**, **Juliëtte** & **Lotte**, zonder jullie was het niet gelukt om de metingen uit te voeren. Ik heb genoten van jullie enthousiasme, betrokkenheid en nieuwsgierigheid.

Het Motion Lab: **Thijs**, **Chantal**, **Christian**, **Athra**, **Sasha** & nogmaals **Juha**. Ik vond het ontzettend tof om onderdeel te zijn van jullie team en vind het knap hoe strak jullie de zaken voor elkaar hebben. Hoewel het werk vanaf verschillende locaties werd uitgevoerd, was de weekstart op maandag een fijn moment om iedereen te kunnen spreken. Dankjulliewel voor de fijne samenwerking.
Christian, bedankt dat je me de kans hebt gegeven om mezelf via de postdoc verder te verdiepen in de biomechanica van het menselijk bewegen en in het ontwikkelen van spier-skeletmodellen. Ik heb er nog geen moment spijt van gehad en ben ontzettend gemotiveerd om het maximale uit de projecten te halen.

Chengxiang, **Oran**, thank you for the great collaboration over the past few years! It has been a pleasure working with you on the development of prosthetics, always with plenty of room for joy and enthusiasm. I also really enjoyed the glimpse into Chinese culture and cuisine.

Alle collega's van Bewegingswetenschappen, bedankt voor de fijne en stimulerende werksfeer. In het bijzonder mijn kamergenoten **Dagmar**, **Eline** & **Pim**. **Dagmar** & **Pim**, dankjulliewel voor het wegwijs maken tijdens de start van mijn PhD en het bespreken en klagen over van alles. **Eline**, ik bewonder je passie voor onderzoek en laat me hier graag door motiveren. Daarnaast zorgt je interesse, openheid en de gedeelde passie voor sport ook daarbuiten voor een fijne band. **Anadi**, **Bas**, **Tom** & **Samruddhi**, thank you for the fun during game nights. **Samantha**, **Roos**, **Jelmer**, **Rowie**, **Bart**, **Verena**, **Leila**, **Rifko** & alle andere collega's op de tweede verdieping, bedankt voor alle gezelligheid tijdens koffiepauzes, congressen, uitjes en borrels. Ondanks dat ik de komende jaren helaas wat minder vaak op kantoor zal zijn, ben ik ontzettend blij dat ik kan blijven!

Ook wil ik graag mijn paranimfen bedanken voor alle hulp ter voorbereiding op mijn promotie. Ik ben ontzettend blij dat jullie naast me staan tijdens mijn verdediging.
Alexander, of het nu is tijdens een normale koffiepauze, een avondje Kolonisten van Catan of de 4 Mijl van Groningen, je fijne persoonlijkheid komt de sfeer altijd ten goede. Mocht ik in de toekomst je algoritme nodig hebben om kaarten voor de Marathon Rotterdam te kunnen bemachtigen, weet ik je te vinden!
Rob, sinds de start van de KEI-week in Groningen dacht ik: ik mag die lange Brabander wel. Ik ben dan ook ontzettend blij dat je, na al die jaren samen in Stad,

de paranimf bij mijn promotie wilt zijn. Ik vind het altijd heerlijk om het delen van BW-gerelateerde updates en struggles te combineren met ‘zwammen’ over van alles en niks. Wat mij betreft komen er nog veel van deze avonden en fietsritten bij!

Alle mede-grondleggers van **Café de Knalpot**. Mijn dank richting jullie mag hier zeker niet ontbreken. Het feit dat onze vriendengroep het al sinds de basisschool volhoudt, ondanks dat we zo verschillend zijn, zegt genoeg over hoe hecht we zijn. Het direct voor elkaar klaarstaan, maar elkaar ook de waarheid vertellen wanneer dat nodig is, is denk ik wat onze vriendschap zo sterk maakt. Dit heeft er de afgelopen jaren zeker ook voor gezorgd dat ik mijn PhD-onderzoek altijd heb kunnen relativeren. Dank voor alle onvergetelijke (en absurde) herinneringen en de avonden om hier iedere keer opnieuw weer stuk om te kunnen gaan.

André, **Marleen** & **Pleun**, bedankt voor het warme welkom in de familie en het me direct thuis laten voelen de afgelopen jaren. Jullie interesse en steun heb ik altijd gevoeld en waardeer ik enorm.

Manon, **Sanne**, **Tom**, het jongvee, **Len** & **Jeroen**, & de nieuwe kalveren, ik ben ontzettend blij met onze band en dat we altijd op elkaar kunnen rekenen. Ik vind het ontzettend tof om te zien hoe iedereen zijn eigen weg kiest en ben super benieuwd hoe dat zich de komende jaren verder zal ontwikkelen.

Pap & **Mam**, ik wil jullie ontzettend bedanken voor alle steun de afgelopen jaren. Jullie hebben me altijd het vertrouwen en de ruimte gegeven die ik nodig had, maar staan er altijd wanneer het nodig is. Jullie hebben ons altijd aangemoedigd te doen wat we leuk vinden, en er vervolgens ook volledig voor te gaan. Als ik dit niet van jullie had meegekregen, zou mijn promotietraject zonder twijfel minder soepel zijn verlopen. Ik zeg dit waarschijnlijk niet vaak genoeg, maar ik ben jullie ontzettend dankbaar!

Lieve **Hilke**, bedankt voor je onvoorwaardelijke steun de afgelopen jaren! Ik ben enorm trots op je en heel erg dankbaar dat ik alles met je kan delen. Ik ben ontzettend blij met onze eigen plek en kan niet wachten om samen met jou nog heel veel nieuwe en bijzondere momenten te beleven. Ik hou van jou!

About the author

Thijs Tankink was born on December 20th, 1998, in Enschede, the Netherlands. He attended pre-university education (VWO) at the Assink Lyceum in Eibergen and Haaksbergen. After graduating, Thijs studied Human Movement Sciences at the University of Groningen, where he obtained his Bachelor's degree in 2020 and his Master's degree in 2022. During his Master's thesis, he focused on individually optimizing the rollover profile of running shoes using human-in-the-loop optimization to enhance ankle work and running economy.

After completing his Master's, Thijs was awarded a Master-PhD position at the Department of Human Movement Sciences at the University Medical Center Groningen (UMCG). During his PhD, he investigated human-in-the-loop optimization protocols for enhancing gait performance through a number of assistive technologies, spanning from footwear to prosthetic ankle-foot devices. In 2023, he started combining his PhD research with work as a lab technician at the GRAIL Lab in the Center for Rehabilitation Beatrixoord at the UMCG. In addition to his research activities, Thijs was involved in education and successfully obtained his University Teaching Qualification (UTQ) in March 2025. He contributed to several Bachelor's courses and supervised multiple Bachelor's and Master's students.

In 2026, Thijs began a postdoctoral position at the Department of Human Movement Sciences at the UMCG, focusing on the development of biomechanical models for individualized diagnosis and treatment of complex movement disorders.

Scientific output

Journal publications

Tankink, T. , Houdijk, H., & Hijmans, J. M. (2024). Human-in-the-loop optimized rocker profile of running shoes to enhance ankle work and running economy. *European Journal of Sport Science, 24 (1), 164-173*.

Tankink, T., Hijmans, J. M., Carloni, R., & Houdijk, H. (2024). Human-in-the-loop optimization of rocker shoes via different cost functions during walking. *Journal of Biomechanics, 166, 112028*.

Tankink, T., Houdijk, H., Tabucol, J., Leopaldi, M., Hijmans, J. M., & Carloni, R. (2025). Human-in-the-loop optimization of the stiffness and alignment of a prosthetic foot to reduce the metabolic cost of walking. *IEEE Transactions on Neural Systems and Rehabilitation Engineering, 33, 2823-2833*.

Tankink, T., Hijmans, J. M., Carloni, R., & Houdijk, H. (2025). Time course of motor learning during human-in-the-loop optimization of a prosthetic foot. *Human Movement Science, 104, 103418*.

Tankink, T., Houdijk, H., Carloni, R., & Hijmans, J. M. (2026). Correlation between metabolic cost and perceived comfort during human-in-the-loop optimization of a prosthetic foot. *Gait & Posture, 110111*.

Submitted for publication

Tankink, T., Hijmans, J. M., Houdijk, H., & Carloni, R. (2025). Effects of walking speed on human-in-the-loop optimized settings and performance of a prosthetic foot: a case-series.

A

Conference contributions

ESMAC 2023, Athens, Greece. *Oral presentation*

ISCOMS Congress 2024, Groningen, the Netherlands. *Workshop leader*

National Congress Sport, Physical Activity and Health 2024, Sittard, the Netherlands. *Oral presentation*

Dutch Congress of Rehabilitation Medicine 2024, Utrecht, the Netherlands. *Oral presentation*

7th RehabMove Congress 2025, Groningen, the Netherlands. *Oral presentation*

ISCOMS Congress 2025, Groningen, the Netherlands. *Workshop leader*

I.S.P.O. 20th World Congress 2025, Stockholm, Sweden. *Oral & poster presentation*

Dynamic Walking Congress 2025, Aachen, Germany. *Oral presentation*

I.S.P.O. Dutch Annual Congress 2025, The Hague, the Netherlands. *Oral presentation*

Symposium Dutch HealthTec Academy 2025, Utrecht, the Netherlands. *Workshop leader*

SMALLL Congress 2025, Rotterdam, the Netherlands. *Poster presentation*

Dutch Prosthetics Days 2026, Lelystad, the Netherlands. *Oral presentation*